UCUENCA

Universidad de Cuenca

Facultad de Ingeniería

Doctorado en Recursos Hídricos

Evaluating electrical conductivity as a surrogate tracer to determine the factors controlling event and pre-event water flow partitioning at a tropical montane Andean ecosystem

Trabajo de titulación previo a la obtención del título de Doctor (PhD) en Recursos Hídricos.

Autor:

Patricio Xavier Lazo Jara

ORCID: 0000-0001-5064-7118

Director:

Patricio Javier Crespo Sánchez

ORCID: 0000-0001-5126-0687

Co-directora:

Catalina Segura

ORCID: 0000-0002-0924-1172

Cuenca, Ecuador

2024-09-17

Resumen

Comprender los procesos hidrológicos es crucial para la correcta gestión de los recursos hídricos, especialmente en los ecosistemas andinos, donde la mayoría de ellos permanecen sin monitoreo y poco estudiados. Aunque varios intentos han aumentado nuestro conocimiento sobre estos temas mediante el uso de trazadores, todavía existe la necesidad de encontrar formas de evaluar procesos subhorarios, principalmente debido a limitaciones en recursos logísticos y económicos. Estos procesos subhorarios son difíciles de estudiar en cuencas con escorrentía de rápida respuesta, donde los caudales máximos se alcanzan muy rápidamente, obviándolos la mayoría de las veces. Esto tiene un papel importante en la gestión del agua, ya que brinda información sobre la dinámica de almacenamiento y liberación dentro de la cuenca, pudiendo variar según sus características, el uso de la tierra y el clima de la misma, de ahí la necesidad de determinar cuáles de ellos son los factores que controlan dichos procesos. Para llenar este vacío de conocimiento, se debe realizar un análisis exhaustivo de los procesos hidrológicos a escala de evento mediante la modelación de separación de flujo de agua de evento y pre-evento. La separación de flujo asume que el caudal de un evento de lluvia-escorrentía puede separarse en dos o más componentes de flujo, siendo los dos componentes comúnmente usados el agua de evento —entra al sistema hidrológico durante el evento de lluvia-escorrentía (e.g., precipitación) y el agua de pre-evento—almacenada en el sistema antes de que inicie el evento de lluvia-escorrentía (e.g., agua de suelos o subterránea). Esta tesis busca determinar los factores espaciales y temporales que controlan la fracción de agua de evento mediante el uso de datos de alta resolución. Para este fin, se siguieron tres objetivos específicos: (1) evaluar si el uso de conductividad eléctrica e isótopos estables para eventos monitoreados bajo condiciones hidrometeorológicas variables produce resultados de separación de flujo de evento y pre-evento similares, (2) examinar si modelos de diferente complejidad producen resultados de separación de agua de evento y pre-evento similares cuando se usa conductividad eléctrica y el oxígeno-18, y (3) determinar cuáles son los factores espaciales y temporales que controlan la separación de flujo de evento y pre-evento en un ecosistema andino montano tropical mediante el uso de datos de conductividad eléctrica de alta resolución.

Para esta tesis, se midió las concentraciones de oxígeno-18 y conductividad eléctrica en el caudal y la precipitación en una cuenca andina de montaña tropical (3505 a 3900 m s.n.m.) con alta resolución temporal (p. ej., 6 h, 4 h, 1 h, 5 min). Estos datos, junto con datos hidrometeorológicos de alta frecuencia, se utilizaron en combinación con modelos asistidos

por trazadores para estimar las fracciones de agua del evento y pre-evento de varios eventos de lluvia y escorrentía en condiciones de flujo variable. Además, los resultados del modelo se correlacionaron con variables hidrometeorológicas y características del paisaje.

Los resultados de esta tesis mostraron que la conductividad eléctrica podría usarse como una alternativa al oxígeno-18 como trazador para análisis de agua de evento y pre-evento, lo que aumenta en gran medida la resolución temporal de las concentraciones del trazador y al mismo tiempo reduce la incertidumbre del análisis de los modelos utilizados. Los resultados mostraron una gran similitud en una amplia gama de condiciones de flujo, lo que garantiza la coherencia de las fracciones estimadas: el 89 % de los eventos monitoreados mostraron diferencias inferiores al 20 % en la fracción de agua de pre-evento, independientemente de las condiciones antecedentes de humedad y lluvia. Esto fue posible debido a un comportamiento cuasi-conservativo de la conductividad eléctrica relacionado con la presencia de suelos riparios ricos en materia orgánica (tipo turba) superpuestos a un lecho de roca compacto a lo largo de la cuenca. Esto resalta el potencial de la conductividad eléctrica para obtener datos con alta frecuencia temporal y al mismo tiempo reducir los costos necesarios para implementar y mantener la recopilación de datos de trazadores durante largos períodos de tiempo. Además, los resultados de la comparación de modelos con diferentes complejidades también mostraron una gran similitud en sus estimaciones de las fracciones de agua de evento y pre-evento, siempre que se encuentren concentraciones apropiadas de agua del evento (Ce) y pre-evento (Cp) para el modelo más simple. De hecho, Cp demostró ser el factor más importante para que las estimaciones sean precisas, mientras que Ce tiene poca influencia en los resultados. Por lo tanto, la mejor manera de determinar Cp resultó ser asumiendo la concentración de una muestra de caudal tomada antes del comienzo de cada evento. Estos hallazgos permitirán reducir los recursos logísticos y económicos necesarios para evaluar adecuadamente la separación de flujo y llevar a cabo evaluaciones casi continuas con alta precisión en ecosistemas montanos altoandinos.

Los resultados anteriores permitieron el análisis de varios factores espaciales y temporales que controlan las fracciones de agua de evento y pre-evento. Esto permitió obtener datos hidrometeorológicos y de trazadores de alta frecuencia de un gran número de eventos de lluvia y escorrentía (n=72). Las correlaciones mostraron que el principal factor temporal de control fue la cantidad de lluvia con una correlación positiva fuerte (es decir, $r>0,7$) y significativa (es decir, $p<0,05$) con la fracción de agua de evento, mientras que el tipo de suelo, la cubertura vegetal y la topografía fueron altamente correlacionados al considerar

los factores espaciales. Estos resultados sugieren una mayor conectividad hidrológica del subsuelo poco profundo entre las laderas y los humedales de rivera, lo que conlleva a un aumento de la fracción de agua de los eventos que muestran flujos máximos más altos al superar un umbral. En general, nuestros hallazgos sugieren que los datos de alta resolución temporal son extremadamente necesarios para evaluar adecuadamente la separación de flujo de agua de evento y pre-evento, ya que ayuda a obtener una comprensión completa del comportamiento hidrológico de la cuenca a escala de evento que puede ayudar en la implementación de estudios con base científica y estrategias de gestión del agua que incluyen muchos procesos que a menudo se pasan por alto.

Palabras clave del autor: humedales, separación hidrográfica, procesos hidrológicos, escala de evento, trazadores, páramo

El contenido de esta obra corresponde al derecho de expresión de los autores y no compromete el pensamiento institucional de la Universidad de Cuenca ni desata su responsabilidad frente a terceros. Los autores asumen la responsabilidad por la propiedad intelectual y los derechos de autor.

Repositorio Institucional: https://dspace.ucuenca.edu.ec/

Abstract

Understanding the hydrological processes are crucial for the correct management of water resources, especially in Andean ecosystems where most of them remains ungauged and understudied. Although, several attempts have increased our knowledge on these topics by using tracers, there is still the need to find ways to adequality asses sub-hourly processes, mainly due to logistical and economical resources limitations. These sub-hourly processes are usually overlooked most of the times because of the difficult to study over fast runoff response catchments where peak flows are reached very quickly. These sub-hourly processes have a major role in water management as it gives insights into storage and release dynamics within the catchment that can vary based on catchment characteristics, land use, and climate; hence, the need to determine which of those are the controlling factors. In order to fill this knowledge gap, a thorough analysis of event scale processes must be conducted by using an event and pre-event flow partitioning modelling. Flow partitioning assumes that stormflow during a rainfall-runoff event can be divided in two or more flow components, the two components commonly considered are event water—entering a hydrological system during a rainstorm event (e.g., precipitation) and pre-event water—stored in the system before the beginning of an event (e.g., soil or groundwater). This thesis aims to determine the spatial and temporal factors controlling event water fraction by using high-resolution data. To this end, three specific objectives were followed: (1) to assess whether the use of electrical conductivity and stable isotopes for events monitored under variable hydrometeorological conditions yield similar event and pre-event flow partitioning results, (2) to examine if models of different complexity yield similar flow partitioning results when using electrical conductivity and Oxygen-18, and (3) to determine what are the spatial and temporal factors controlling flow partitioning at a tropical montane Andean ecosystem by using electrical conductivity high-resolution data.

For this thesis, we measured Oxygen-18 and electrical conductivity concentrations at streamflow and precipitation over a tropical montane Andean catchment (3505 to 3900 m.a.s.l.) at high temporal resolution (e.g., 6h, 4h, 1h, 5min). This data together with high frequency hydrometeorological data were used in combination with tracer-aided models to estimate the event and pre-event water fractions of several rainfall-runoff events under variable flow conditions. In addition, the modelling results were correlated with hydrometeorological variables and landscape features.

The results of this thesis showed that electrical conductivity could be used as an alternative to Oxygen-18 as a tracer for event and pre-event water flow partitioning analyses which highly increases the temporal resolution of tracer concentrations while reducing the uncertainty of the tracer-aided model. The results showed great similarity under a large range of flow conditions, reassuring the consistency of the estimated fractions with 89% of the monitored events showing differences lower than 20% in pre-event water fraction regardless of the antecedent moisture and rainfall conditions. The use of electrical conductivity was possible due to a quasi-conservative behavior related with the presence of organic-rich riparian soils (peat-type) overlying compact bedrock across the catchment. This highlights the potential of electrical conductivity to obtain high temporal frequency data while lowering the costs needed to implement and keep tracer data collection up for long time periods. In addition, results from the comparison of models with different complexities also showed great similarity in their estimations of the event and pre-event water fractions as long as appropriate concentrations of event (Ce) and pre-event (Cp) water for the simpler model are set. In fact, Cp showed to be the most important factor for improving accuracy while Ce had little influence on the results. Hence, the best way to determine Cp was the concentration of a streamflow sample taken before the beginning of each event. These findings will allow to reduce the logistical and economical resources needed to adequately assess hydrograph separation and to carry out quasi-continuous assessments of flow partitioning with high accuracy in high-Andean montane ecosystems.

The previous results led to the analysis of several spatial and temporal factors controlling event and pre-event water fractions. This allowed us to obtain tracer and hydrometeorological high-frequency data from a large number of rainfall-runoff events (n=72). The correlations showed that the main temporal controlling factor was rainfall amount with a strong (i.e., $r>0.7$) and significant (i.e., $p<0.05$) positive correlation with the event water fraction, whereas, soil type, vegetation cover, and topography were highly correlated when considering the spatial factors. These results suggested an enhanced shallow subsurface hydrological connectivity between hillslopes and riparian wetlands which follow in an increase of event water fraction for events that show higher peak flows while a threshold is exceeded. Overall, our findings suggests that high temporal resolution data is extremely necessary to adequately assess event and pre-event water fraction flow partitioning as it helps to obtain a complete understanding of catchment hydrological behavior at scale event. This improved understanding could aid in the implementation of

science-based water management strategies that includes many processes that are often overlooked.

Author Keywords: wetlands, hydrograph separation, hydrological processes, event scale, tracers, paramo

The content of this work corresponds to the right of expression of the authors and does not compromise the institutional thinking of the University of Cuenca, nor does it release its responsibility before third parties. The authors assume responsibility for the intellectual property and copyrights.

Institutional Repository: https://dspace.ucuenca.edu.ec/

Director:

Prof. Dr. Patricio Crespo Sánchez

Department of Water Resources and Environmental Sciences University of Cuenca

Co-director:

Prof. Dr. Catalina Segura

Department of Forest Engineering, Resources, and Management Oregon State University

Jury committee:

Prof. Dr. Ana Elizabeth Ochoa, Universidad del Azuay

Prof. Dr. Esteban Samaniego, Universidad de Cuenca

Prof. Dr. Edison Timbe, Universidad de Cuenca

Dean of the Faculty of Engineering

Prof. Dr. Lorena Sigüenza

Rector

Prof. Dr. María Augusta Hermida

Evaluating electrical conductivity as a surrogate tracer to determine the factors controlling event and pre-event water flow partitioning at a tropical montane Andean ecosystem

Thesis submitted in partial fulfilment of the requirements for the degree of Doctor of Philosophy in Water Resources

Patricio Xavier Lazo Jara

Spanish translation of the title:

Evaluación de la conductividad eléctrica como trazador sustituto para determinar los factores que controlan la partición del flujo en agua de evento y pre-evento en un ecosistema andino montano tropical

Please refer to this work as follows:

Lazo, Patricio X., 2024. Evaluating electrical conductivity as a surrogate tracer to determine the factors controlling event and pre-event water flow partitioning at a tropical montane Andean ecosystem. PhD Thesis, Universidad de Cuenca, Escuela Politécnica Nacional and Universidad Técnica Particular de Loja, Ecuador

Faculty:

Faculty of Engineering, University of Cuenca.

Department:

Department of Water Resources and Environmental Sciences, University of Cuenca.

Universities:

Universidad de Cuenca, Escuela Politécnica Nacional y Universidad Técnica

Particular de Loja.

City:

Cuenca, Ecuador

Contents

Resumen 1
Abstract 4
Contents 10
List of Figures 14
List of Tables 15
Acknowledgments 16
CHAPTER 1 19
1. Introduction and Thesis Outline 19
1.1. Introduction 19
1.2. Objectives 23
1.3. Study site 23
1.4. Outline of the thesis 25
CHAPTER 2 29
2. Flow partitioning modelling using high-resolution electrical conductivity data during variable flow conditions in a tropical montane catchment 29
2.1. Abstract 29
2.2. Motivation for the next chapter 30
CHAPTER 3 31
3. A simple mixing model using electrical conductivity yields robust hydrograph separation in a tropical montane catchment 31
3.1. Abstract 31
3.2. Motivation for the next chapter 32
CHAPTER 4 33
4. Spatial and temporal factors influencing hydrograph separation during variable flow conditions in a tropical montane catchment 33
4.1. Abstract 33
CHAPTER 5 35
5. Conclusions 35
5.1. Synthesis and conclusions 35
5.2. Future research 41
6. References 44

APPENDIX 71

Appendix 1. a) Volumetric sequential rainfall sampler located in the study site. The sampler was constructed using 4 plastic circular funnels (two of 250 mm diameter and two of 300 mm diameter) connected to ten 500 ml glass bottles. All bottles were sequentially connected by plastic tubes of 5 mm diameter. Each bottle had a glass pipette of 5 mm diameter introduced through their top while the rest of the bottle was hermetically sealed to prevent pressure decompensation. The top of the pipette was outside the glass bottle, while its bottom was inside at a level where the volume collected is 160 ml (corresponding to 1.12 mm of rainfall). Therefore, water entered the first bottle until reaching 160 ml volume, once the atmospheric pressure was equilibrated water was diverted into bottle 2 and so on until rain stopped or bottle 10 was filled. The latter almost never occurred, i.e., only 2 times during the 20 months monitoring period. The bottles were placed inside a wooden structure covered with aluminum foil and batting cotton for insulation to avoid isotopic fractionation due to evaporation, b) Sampler schematic representation showing: A-Glass bottle (500 ml volume), B-Plastic cap, C-glass pipette (5 mm diameter) to equilibrate atmospheric pressure , D-plastic tube (5 mm diameter) connecting the glass bottles in sequence, and E-Y connector). 72

Appendix 2. Relationship between $\delta^{2}H$ and $\delta^{18}O$ values in precipitation water samples collected with the volumetric autosampler. Red line represents the long-term Local Meteoric Water Line for the study site obtained from Mosquera *et al*. (2016a).....73

Appendix 3. Modules, equations, and parameters of the four Tracer-Based Streamflow Partitioning Analysis (TraSPAN) model structures. (Mosquera et al., 2018) 74

Appendix 4. Pre-event water fractions (PEWs) estimated using model structures a) 1, b) 2, c) 3, and d) 4 and calibrated for Oxygen-18 (black dots) and electrical conductivity (EC; red dots). Vertical lines represent uncertainty in PEWs corresponding to the 5–95% confidence limits of the possible solutions from the parameter sets within the range of behavioral solutions. 76

Appendix 5. Differences in pre-event water fractions (PEWs) estimated using Oxygen-18 and electrical conductivity for calibration of model structures a) 1, b) 2, c) 3, and d) 4. Dots represent the difference between the PEWs which produced the highest KGE vales for each tracer. Solid horizontal black line represents no difference (i.e., 0%). Dashed horizontal red lines represent the threshold for acceptable differences (±20%). Black vertical lines represent the differences in PEWs considering the estimated uncertainties determined for model calibration with each tracer (i.e., 5–95% confidence limits of behavioral solutions). The dots' colors correspond to events with 0 (red), 1 (black), and 2 (blue) water samples collected during peak flow. Sampling factor is equal to the total number of samples taken during an event divided by the duration of the event. 77

Appendix 6. Hydrograph separatioin performed during 37 rainfall-runoff events showing the pre-event water estimation obtained using the combination of C_e and C_p that showed the best results with $\delta^{18}O$ and EC. Error bars correspond to the uncertainty estimated by using the methodology proposed by Genereux (1998).....78

Appendix 7. Stable isotopic ($\delta^{18}O$) and electrical conductivity (EC) pre-event (PE) and event (E) water concentrations for each rainfall-runoff event (n=37) using the different sample options

described in Table 1 (i.e., PE1 to PE6, E2 to E6). E1 is not included in the table as it corresponds to several values depending on the number of samples collected during each monitored event as described in Table 3.1. 97

Appendix 8. Hydrometeorological variables for each of the rainfall-runoff events at M1 microcatchment. P means precipitation, Q means streamflow, RC means Runoff Coefficient, and Ant P means antecedent precipitation with the days considered are presented within the brackets. tot, average, and max, represents total, average, and maximum values.....99

Appendix 9. Hydrometeorological variables for each of the rainfall-runoff events at M2 microcatchment. P means precipitation, Q means streamflow, RC means Runoff Coefficient, and Ant P means antecedent precipitation with the days considered are presented within the brackets. tot, average, and max, represents total, average, and maximum values.....102

Appendix 10. Hydrometeorological variables for each of the rainfall-runoff events at M3 microcatchment. P means precipitation, Q means streamflow, RC means Runoff Coefficient, and Ant P means antecedent precipitation with the days considered are presented within the brackets. tot, average, and max, represents total, average, and maximum values.....105

Appendix 11. Hydrometeorological variables for each of the rainfall-runoff events at M4 microcatchment. P means precipitation, Q means streamflow, RC means Runoff Coefficient, and Ant P means antecedent precipitation with the days considered are presented within the brackets. tot, average, and max, represents total, average, and maximum values.....108

Appendix 12. Hydrometeorological variables for each of the rainfall-runoff events at M5 microcatchment. P means precipitation, Q means streamflow, RC means Runoff Coefficient, and Ant P means antecedent precipitation with the days considered are presented within the brackets. tot, average, and max, represents total, average, and maximum values.....111

Appendix 13. Hydrometeorological variables for each of the rainfall-runoff events at M6 microcatchment. P means precipitation, Q means streamflow, RC means Runoff Coefficient, and Ant P means antecedent precipitation with the days considered are presented within the brackets. tot, average, and max, represents total, average, and maximum values.....114

Appendix 14. Hydrometeorological variables for each of the rainfall-runoff events at M7 microcatchment. P means precipitation, Q means streamflow, RC means Runoff Coefficient, and Ant P means antecedent precipitation with the days considered are presented within the brackets. tot, average, and max, represents total, average, and maximum values.....117

Appendix 15. Linear regression between the hydrometeorological variables presenting the highest correlation with the event water fraction (Q_e) at catchment M1. P = precipitation, Q = streamflow. 120

Appendix 16. Linear regression between the hydrometeorological variables presenting the highest correlation with the event water fraction (Q_e) at catchment M2. P = precipitation, Q = streamflow. 121

Appendix 17. Linear regression between the hydrometeorological variables presenting the highest correlation with the event water fraction (Q_e) at catchment M3. P = precipitation, Q = streamflow. 122

Appendix 18. Linear regression between the hydrometeorological variables presenting the highest correlation with the event water fraction (Q_e) at catchment M4. P = precipitation, Q = streamflow. 123

Appendix 19. Linear regression between the hydrometeorological variables presenting the highest correlation with the event water fraction (Q_e) at catchment M5. P = precipitation, Q = streamflow. 124

Appendix 20. Linear regression between the hydrometeorological variables presenting the highest correlation with the event water fraction (Q_e) at catchment M7. P = precipitation, Q = streamflow. 125

List of Figures

Fig. 1.1. Zhurucay Ecohydrological Observatory showing the location of the meteorological station and the outlet of the nested catchments (M1-M7) used to collect water and tracer data during the period September 2017 to October 2018. 24
Fig. 1.2. Outline of the structure of the doctoral dissertation including the main methods for each.....28
Fig. 5.1. Assumptions in TraSPAN model structure with the time-variable fraction of P_{eff} routed as event water and two reservoirs in parallel for the event and pre-event runoff components. (Mosquera et al., 2018).....37
Fig. 5.2. Assumptions of the Two-component mixing model with q corresponds to streamflow, c is concentration, and 1, 2, and 3 corresponds to event, pre-event, and output respectively.....38
Fig. 5.3. Graphical scheme of the factors controlling the event water fraction with their corresponding catchment dynamics and hydrological processes.....40

List of Tables

Table 1.1. Main landscape features of the nested system of catchments of the Zhurucay Ecohydrological Observatory (M1-M7). 25
Table 5.1. Comparison between the use of EC and Oxygen-18 as tracer when monitoring rainfall-runoff events 36

Acknowledgments

A long journey with a satisfying end. That is how this period of my life could be defined. A time where my mind and body has been tested to its limits, but my resilience showed up to the task. This time of my life I have acquire a lot of knowledge about modelling, programing, and hydrological processes that will surely help me over the years to come in both, my professional and personal future, but the most important thing that this journey gave me was the sense that anything that life is going to throw at me, I will be able to overcome.

I would like to thank my advisors Patricio Crespo, Catalina Segura, and Giovanny Mosquera. To Patricio for not letting me throw the towel when things got complicated, for always supporting me and finding ways to help me through all my academic studies and personal life, his guidance have formed my professional career, and I could not ask for a better advisor. To Catalina for taking a stranger into her guidance and trust him to carry on this study, her academic support was key to develop my doctoral research and taking it to the highest level. To Giova for his unwavering support and motivation since our undergrad studies, and most important for his unvaluable friendship that I always cherish. All of you have my deepest gratitude and respect.

I also thank the members of my review committee, Ana Ochoa, Esteban Samaniego, and Edisson Timbe. Their comments, accurate and fulfilling, were always well received and helped to improve the quality of this thesis.

I thank the projects that made possible the publication of the articles presented in this thesis. The funding for this research comes from DFG RESPECT 386807763 and the Vice-rectorate of Investigation of the University of Cuenca (VIUC) through the project “From field scale eco-hydrological process understanding to landscape scale water fluxes”, and from the International Atomic Energy Agency (IAEA) and the Vice-rectorate of Investigation of the University of Cuenca (VIUC) through research contracts 22906 “Evaluation of Non-Stationary Hydrological Conditions in the Andean Páramo” and 22905 “Identification of Tap Water Sources and Water Supply Structure in a Mesoscale Tropical Andean City”. I also thank Comuna Chumblín Sombrederas (San Fernando, Azuay) for granting access to its communal land reserve during the development of this thesis. Thanks to Dundee Precious Metals Ecuador for their support in the logistics for the field work.

I would like to thank all the members of the Department of Water Resources and Environmental Sciences for all their support during my doctoral research, especially to those that helped me in the formidable field work that this thesis required: Juan Pesantez, Franklin Marín, Pablo Peña, Viviana Arízaga, Darío Zhiña, Mishel Palacios, Mateo Jerves, Juan Cabrera, and Karina Larco.

Last but not least, I would like to extend my gratitude and love to my wife and kids, they lived all this journey by my side and were extremely important for me to complete it. To my dear kids Xavier and Bernarda, you really are the fuel in my life, your smiles always were recomforting when things got difficult, every hug and every laugh, every kiss and every game, every joke and every “I love you”. All of it was necessary to accomplish anything in my life, you will always have my support in everything you do as you always supported me. I love you deeply. To my wife Andrea, I could not do it without you beside me, I could not chose a better partner to share my life with, your love and support during the most difficult times is highly appreciated, your company always make me a better person, thank you for your patience, I know it was not easy for you to endure this journey, sometimes it was harder for you than for me, but have no doubt that I will always be thankful and will always love you.

To Andrea, Xavier and Bernarda,

your love and support will always be needed for me to keep going forward

CHAPTER 1

1. Introduction and Thesis Outline

1.1. Introduction

Tropical montane Andean ecosystems are crucial in providing water resources to communities downstream as they play an important role in hydrological services (Aparecido et al., 2018) such as providing water for different uses (i.e., drinking, irrigation, electricity generation (Célleri and Feyen, 2009), water regulation, and production (Monge-Salazar et al., 2022; Mosquera et al., 2016a, 2015), water storage (Lazo et al., 2019), and essential biogeochemical processes (Pesántez et al., 2018). Thus, their importance has promoted several studies focusing on understanding the runoff generation processes with emphasis on determining their spatial and temporal controlling factors; where rainfall, soil type, vegetation cover, land use, hillslope-riparian zone connectivity, and topography distribution showed to play a key role at long-term scale analysis (e.g., Carrillo-Rojas et al., 2016; Correa et al., 2019, 2017; Hamel et al., 2017; Larco et al., 2023; Mosquera et al., 2023, 2022; Pesántez et al., 2023; Wright et al., 2017).

This information has improved the correct management of water resources and the development of several indicators of Andean ecosystems' current conservation states, which are constantly threatened by anthropogenic activities. However, it is also crucial to gain a fully understanding of these processes at finer scales such as during rainfall-runoff events. Event scale processes are important to (i) refine hydrological models by improving prediction reliability (van Kempen et al., 2021), (ii) to aid in early warning systems and mitigating flow related risks by improving flash flood prediction (Potdar et al., 2021), iii) to manage water quality during extreme events (Ebrahimi et al., 2024), (iv) capturing key characteristics of hydrological response during extreme events (Michelon et al., 2021), and (v) to evaluate climate change impacts over extreme events (Ombadi et al., 2023). These will help to provide valuable insights such as resilience, sustainability, and safety for water resources management and risk assessment by also enhancing flood prediction, climate impact assessments, and contributing to better hydrological modelling. Hence, the need to further investigate these processes at event scale which is often complex due to temporal and

logistic limitations, especially in Andean catchments, where most ecosystems are remote and ungauged.

Understanding the controlling factors aforementioned require a thorough analysis that could only be achieved by using a combination of hydrometric and tracer data. This approach has proved to be the most informative when analyzing runoff processes (Birkel and Soulsby, 2015) . It unifies two speed concepts that most of the times are considered separately: celerity and velocity (McDonnell and Beven, 2014). Celerity is defined as the speed with which a perturbation to the flow propagates through the flow domain such as a flood wave moving down a river, while velocity is used to define the mass flux of the water itself such as the tracer speed through the hydrologic system. This combined method could be used to i): explore the mixing relationships between fluxes and storages (van Huijgevoort et al., 2016), ii) infer travel time distributions (McGuire and McDonnell, 2006), iii) evaluate model performance as an extra criteria besides the more common hydrometric-based goodness of fit measures (Fenicia et al., 2008; Uhlenbrook and Sieber, 2005), and iv) separate and quantify the contributions of runoff components during different hydrological conditions at event scale (Klaus and McDonnell, 2013). The latter has been widely assessed by using event and pre-even water hydrograph separation, also referred as flow partitioning, which separates the flow in two fractions: (i) the water entering the system (i.e., event water) and (ii) the water that was stored at the catchment (i.e., pre-event water). This methodology was used as a tool to indirectly gain insights into: (i) rainfall-runoff processes (e.g., Goller et al., 2005; Hrachowitz et al., 2011; St Amour et al., 2005) such as precipitation leading to soil saturation and the connectivity among saturated areas that promotes increases at streamflow, (ii) surface and subsurface flow paths of water (e.g., Camacho Suarez et al., 2015; Laudon et al., 2004; Pearce et al., 1986) such as vertical and lateral flow movement that regulates the amount of water released and stored, and (iii) runoff generation thresholds (McGlynn and McDonnell, 2003; McGuire and McDonnell, 2010; Tweed et al., 2016) which are mostly determined by the catchment characteristics .

High-resolution data (i.e., sub-hourly) has proven to be crucial in obtaining reliable modelling results by greatly reducing uncertainty and promoting an adequate comprehension of the hydrological processes by increasing insights into catchment's functioning which aids the processes conceptualization (Birkel and Soulsby, 2015). This high-resolution is easier to obtain when dealing with hydrometric data because of the number of devices available on the market to gather streamflow and rainfall data, which are often cheaper and low

maintenance, making them very affordable to be implemented in almost every monitored catchment worldwide. This is not the case for tracer data where high-resolution is scarce and reduced to few studies during small periods of time (i.e., 4 months)(e.g., Wang et al., 2019), which is mainly the result of stable isotopes being commonly used because of their conservative behavior (Klaus and McDonnell, 2013). Stable isotopes require a significant number of resources to achieve a high-resolution sampling and analysis field set-up, even though several initiatives have been carried into improving the technology and analysis time (e.g., Herbstritt et al., 2019; Sahraei et al., 2020; Tweed et al., 2016; von Freyberg et al., 2017), sustaining this type of set-up over longer periods remains challenging, especially in the Andean tropics. The main problem when sustaining these set-ups is that stable isotopes require very expensive high-level equipment that is not adequate for extreme climate conditions, often of considerable size with high demanding energy and maintenance needs, these resources are not always available or sustainable over time for remote catchments. Hence, the need to find an alternative tracer that guarantees similar results than stable isotopes in terms of event and pre-event water fractions with low implementation requirements.

In this sense, many studies have used different tracers in event and pre-event flow partitioning such as chloride (e.g., Brown et al., 1999; Leaney et al., 1993; Monteith et al., 2006; Turner et al., 1987), silica (e.g., Durand et al., 1993; Hooper and Shoemaker, 1986; Munyaneza et al., 2012; Nolan and Hill, 1990), alkalinity (e.g., Ribolzi et al., 1996), sodium (e.g., Pionke et al., 1993; Suecker et al., 2000) and calcium (Johnson et al., 2023). All these studies have showed that similarity depends on the grade of tracer conservative behavior on the catchment in which it is applied. Hence, Electrical conductivity (EC) studies has showed the highest potential because it is easy to measure and quantify, being able to obtain this data from very affordable automatic sensors that could be installed in combination with the streamflow sensors, at the same resolution (e.g., sampling every 5 minutes) (Cano-Paoli et al., 2019; Saraiva Okello et al., 2018), Thus, allowing a sustained high-resolution set-up to monitor a great number of rainfall-runoff events, avoiding a significant loss of information as a result of low-resolution sampling (Kirchner et al., 2004). Thus, EC has showed contrasting results, while some studies reported similar results (e.g., Camacho Suarez et al., 2015; Cano-Paoli et al., 2019; Meriano et al., 2011; Mosquera et al., 2018; Vidon and Cuadra, 2010), other found great differences (e.g., Hayashi et al., 2012; Laudon and Slaymaker, 1997; Pellerin et al., 2008). This suggests that EC could not be used in all

catchments and highlights the need for a proper comparison between EC and stable isotopes during several rainfall-runoff event conditions at the highest possible resolution. This is viable in Andean ecosystem where low temperatures, non-saline soils, and stable river beds without salts are common, reducing EC variability; and therefore, enhancing its conservative behavior, making these ecosystems a perfect field laboratory to test this tracer.

Another important aspect of event and pre-event flow partitioning is the use of different modelling frameworks that aim for a more realistic representation of the catchment. Although, many authors have proposed the use of complex models that try resemble the variety of internal catchment processes than simpler ones (Stadnyk et al., 2013; Vaché and McDonnell, 2006), they require numerous resources such as high-level equipment, high-resolution data and a large amount of computational capacities that are not always available. These complex models are often accompanied by several parameters that need to be calibrated and could lead to overparameterization (Seibert et al., 2019). However, catchment hydrologists need to identify when a complex model is necessary over a simpler one by analyzing the objectives of the modelling and the results needed to fulfil these objectives. Most of the time the preference of a complex model is based only on the fact that it could have less uncertainty or the inclusion of more processes to increase the catchment representation, but this could not always be accurate. A proper comparison between models of different complexity is needed under several conditions to accept or reject their use and determine under which conditions they are similar. This will have the potential to implement models, such as event and pre-event flow partitioning over ungauged catchments where information is scarce.

High-resolution data in combination with a straightforward framework is highly important to explore spatial and temporal controlling factors of event and pre-event flow partitioning as they provide a great number of monitored and analyzed rainfall-runoff events. Many of the studies exploring this subject have failed to monitor a large number of rainfall-runoff events, therefore; have omitted several catchment event conditions where the relationships between landscape organization, hydrometric variables, and catchment hydrological response change as dominant runoff generation processes vary (Carey et al., 2013; Tetzlaff et al., 2009). Soils, geology, topology, topography, precipitation, antecedent wetness conditions among others influence the short-term runoff responses (Buttle, 2006) as a result of different studies developed using the combined hydrometric and tracer approach, thus; failed to capture all the meteorological conditions in which these occur because of the small number

of events monitored and the assumption that one event could be used to represent several conditions which created an incomplete understanding of the runoff processes at event scale, especially over the Andean tropics where a scarce number of these studies have been developed. Hence, spatial and temporal controlling factors at event scale must be adequately assessed.

This thesis aims to fill this knowledge gap by analyzing the spatial and temporal controlling factors of event and pre-event water fractions by finding a surrogate tracer that allows a combined hydrometric and tracer high-resolution data, resulting in an extended number of rainfall-runoff events monitored avoiding an incomplete set that could bias the analysis of controlling factors over a simple modelling framework. Filling this gap is very important for the correctly identification of the variability of fast occurring rainfall-runoff processes that increase the understanding of catchment hydrology in the Andean tropics to support water management plans.

1.2. Objectives

The main objective of this thesis was to determine which factors control event and pre-event flow partitioning at a tropical montane Andean ecosystem by using high-resolution electrical conductivity data as a surrogate tracer. The specific objectives can be summarized as:

1. To assess whether the use of electrical conductivity and stable isotopes for events monitored under variable hydrometeorological conditions yield similar flow partitioning results.
2. To examine if models of different complexity yield similar flow partitioning results when using electrical conductivity and Oxygen-18.
3. To determine what are the spatial and temporal factors controlling flow partitioning at a tropical montane Andean ecosystem by using electrical conductivity high-resolution data.

1.3. Study site

The Zhurucay Ecohydrological Observatory (ZEO) is a tropical montane páramo catchment located west of the Pacific-Atlantic water continental divide in the southern Ecuadorian Andes (3°04′S, 79°14′W) at an elevation ranging from 3505 to 3900 m a.s.l. (Fig. 1.1). Despite this, the local climate is mainly influenced by recycled atmospheric moisture of the Amazon forest stemming east of the Andean mountain range (Esquivel-Hernández et al.,

2019; Zhiña et al., 2022). The catchment has a drainage area of 7.53 km^2 where a generally cold and frequently cloudy and foggy climate is observed, with annual temperatures averaging 6.3±1.24°C and a mean relative humidity of 92.3±8.3% (Larco et al., 2023) , which results in a relatively low annual evapotranspiration ratio (ET/P) of 0.49 (Ochoa-Sánchez et al., 2020). The annual precipitation (± standard deviation) averaged 1222±22 mm at 3780 m a.s.l. (Larco et al., 2023), with light rainfall in the form of drizzle (intensities<5mm/hr) accounting for a 90% of the water inputs year-round (Padrón et al., 2015). This constant precipitation input causes soils to maintain high humidity, promoting a shallow subsurface flow at the top soil layer (Mosquera et al., 2016c), resulting in a flashy streamflow response to rainfall (Lazo et al., 2023; Mosquera et al., 2016b, 2015).

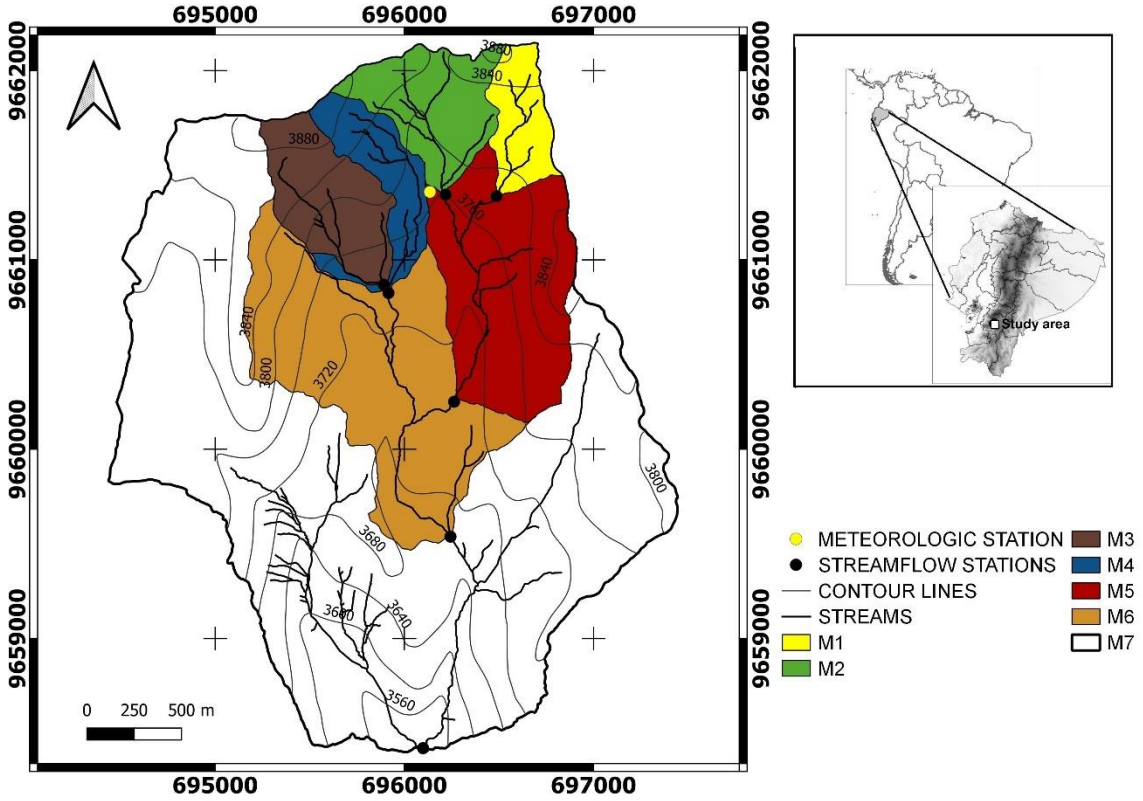

Fig. 1.1. Zhurucay Ecohydrological Observatory showing the location of the meteorological station and the outlet of the nested catchments (M1-M7) used to collect water and tracer data during the period September 2017 to October 2018.

Geology consists of three types of formations. Quimsacocha formation has basaltic flows in combination with plagioclases, feldspars, and andesitic pyroclastics. Turi formation is composed mainly of tuffaceous andesitic breccias, conglomerates, horizontal stratified

sands, and Quaternary deposits dominated by glacial moraines. The soils at the catchment were identified as Andosols and Histosols (IUSS Working Group WRB, 2015), which are humic and acidic and present high water retention capacity (Mosquera et al., 2021; Quichimbo et al., 2012). Vegetation cover consists of tussock grass (Calamagrostis sp.) above andosols mainly located at hillslopes (71% of catchment area; Table 1.1), and cushion plants (*Plantago rigida, Xenophyllum humile, Azorella* spp.) on top of Histosols mainly found at valley bottoms (29% of catchment area; Table 1.1).

Table 1.1. Main landscape features of the nested system of catchments of the Zhurucay Ecohydrological Observatory (M1-M7).

Micro catchment	Area (km^2)	Slope (%)	Soil type		Vegetation cover		Geology		
			Andosol (%)	Histosol (%)	Tussock grass (%)	Cushion plants (%)	Quimsacocha Formation (%)	Turi Formation (%)	Quaternary deposits (%)
M1	0.20	14	85	15	85	15	100	0	0
M2	0.38	24	83	17	87	13	66	1	33
M3	0.38	19	80	20	78	22	59	41	0
M4	0.65	18	76	24	79	21	50	48	1
M5	1.40	20	78	22	78	22	70	1	30
M6	3.28	18	74	26	73	27	50	30	20
M7	7.53	17	72	28	71	29	56	31	13

Because of the location of sampling equipment, only M6 was used for the analyses of chapters 2 and 3, whereas the complete nested monitoring systems were used for the analysis of chapter 4.

1.4. Outline of the thesis

The outline of the thesis with its main methods is presented in Fig. 1.2. Chapter 1 addresses an overview of the event and pre-event flow partitioning at event scale, knowledge gaps, and their importance to hydrological processes at Andean ecosystems. In addition, the main objectives of the thesis and the study site where the thesis have been conducted were also showed in chapter 1. The following chapters developed the three objectives proposed in this thesis. Study site was the same for all the published papers, thus; its description has been

omitted from chapters 2, 3, and 4 as it was previously presented in chapter 1. The complete list of references is provided at the end of this document, this encompasses the references of the entire thesis.

Chapter 2 develops the first objective of the thesis. In this chapter a tracer-aided model was used to perform event and pre-event water flow partitioning to compare the results obtained with two tracers: Oxygen-18 and electrical conductivity. This chapter showed a published paper in the journal “Journal of Hydrology”. Corroborating that EC brings the same results as Oxygen-18 at event and pre-event flow partitioning will allow high frequency tracer sampling (i.e., 5-minutes resolution) that will increase the number of monitored events at a wide range of hydrometeorological conditions, and also allowing the capture of samples covering the rising limb, the peak, and the recession of all the events. This also means capturing tracer data at the same resolution than streamflow data while reducing the uncertainty of the model, information that will be valuable for the following chapters.

Chapter 3 corresponds to the second objective of the thesis. In this chapter a comparison of event and pre-event flow partitioning models of different complexity was performed. The results obtained by using the complex tracer-aided model in chapter 2 was compared with the results obtained with the two-component mixing model, a simpler framework widely used worldwide. For this, 36 combinations of event and pre-event fraction concentrations for the simpler model were tested to determine which one gives similar results than the complex model. This chapter have determined the importance of characterizing pre-event water fraction concentration for each event individually, rather than assuming one value for every event, highlighting the importance of high-frequency sampling. The results of this chapter helped to reduce the number of computational resources and time needed to evaluate a large number of rainfall-runoff events that will be obtained from using EC as a tracer for event and pre-event water flow partitioning, and also how to determine the concentrations needed for further analysis which will be very useful when analyzing the controlling factors. This chapter represents a published paper in the journal “Journal of Hydrology”.

Chapter 4 encompasses the third objective of the thesis. This chapter benefits from the results obtained from chapters 2 and 3 to obtain a large dataset of high-frequency (i.e., 5-minutes resolution) monitored rainfall-runoff events over the course of the 2017-2018 hydrological year. This large dataset was evaluated with the two-component mixing model to determine the event and pre-event water fractions and was compared with several

hydrometeorological variables and landscape features to determine the factors controlling event water fraction. High-frequency allowed the identification of threshold related factors, giving insights into the dynamics of saturated contributing areas during rainfall-runoff events, highlighting the need of further investigation of these processes.

Finally, chapter 5 provides a synthesis of the main findings of the thesis. The accompanying discussion aims to encourage the use of tracers that allows high-frequency monitoring to adequately determine event scale hydrological processes that are not easily observed with regular monitoring set-ups especially in Andean ecosystems given their importance on providing several hydrological services, and many opportunities of developing such line of work in future research.

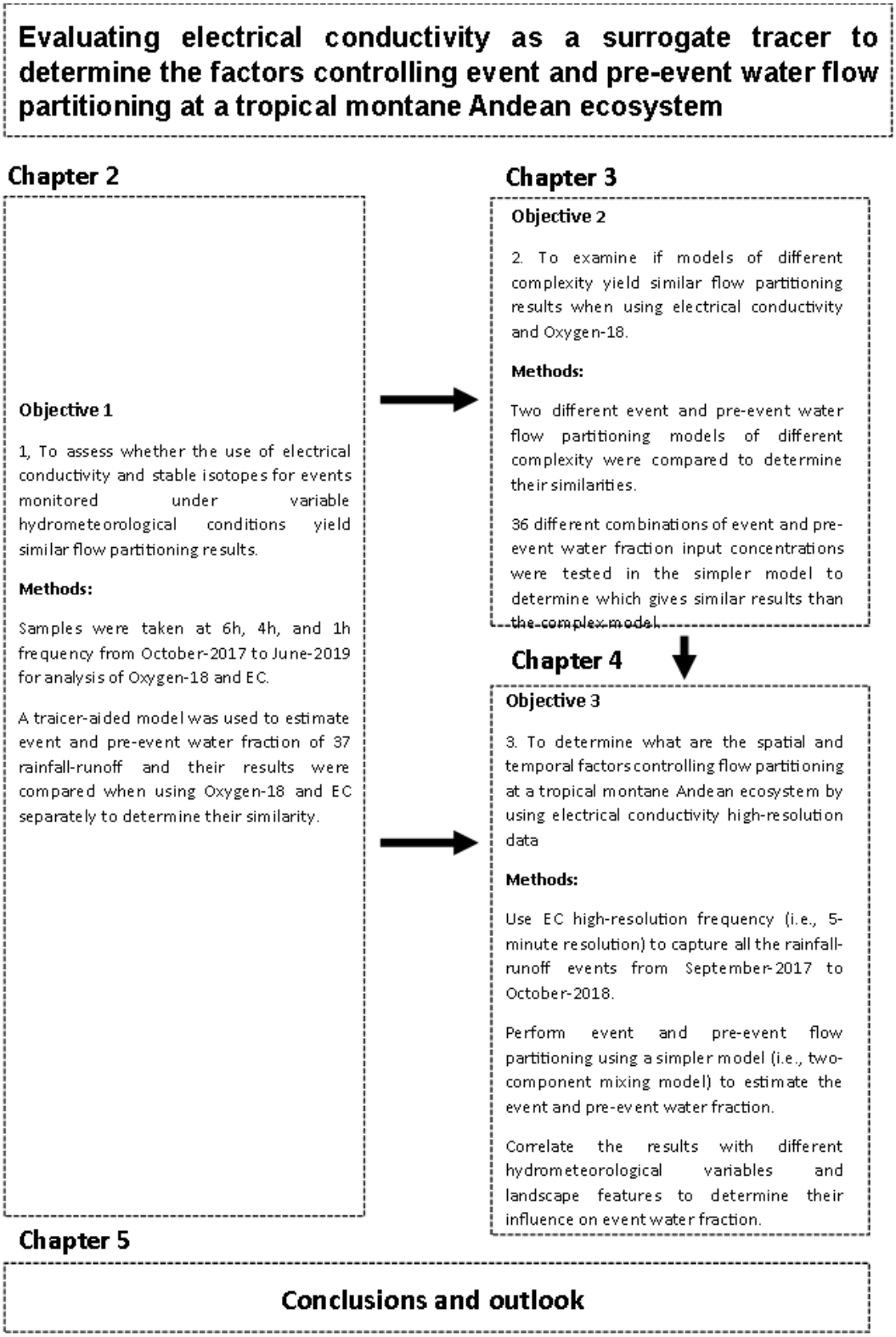

Fig. 1.2. Outline of the structure of the doctoral dissertation including the main methods for each.

CHAPTER 2

2. Flow partitioning modelling using high-resolution electrical conductivity data during variable flow conditions in a tropical montane catchment

Based on: Lazo, P.X., Mosquera, G.M., Cárdenas, I., Segura, C., Crespo, P., 2023. Flow partitioning modelling using high-resolution electrical conductivity data during variable flow conditions in a tropical montane catchment. J. Hydrol. 617, 128898. doi:10.1016/J.JHYDROL.2022.128898

Link: https://www.sciencedirect.com/science/article/abs/pii/S0022169422014688?via%3Dihub

2.1. Abstract

Tracer-aided hydrological models (TAHMs) are one of the most powerful tools to identify new (event) and old (pre-event) water fractions contributing to stormflow because they account both for streamflow and tracer mixing dynamics in model calibration. Nevertheless, their representativeness of hydrograph dynamics is often limited due to the unavailability of high-resolution conservative tracer data (e.g., water stable isotopes or chloride). Hence, there is a need to identify alternative tracers that yield similar flow partitioning results than "ideal" ones while requiring fewer financial resources for high-frequency monitoring (e.g., sub-hourly). Here, we compare flow partitioning results of a TAHM calibrated using high-frequency electrical conductivity (EC) and water stable isotope (18O) data collected during 37 rainfall-runoff events monitored during variable hydrometeorological conditions in the Zhurucay Ecohydrological Observatory (ZEO), a tropical alpine catchment located in southern Ecuador. When the model was calibrated using the sampling resolution of stables isotopes (6-hours to 1-hour), no statistically significant differences of pre-event water fractions (PEWs) using both tracers for model calibration were found. PWE differences between both tracers for 89% of the events were <20% regardless of the events' antecedent moisture and rainfall conditions. Model transfer functions were also similar suggesting that catchment internal processes inferred using both tracers are comparable. Events presenting larger differences (n=4; up to 27% PEW difference) had no samples collected during peak flow. Calibration of the model using EC data collected at sub-hourly intervals (every 5-minutes) showed a significant increase in model performance as compared to the frequency of collection of isotopic data. Similarity in flow partitioning results can be attributed to a quasi-

conservative nature of EC due to the presence of organic-rich riparian soils (peat-type) overlying compact bedrock across the catchment. Findings also highlight the importance of capturing rapidly occurring catchment mixing processes though high-temporal frequency monitoring of tracer data. Our study encourages the value of assessing the use of alternative tracers, such as EC, to identify fast occurring rainfall-runoff processes, while lowering the costs needed to implement and sustain tracer data collection for long time periods.

2.2. Motivation for the next chapter

The objective of this chapter was to determine if Electrical Conductivity (EC) yielded similar flow partitioning results than Oxygen-18 when calibrating a Tracer-aided hydrological model during a large range of hydrometeorological conditions. The chapter showed that EC could be used as an alternative tracer because it presented a quasy-conservative behavior allowing an increase in sampling resolution, that also increases the performance of the model. These findings serve to identify the best model structure for the catchment and obtain a high-resolution EC database, that were used in the next chapter to find out if these similarities could also be obtained when using a less complex model that could reduce the resources needed to evaluate flow partitioning and evaluate the input data needed to obtain reliable results.

CHAPTER 3

3. A simple mixing model using electrical conductivity yields robust hydrograph separation in a tropical montane catchment

Based on: Lazo, P.X., Mosquera, G.M., Cárdenas, I., Segura, C., Crespo, P., 2024. A simple mixing model using electrical conductivity yields robust hydrograph separation in a tropical montane catchment. J. Hydrol. 131632. doi:https://doi.org/10.1016/j.jhydrol.2024.131632

Link: https://doi.org/10.1016/j.jhydrol.2024.131632

3.1. Abstract

Hydrograph separation assessment is crucial to understand stormflow generation at catchments worldwide. Tracer-based methods provide robust estimations of event (or new) and pre-event (or old) water fractions as they account for external and internal catchment hydrological behavior. While models of different mathematical and computational complexity are often used in tracer-based hydrograph separation studies, direct comparisons between those models are limited. Here, we compare hydrograph separation results yielded by the simplest Two-Component Mixing Model (TCMM) and a Tracer-based Streamflow Partitioning ANalysis model (TraSPAN) assumed to provide robust results as it combines conceptual rainfall-runoff modelling with tracers' mass balance. We carried out the analysis using high temporal frequency (sub-daily to sub-hourly) data of two tracers, Oxygen-18 and Electrical Conductivity (EC), monitored during 37 rainfall-runoff events with different hydrometeorological conditions in a high-Andean páramo catchment located at the Zhurucay Ecohydrological Observatory in southern Ecuador. Both approaches yield similar estimations of event and pre-event water fractions regardless of the tracer used as long as appropriate concentrations of event (Ce) and pre-event (Cp) water for the TCMM are determined. Although the estimate of Ce has little influence with one rainfall sample collected during the event being sufficient to obtain reliable results, results hinge heavily on the estimate of Cp. We found that the TCMM yields similar results than TraSPAN when Cp is represented by the stream water concentration corresponding to a sample collected prior to the beginning of each of the events. We conclude that the combination of a simple framework (TCMM) with sub-hourly EC measurements provides reliable hydrograph

separation results when representative Cp samples are used. These findings will allow to lower the logistical and economical resources needed to adequately assess hydrograph separation and to carry out quasi-continuous assessments of flow partitioning with high accuracy in high-Andean páramo catchments.

3.2. Motivation for the next chapter

The objective of this chapter was to test if a simple mixing model yields similar results than a more complex tracer-aided hydrological model. This chapter showed the ideal combination of input tracer data to obtain reliable event and pre-event water fractions when performing hydrograph separation, where the selection of pre-event water fraction concentration has a major influence, contrary to event water fraction concentration. The chapter also corroborates that EC could be used as an alternative to Oxygen-18, therefore; the following chapter uses this information to create a combined 5-minute resolution streamflow and EC database that allows monitoring of almost every rainfall-runoff event at the catchment. This made possible the capture of all the hydrometeorological conditions in which these events can occur to adequately determine the factors controlling event and pre-event water flow partitioning at event scale.

CHAPTER 4

4. Spatial and temporal factors influencing hydrograph separation during variable flow conditions in a tropical montane catchment

Based on: Lazo, P.X., Mosquera, G.M., Cárdenas, I., Segura, C., Crespo, P., 2024. Spatial and temporal factors influencing high-temporal frequency hydrograph separation during variable flow conditions in a tropical montane catchment. In review.

4.1. Abstract

Determining the factors influencing runoff generation through key hydrological indicators such as the event (Qe) and pre-event (Qp) water fractions contributing to total stormflow is key to water resources management at montane ecosystems. As a result, tracer-aided hydrograph separation has become an important tool for flow partitioning at catchment scale. However, a sustained high-resolution sampling is often difficult to achieve due to logistic and economic constraints that result in few rainfall-runoff events generally monitored, leading to an incomplete understanding of catchment hydrological behavior across the wide range of hydrometeorological conditions occurring throughout the year. Here, we used high-frequency hydrometeorological (precipitation and streamflow) and tracer data (electrical conductivity, EC) to determine the spatial and temporal factors influencing hydrograph separation in a nested system of tropical montane catchments during 72 rainfall-runoff events representing 90% of the events during the period September-2017 to October-2018. Temporally, Qe was positive strongly and significantly correlated with precipitation amount. Spatially, soil type, vegetation cover, and topography were highly correlated with Qe for each of the monitored events. Although, a dominance of Qp contribution to total stormflow was observed regardless of intra-event and antecedent hydrometeorological conditions for all events, the results suggest that enhanced shallow subsurface hydrological connectivity between hillslopes and riparian wetlands results in an increase of Qe for events showing higher peak flows. Our findings highlight the importance of acquiring high-frequency data to obtain a complete understanding of catchment hydrological behavior that can aid in the implementation of science-based water management strategies.

CHAPTER 5

5. Conclusions

5.1. Synthesis and conclusions

This thesis is supported by the three main objectives developed in chapters 2, 3, and 4. The first objective involved the comparison between electrical conductivity (EC) and Oxygen-18 to determine if EC could become a surrogate when performing event and pre-event flow partitioning by using a complex tracer-aided hydrological model (TraSPAN). This allowed the use of EC to evaluate models with different complexity in objective 2, where a simple Two-component mixing model (TCMM) was compared with the TrasPAN to determine under which conditions TCMM provides similar results. Building on the results from objectives 1 and 2, objective 3 used EC to obtain high-resolution (i.e., every 5 minutes) hydrograph separation. Seventy-two rainfall-runoff events that covered all the hydrometeorological conditions were used, to understand the spatial and temporal controlling factors of event and pre-event water fractions.

In objective 1 (chapter 2), the TraSPAN model was calibrated using high-resolution EC and Oxygen-18 data as tracers. A total of 37 rainfall-runoff events were monitored, and 4 model structures were tested. The comparison showed that EC gave similar results than Oxygen-18, not only in the estimates of water fractions but also in catchment internal processes, as demonstrated by the similarity of the Transit Time Distributions when calibrating the model structures. This chapter showed that the catchment's soils high-water storage and retention capacity allows a very good mixing of the water in the system where no major chemical reactions occur. In addition, the mixing processes are developed in low temperatures also limiting the chemical reactions. Other important aspect of the catchment is the low groundwater contribution to the streams causing that the majority of the water comes from the well-mixed soil water. The combination of these specific catchment features benefits EC quasi-conservative behavior. This opens the possibility of increasing the sampling resolution of the tracer with little effort and sustaining this set-up over longer periods, especially in remote places where logistics are complicated and financial support is scarce. This chapter also highlights the importance of high resolution to improve model accuracy to better understand intra-event rainfall-runoff processes that appear at finer temporal resolutions and

how internal catchment processes influences the behavior of certain elements that could be more suitable tracers than others to improve the sampling resolution.

The use of EC as a surrogate tracer also presents financial benefits that could result in a sustainable and economical monitoring program. A comparison of the cost when using $\delta^{18}O$ and EC is showed in Table 5.1 where a difference of almost $1000000 is observed when considering the monitoring of 7 sampling points. This information could be crucial for decision makers when managing monitoring resources over remote and ungagged ecosystems such as Andean páramo.

Table 5.1. Comparison between the use of EC and Oxygen-18 as tracer when monitoring rainfall-runoff events.

Item	Unitary cost Electrical conductivity	Needed	Total	Unitary cost Oxygen-18	Needed	Total
Equipment	$ 3,200.00	1	$ 3,200.00	$ 7,000.00	3	$ 21,000.00
Laboratory analysis	$ -	NA	NA	$ 12.00	8760	$ 105,120.00
Transportation	$ 60.00	24	$ 1,440.00	$ 60.00	156	$ 9,360.00
Salary	$ 50.00	24	$ 1,200.00	$ 50.00	156	$ 7,800.00
1-year 5-minute resolution			$ 5,840.00	1-year hourly resolution		$ 143,280.00
7 sampling points			$ 40,880.00	7 sampling points		$ 1,002,960.00

Objective 2 (chapter 3) compares two tracer-aided models of different complexity, the TraSPAN and the TCMM. Both models perform event and pre-event flow partitioning. The complexity of the models differ as TraSPAN corresponds to a structure that estimates the effective precipitation, which routed the input flow into 4 buckets, 2 corresponding to the event water fraction with slow and fast movement, and the other 2 corresponding to the pre-event water fraction with slow and fast movement. This model is calibrated to match not only streamflow data but also tracer data (Fig. 5.1). The TCMM on the other hand, is a basic

mass balance model in which the input data corresponds to the event water fraction with its concentration, and the pre-event water fraction with its concentration. It consists in only one bucket where these to fractions mixes resulting in the streamflow with its concentration (Fig. 5.2).

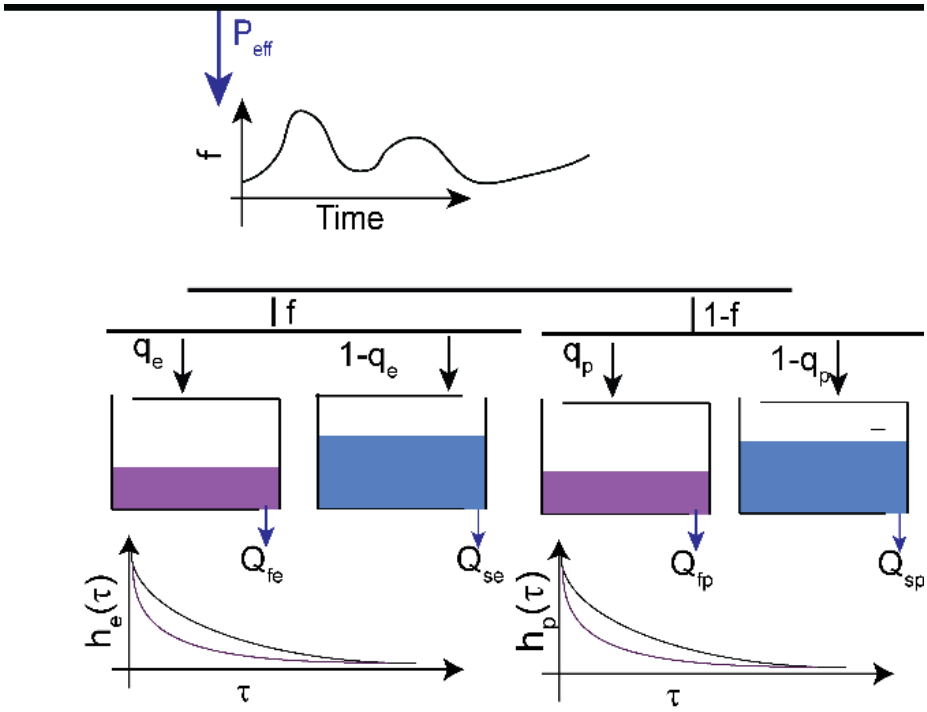

Fig. 5.1. Assumptions in TraSPAN model structure with the time-variable fraction of P_{eff} routed as event water and two reservoirs in parallel for the event and pre-event runoff components. (Mosquera et al., 2018)

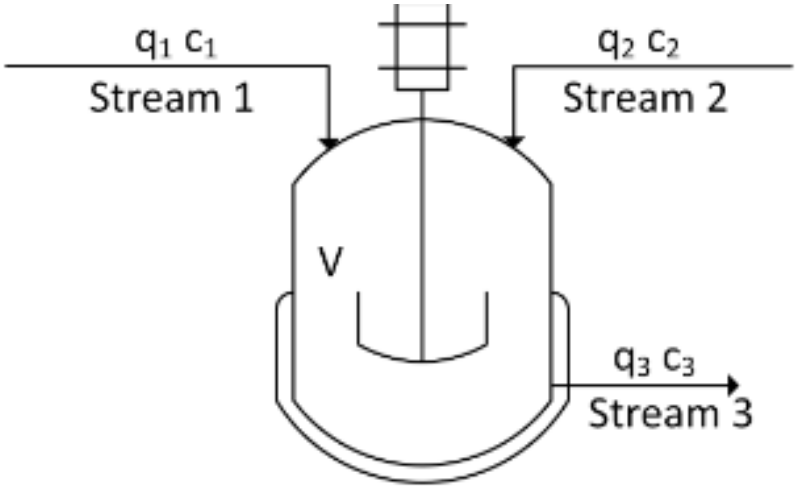

Fig. 5.2. Assumptions of the Two-component mixing model with q corresponds to streamflow, c is concentration, and 1, 2, and 3 corresponds to event, pre-event, and output respectively.

This chapter showed that the similarities between the results of these two models depending on the accuracy when selecting the input event and pre-event water concentrations. In fact, the concentration that most influences the accuracy of the results corresponded to the pre-event water fraction, highlighting that the selection of the concentration must be specific for each event rather than a single value (i.e,, baseflow concentration) for all of them regardless of the tracer used. This is assumed to be correct in most of the event and pre-event water flow partitioning studies worldwide, however; it could not be true in regions such as Andean humid paramo catchments, where hydrological behavior is dominated by peat-type riparian soils with little to no contributions of deep groundwater flow to the total streamflow. This chapter also revealed a low intra-event variability in rainfall concentrations, responsible for the event water fraction at the catchment. This low variability is primarily due to the constant input of low-intensity precipitation through the year. Hence, the event water concentration could be easily determined with a single sample of rainfall during the event in catchments without ice-melt. The similarity between the results obtained with models of different complexity suggest a good quality in the results of simple models over Andean paramo catchments. Ungauged catchments could benefit from these results as simple models reduces computational time and allocated resources. This thesis encourages this type of comparisons in other Andean catchments.

Overall, the findings obtained in chapters 2 and 3 highlight the importance of catchment hydrological behavior in the selection of the tracers to be used for the analysis. This hydrological behavior could also have an impact on the complexity level of the models that could be used to perform hydrograph separation. These results showed that the combination of high-resolution EC data with a simple mathematical framework could reduce the logistical and economic resources required for this type of analysis. This showed an excellent opportunity to progress in the understanding of catchment hydrology in the region by determining the factors controlling the event and pre-event flow partitioning.

This led to objective 3 (chapter 4) in which we learn from chapters 2 and 3 the models and methods to be used to obtain high-resolution tracer data. This helped to obtain a great number of rainfall-runoff events to be analyzed by using the TCMM. Thus, an accurate estimation of event and pre-event water fractions was achieved. An extended high-resolution

EC monitoring of the nested set-up in the catchment allowed the monitoring of 90% of the rainfall-runoff events that occurred during the hydrological year, something that has not been achieved by any hydrograph separation study. This chapter highlights the need for further investigation on event scale processes that takes advantage of high temporal resolution data. This will encourage to reevaluate event scale processes at different catchments where high-resolution is achieved. The aim of this chapter is to monitor all the event hydrometeorological conditions, resulting in a complete database that captures all the hydrological processes at a event scale. This chapter also showed how spatial and temporal factors influence the runoff response to rainfall at the catchment. Precipitation was the most important temporal factor influencing the event water production, but it was the precipitation quantity rather than the precipitation intensity what controlled how much event water contributed to the streamflow resulting in a positive correlation between precipitation amount and event water fraction. Higher precipitation increases the number of saturated areas among the catchments and the connectivity between hillslopes and riparian zones, leading to the occurrence of saturation overland flow that promotes a dominance of event water at event scale. Furthermore, the most important spatial controllers were the type of soils, the vegetation cover, and the average slope of the catchment; however, not all these factors influenced equally to all the events. Some events depend just in one of the factors at some point, while others rely on a combination of them. These influences highly depend on the amount of water exiting the catchment as streamflow (i.e., peak flow) with responses depending in soil type, steepness of the slope, or a combination of both. Histosols and cushion plants presented a positive correlation with the event water fraction during low to medium peak flow values. Their high retention capacities enhance rapid saturation of riparian zones increasing the connectivity between saturated areas and hillslope zones which results in surface runoff with high event water fractions.

A threshold behavior was observed with opposing correlations (i.e., positive or negative) depending on the peak flow regarding the average slope of the catchment (i.e., topography). This suggests that when a threshold is reached (i.e., peak flow = 0.036mm/s), the factors changed the way in which they influence the catchment hydrological response. We assumed that the steepness of the slope favors the rapid lateral movement of subsurface flow at low and medium peak flow values, but the correlation shifts when the threshold is reached. This phenomenon results from the increased connectivity of the saturated areas that contribute to the streamflow as flatter large areas became saturated faster as the events increase their

peak flows, enhancing the occurrence of overland flow and their connectivity with the hillslopes, which also leads to a rapid lateral movement of subsurface flow increasing the amount of event water contributing to the stream over higher streamflow values. Fig. 5.3 shows a summary of the methods used and the relationships between the controlling factors with the catchment dynamics and hydrological processes.

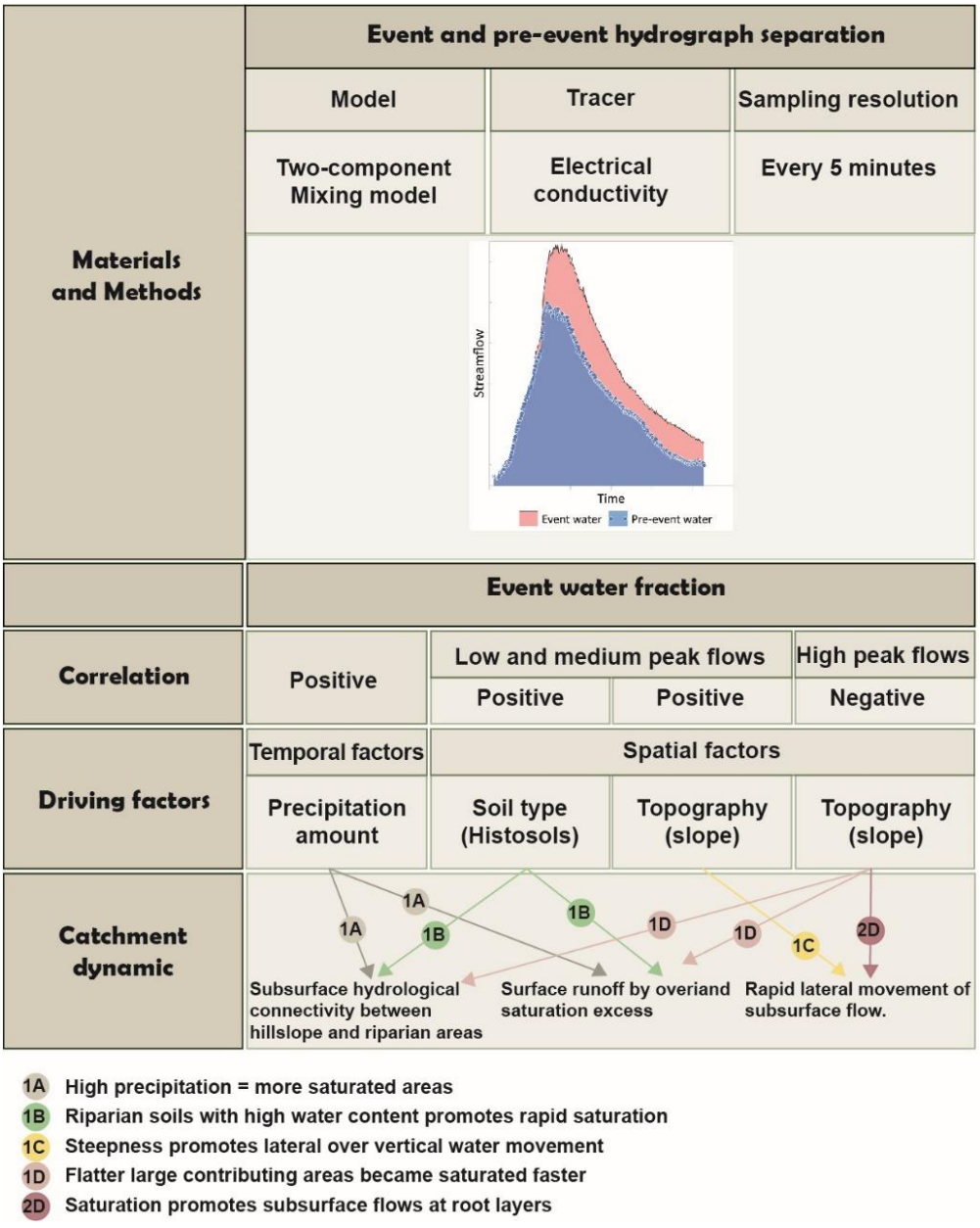

Fig. 5.3. Graphical scheme of the factors controlling the event water fraction with their corresponding catchment dynamics and hydrological processes

This thesis helped to gain a deeper understanding of the hydrological processes identified also by other studies such as Mosquera, (2020) and Pesántez, (2023). They showed that the ZEO presented saturation hotspots of soil water storage that varies according to the catchment conditions. This is clearly related with the connectivity between saturation areas also identified by this study, which is controlled by the type of soils, the slopes within the catchment, and the amount of precipitation. The occurrence of this hotspots could be also responsible for the increase of Q_e at higher peak flows. The soils connectivity was also observed by their studies where the connectivity between riparian soils and hillslopes contribute to the runoff generation. Our study align with this finding as this connectivity increases the saturation of the soils and the occurrence of overland flow which increases the event water fraction at the catchment. The threshold behavior on the controlling factors during rainfall-runoff events helped to determine that the dominance of vertical flow paths on these soils observed by Mosquera, (2020) is replaced by a dominance of lateral flow at higher peak flows resulting from the connectivity between saturated areas and the hillslopes. This thesis also depicted the importance of high-resolution data as it helps to identify processes such as the aforementioned that are often missing at lower resolutions. The new knowledge presented at this thesis could only be obtained by the use of EC as a tracer which allowed the tracer sampling every 5 minutes These clearly shows that the findings identified in this study helped to increase our knowledge over hydrological processes and this could only be achieved by analyzing the catchment at event scale.

Overall, chapter 4 showed the great potential of the methodology developed in previous chapters using a high-temporal resolution that allows the gathering of vast amounts of data during longer periods to improve our knowledge of event-scale runoff generation processes. These findings highlight the opportunity to improve the understanding of catchment hydrological behavior at a scale event over the Andean paramo by bringing crucial information to improve soil conservation and water management practices.

5.2. Future research

The results obtained in this thesis helped to acquire high-resolution tracer data and the identification of spatial and temporal factors controlling event water fraction. These findings promote future research in many ways:

- **Electrical conductivity as a reliable tracer:** The findings of chapters 2 and 3 confirmed the great potential of electrical conductivity (EC) as an alternative tracer

regarding event and pre-event hydrograph separation, by providing 1-minute measurements intervals. This reduces the logistical and economical resources needed to maintain this type of monitoring on the long-term. This needs to be tested over different catchments even at the Andes where different features could greatly influence EC behavior. It would be highly valuable to study if this tracer could be used beyond hydrograph separation given its quasi-conservative behavior. For instance, the estimation of Mean Transit Times (MTT) using high-resolution data or a detailed characterization of different water sources during wet and dry seasons.

- **The ability to measure EC at high temporal and spatial resolution:** It can serve to reduce the uncertainty of tracer-aided hydrological models. This could lead to improving the identification of runoff generation processes by revealing sub-hourly processes that occur during rainfall-runoff events.
- **In event and pre-event flow partitioning:** An evaluation of hydrograph separation is needed to adequately select the pre-event concentration used in past studies. Several studies have been conducted using a single value to represent the pre-event water concentration for all the events analyzed (e.g., baseflow concentration). This thesis determined that a value should be selected for each event as it highly influences the results. Hence, further investigation is recommended by using high-resolution sampling techniques to determine which value should be used as event and pre-event concentrations over the Andean paramo.
- **Regarding hydrological models´ selection:** the results of chapter 4 have shown that the complexity of tracer-aided hydrological models used could be reduced depending on catchment characteristics. Further investigation is needed to guarantee that computational resources are allocated where most required. To gain a fully comprehension of catchment hydrological response and their processes involved, a multi-model approach should be implemented rather than using only one option. This will facilitate the evaluation of the catchment and to include the majority of the identified processes.
- **In determining hydrological thresholds at a event scale:** Following the results in chapter 4, we encourage further investigation to determine thresholds that occur at fast runoff response ecosystems such as Andean paramo. This high-resolution methodology showed the potential to identify thresholds that will not be discovered unless sub-hourly data were collected. The correct identification of these processes

is very important to improve water management programs, especially in the Andean ecosystems where most of the population downstream obtain their water supply.

- **Connectivity between saturated areas:** Chapter 4 showed the importance of the saturated areas dynamics at event scale; further investigation into this topic is hugely needed not only at Andean ecosystems but worldwide. This is highly important to improve our knowledge about catchment hydrological dynamics and help conservation programs to adequately allocate resources on critical zones that must be looked after. In addition, this will also help to improve model conceptualization, which will result in a better interpretation of catchment hydrological processes.
- **Effect of net radiation over event water fraction:** Net radiation over catchments influences the interception and evaporation rates at event scale and thus, affecting the effective precipitation. Hence, the understanding of its influence over event water fraction must be achieved as it could play an important role on catchment hydrological processes moreover as climate change could significantly change the net radiation and affect the runoff generation processes.

6. References

Akaike, H., 1974. A new look at the statistical model identification. IEEE Trans. Automat. Contr. 19, 716–723. doi:10.1109/TAC.1974.1100705

Ali, G.A., Roy, A.G., Turmel, M.-C., Courchesne, F., 2010. Source-to-stream connectivity assessment through end-member mixing analysis. J. Hydrol. 392, 119–135. doi:10.1016/j.jhydrol.2010.07.049

Aparecido, L.M.T., Teodoro, G.S., Mosquera, G., Brum, M., Barros, F. de V., Pompeu, P.V., Rodas, M., Lazo, P., Müller, C.S., Mulligan, M., Asbjornsen, H., Moore, G.W., Oliveira, R.S., 2018. Ecohydrological drivers of Neotropical vegetation in montane ecosystems. Ecohydrology e1932. doi:10.1002/eco.1932

Bansah, S., Ali, G., 2017. Evaluating the Effects of Tracer Choice and End-Member Definitions on Hydrograph Separation Results Across Nested, Seasonally Cold Watersheds. Water Resour. Res. 53, 8851–8871. doi:10.1002/2016WR020252

Bansah, S., Quaye-ballard, J., Andam-akorfu, S.A., Bam, E., Anornu, G.K., 2019. End-Member Selection in Two-Component Isotope-Based Hydrograph Separation. Open J. Mod. Hydrol. 9, 41–53. doi:10.4236/ojmh.2019.92003

Barthold, F.K., Turner, B.L., Elsenbeer, H., Zimmermann, A., 2017. A hydrochemical approach to quantify the role of return flow in a surface flow-dominated catchment. Hydrol. Process. 31, 1018–1033. doi:10.1002/hyp.11083

Barthold, F.K., Woods, R.A., 2015. Stormflow generation: A meta-analysis of field evidence from small, forested catchments. Water Resour. Res. 51, 3730–3753. doi:10.1002/2014WR016221

Benettin, P., Bailey, S.W., Campbell, J.L., Green, M.B., Rinaldo, A., Likens, G.E., McGuire, K.J., Botter, G., 2015. Linking water age and solute dynamics in streamflow at the Hubbard Brook Experimental Forest, NH, USA. Water Resour. Res. 51(11) 9256-9272. 51, 9256–9272. doi:10.1002/2015WR017552

Benettin, P., Van Der Velde, Y., Van Der Zee, S.E.A.T.M., Rinaldo, A., Botter, G., 2013. Chloride circulation in a lowland catchment and the formulation of transport by travel time distributions. Water Resour. Res. 49, 4619–4632. doi:10.1002/WRCR.20309

Berman, E.S.F., Gupta, M., Gabrielli, C., Garland, T., McDonnell, J.J., 2009. High-frequency field-deployable isotope analyzer for hydrological applications. Water Resour. Res. 45, 10201. doi:10.1029/2009WR008265

Beven, K., Binley, A., 1992. The future of distributed models: Model calibration and uncertainty prediction. Hydrol. Process. 6, 279–298. doi:10.1002/hyp.3360060305

Beven, K., Freer, J., 2001. Equifinality, data assimilation, and uncertainty estimation in mechanistic modelling of complex environmental systems using the GLUE methodology. J. Hydrol. 249, 11–29. doi:10.1016/S0022-1694(01)00421-8

Birkel, C., Dunn, S.M., Tetzlaff, D., Soulsby, C., 2010. Assessing the value of high-resolution isotope tracer data in the stepwise development of a lumped conceptual rainfall–runoff model. Hydrol. Process. 24, 2335–2348. doi:10.1002/HYP.7763

Birkel, C., Soulsby, C., 2015. Advancing tracer-aided rainfall-runoff modelling: a review of progress, problems and unrealised potential. Hydrol. Process. 29, 5227–5240. doi:10.1002/hyp.10594

Birkel, C., Soulsby, C., Tetzlaff, D., 2014. Developing a consistent process-based conceptualization of catchment functioning using measurements of internal state variables. Water Resour. Res. 50, 3481–3501. doi:10.1002/2013WR014925

Birkel, C., Soulsby, C., Tetzlaff, D., Dunn, S., Spezia, L., 2012. High-frequency storm event isotope sampling reveals time-variant transit time distributions and influence of diurnal cycles. Hydrol. Process. 26, 308–316. doi:10.1002/hyp.8210

Birkel, C., Tetzlaff, D., Dunn, S.M., Soulsby, C., 2011. Using lumped conceptual rainfall–runoff models to simulate daily isotope variability with fractionation in a nested mesoscale catchment. Adv. Water Resour. 34, 383–394. doi:10.1016/J.ADVWATRES.2010.12.006

Blume, T., Zehe, E., Bronstert, A., 2008. Investigation of runoff generation in a pristine, poorly gauged catchment in the Chilean Andes II: Qualitative and quantitative use of tracers at three spatial scales. Hydrol. Process. 22, 3676–3688. doi:10.1002/HYP.6970

Bonell, M., Pearce, A.J., Stewart, M.K., 1990. The identification of runoff-production

mechanisms using environmental isotopes in a tussock grassland catchment, eastern otago, New Zealand. Hydrol. Process. 4, 15–34. doi:10.1002/HYP.3360040103

Brocca, L., Melone, F., Moramarco, T., Singh, V.P., 2009. Assimilation of Observed Soil Moisture Data in Storm Rainfall-Runoff Modeling. J. Hydrol. Eng. 14, 153–165. doi:10.1061/(ASCE)1084-0699(2009)14:2(153)

Brown, V.A., McDonnell, J.J., Burns, D.A., Kendall, C., 1999. The role of event water, a rapid shallow flow component, and catchment size in summer stormflow. J. Hydrol. 217, 171–190. doi:10.1016/S0022-1694(98)00247-9

Buttle, J., 2006. Mapping first-order controls on streamflow from drainage basins: the T 3 template. Hydrol. Process. 20, 3415–3422. doi:10.1002/hyp.6519

Buttle, J.M., 1994. Isotope hydrograph separations and rapid delivery of pre-event water from drainage basins. Prog. Phys. Geogr. Earth Environ. 18, 16–41. doi:10.1177/030913339401800102

Camacho Suarez, V. V, Saraiva Okello, A.M.L., Wenninger, J.W., Uhlenbrook, S., Suarez, C., 2015. Understanding runoff processes in a semi-arid environment through isotope and hydrochemical hydrograph separations. Hydrol. Earth Syst. Sci 19, 4183–4199. doi:10.5194/hess-19-4183-2015

Cano-Paoli, K., Chiogna, G., Bellin, A., 2019. Convenient use of electrical conductivity measurements to investigate hydrological processes in Alpine headwaters. Sci. Total Environ. 685, 37–49. doi:10.1016/J.SCITOTENV.2019.05.166

Carey, S.K., Tetzlaff, D., Buttle, J., Laudon, H., McDonnell, J., McGuire, K., Seibert, J., Soulsby, C., Shanley, J., 2013. Use of color maps and wavelet coherence to discern seasonal and interannual climate influences on streamflow variability in northern catchments. Water Resour. Res. 49, 6194–6207. doi:10.1002/wrcr.20469

Carrillo-Rojas, G., Silva, B., Córdova, M., Célleri, R., Bendix, J., 2016. Dynamic Mapping of Evapotranspiration Using an Energy Balance-Based Model over an Andean Páramo Catchment of Southern Ecuador. Remote Sens. 8, 160. doi:10.3390/rs8020160

Cartwright, I., Gilfedder, B., Hofmann, H., 2014. Contrasts between estimates of baseflow help discern multiple sources of water contributing to rivers. Hydrol. Earth Syst. Sci.

18, 15–30. doi:10.5194/HESS-18-15-2014

Cartwright, I., Morgenstern, U., 2018. Using tritium and other geochemical tracers to address the “old water paradox” in headwater catchments. J. Hydrol. 563, 13–21. doi:10.1016/j.jhydrol.2018.05.060

Casper, M.C., Volkmann, H.N., Waldenmeyer, G., Plate, E.J., 2003. The separation of flow pathways in a sandstone catchment of the Northern Black Forest using DOC and a nested Approach. Phys. Chem. Earth, Parts A/B/C 28, 269–275. doi:10.1016/S1474-7065(03)00037-8

Cayuela, C., Latron, J., Geris, J., Llorens, P., 2019. Spatio-temporal variability of the isotopic input signal in a partly forested catchment: Implications for hydrograph separation. Hydrol. Process. 33, 36–46. doi:10.1002/hyp.13309

Célleri, R., Feyen, J., 2009. The Hydrology of Tropical Andean Ecosystems: Importance, Knowledge Status, and Perspectives. Mt. Res. Dev. 29, 350–355. doi:10.1659/mrd.00007

Cey, E.E., Rudolph, D.L., Parkin, G.W., Aravena, R., 1998. Quantifying groundwater discharge to a small perennial stream in southern Ontario, Canada. J. Hydrol. 210, 21–37. doi:10.1016/S0022-1694(98)00172-3

Chapman, T., 1999. A comparison of algorithms for stream flow recession and baseflow separation. Hydrol. Process. 13, 701–714. doi:10.1002/(SICI)1099-1085(19990415)13:5<701::AID-HYP774>3.0.CO;2-2

Christophersen, N., Hooper, R.P., 1992. Multivariate analysis of stream water chemical data: The use of principal components analysis for the end-member mixing problem. Water Resour. Res. 28, 99–107. doi:10.1029/91WR02518

Correa, A., Breuer, L., Crespo, P., Célleri, R., Feyen, J., Birkel, C., Silva, C., Windhorst, D., 2019. Spatially distributed hydro-chemical data with temporally high-resolution is needed to adequately assess the hydrological functioning of headwater catchments. Sci. Total Environ. 651, 1613–1626. doi:10.1016/J.SCITOTENV.2018.09.189

Correa, A., Windhorst, D., Crespo, P., Célleri, R., Feyen, J., Breuer, L., 2016. Continuous versus event-based sampling: how many samples are required for deriving general hydrological understanding on Ecuador’s páramo region? Hydrol. Process. 30, 4059–

4073. doi:10.1002/hyp.10975

Correa, A., Windhorst, D., Tetzlaff, D., Crespo, P., Célleri, R., Feyen, J., Breuer, L., 2017. Temporal dynamics in dominant runoff sources and flow paths in the Andean Páramo. Water Resour. Res. 53, 5998–6017. doi:10.1002/2016WR020187

Cras, A., Marc, V., Travi, Y., 2007. Hydrological behaviour of sub-Mediterranean alpine headwater streams in a badlands environment. J. Hydrol. 339, 130–144. doi:10.1016/J.JHYDROL.2007.03.004

Crawford, J., Hughes, C.E., Parkes, S.D., 2013. Is the isotopic composition of event based precipitation driven by moisture source or synoptic scale weather in the Sydney Basin, Australia? J. Hydrol. 507, 213–226. doi:10.1016/J.JHYDROL.2013.10.031

Crespo, P.J., Feyen, J., Buytaert, W., Bücker, A., Breuer, L., Frede, H.-G., Ramírez, M., 2011. Identifying controls of the rainfall–runoff response of small catchments in the tropical Andes (Ecuador). J. Hydrol. 407, 164–174. doi:10.1016/j.jhydrol.2011.07.021

Delavau, C.J., Stadnyk, T., Holmes, T., 2017. Examining the impacts of precipitation isotope input δ18Oppt) on distributed, tracer-aided hydrological modelling. Hydrol. Earth Syst. Sci. 21, 2595–2614. doi:10.5194/HESS-21-2595-2017

Delsman, J.R., Essink, G.H.P.O., Beven, K.J., Stuyfzand, P.J., 2013. Uncertainty estimation of end-member mixing using generalized likelihood uncertainty estimation (GLUE), applied in a lowland catchment. Water Resour. Res. 49, 4792–4806. doi:10.1002/WRCR.20341

Demand, D., Blume, T., Weiler, M., 2019. Spatio-temporal relevance and controls of preferential flow at the landscape scale. Hydrol. Earth Syst. Sci. 23, 4869–4889. doi:10.5194/hess-23-4869-2019

Detty, J.M., McGuire, K.J., 2010. Threshold changes in storm runoff generation at a till-mantled headwater catchment. Water Resour. Res. 46. doi:10.1029/2009WR008102

DeWalle, D.R., Edwards, P.J., Swistock, B.R., Aravena, R., Drimmie, R.J., 1997. Seasonal isotope hydrology of three Appalachian forest catchments. Hydrol. Process. 11, 1895–1906. doi:10.1002/(SICI)1099-1085(199712)11:15<1895::AID-HYP538>3.3.CO;2-R

Didszun, J., Uhlenbrook, S., 2008. Scaling of dominant runoff generation processes: Nested catchments approach using multiple tracers. Water Resour. Res. 44. doi:10.1029/2006WR005242

Dunkerley, D., 2008. Identifying individual rain events from pluviograph records: a review with analysis of data from an Australian dryland site. Hydrol. Process. 22, 5024–5036. doi:10.1002/hyp.7122

Dunn, S.M., Freer, J., Weiler, M., Kirkby, M.J., Seibert, J., Quinn, P.F., Lischeid, G., Tetzlaff, D., Soulsby, C., 2008. Conceptualization in catchment modelling: simply learning? Hydrol. Process. 22, 2389–2393. doi:10.1002/hyp.7070

Durand, P., Neal, M., Neal, C., 1993. Variations in stable oxygen isotope and solute concentrations in small submediterranean montane streams. J. Hydrol. 144, 283–290. doi:10.1016/0022-1694(93)90176-A

Ebrahimi, S., Azizi, K., Khorram, M., Kashani, A.R., Ali, A.S.A., 2024. Evaluation of hydrological variabilities of water quality models considering event-based scenarios: A case study. Stoch. Environ. Res. Risk Assess. 38, 2425–2449. doi:https://doi.org/10.1007/s00477-024-02687-2

Esquivel-Hernández, G., Mosquera, G.M., Sánchez-Murillo, R., Quesada-Román, A., Birkel, C., Crespo, P., Célleri, R., Windhorst, D., Breuer, L., Boll, J., 2019. Moisture transport and seasonal variations in the stable isotopic composition of rainfall in Central American and Andean Páramo during El Niño conditions (2015–2016). Hydrol. Process. 33, 1802–1817. doi:10.1002/hyp.13438

Fenicia, F., McDonnell, J.J., Savenije, H.H.G., 2008. Learning from model improvement: On the contribution of complementary data to process understanding. Water Resour. Res. 44. doi:10.1029/2007WR006386

Fischer, B.M.C., Rinderer, M., Schneider, P., Ewen, T., Seibert, J., 2015. Contributing sources to baseflow in pre-alpine headwaters using spatial snapshot sampling. Hydrol. Process. 29, 5321–5336. doi:10.1002/HYP.10529

Fischer, Benjamin M. C., Stähli, M., Seibert, J., 2017. Pre-event water contributions to runoff events of different magnitude in pre-alpine headwaters. Hydrol. Res. 48, 28–47. doi:10.2166/nh.2016.176

Fischer, Benjamin M.C., van Meerveld, H.J. (Ilja), Seibert, J., 2017. Spatial variability in the isotopic composition of rainfall in a small headwater catchment and its effect on hydrograph separation. J. Hydrol. 547, 755–769. doi:10.1016/j.jhydrol.2017.01.045

Floury, P., Gaillardet, J., Gayer, E., Bouchez, J., Tallec, G., Ansart, P., Koch, F., Gorge, C., Blanchouin, A., Roubaty, J.L., 2017. The potamochemical symphony: New progress in the high-frequency acquisition of stream chemical data. Hydrol. Earth Syst. Sci. 21, 6153–6165. doi:10.5194/HESS-21-6153-2017

Forster, M.R., 2000. Key concepts in model selection: Performance and generalizability. J. Math. Psychol. 44, 205–231. doi:10.1006/JMPS.1999.1284

Genereux, D., 1998. Quantifying uncertainty in tracer-based hydrograph separations. Water Resour. Res. 34, 915–919. doi:doi:10.1029/98WR00010

Geris, J., Tetzlaff, D., McDonnell, J.J., Soulsby, C., 2017. Spatial and temporal patterns of soil water storage and vegetation water use in humid northern catchments. Sci. Total Environ. 595, 486–493. doi:10.1016/j.scitotenv.2017.03.275

Geris, J., Tetzlaff, D., Soulsby, C., 2015. Resistance and resilience to droughts: hydropedological controls on catchment storage and run-off response. Hydrol. Process. 29, 4579–4593. doi:10.1002/hyp.10480

Goller, R., Wilcke, W., Leng, M.J., Tobschall, H.J., Wagner, K., Valarezo, C., Zech, W., 2005. Tracing water paths through small catchments under a tropical montane rain forest in south Ecuador by an oxygen isotope approach. J. Hydrol. 308, 67–80. doi:10.1016/j.jhydrol.2004.10.022

Gomi, T., Asano, Y., Uchida, T., Onda, Y., Sidle, R.C., Miyata, S., Kosugi, K., Mizugaki, S., Fukuyama, T., Fukushima, T., 2010. Evaluation of storm runoff pathways in steep nested catchments draining a Japanese cypress forest in central Japan: a geochemical approach. Hydrol. Process. 24, 550–566. doi:10.1002/hyp.7550

Gonzales, A.L., Nonner, J., Heijkers, J., Uhlenbrook, S., 2009. Comparison of different base flow separation methods in a lowland catchment. Hydrol. Earth Syst. Sci. 13, 2055–2068. doi:10.5194/HESS-13-2055-2009

Gou, J., Qu, S., Shi, P., Li, D., Chen, X., Wang, Y., Shan, S., Si, W., 2018. Application of Stable Isotope Tracer to Study Runoff Generation during Different Types of Rainfall

Events. Water 2018, Vol. 10, Page 538 10, 538. doi:10.3390/W10050538

Guallpa, M., Célleri, R., Crespo, P., 2022. Efecto del coeficiente teórico de descarga de vertederos sobre la medición de caudales en pequeños ríos Andinos. La Granja 36. doi:10.17163/LGR.N36.2022.06

Guastini, E., Zuecco, G., Errico, A., Castelli, G., Bresci, E., Preti, F., Penna, D., 2019. How does streamflow response vary with spatial scale? Analysis of controls in three nested Alpine catchments. J. Hydrol. 570, 705–718. doi:10.1016/j.jhydrol.2019.01.022

Gupta, H. V., Kling, H., Yilmaz, K.K., Martinez, G.F., 2009. Decomposition of the mean squared error and NSE performance criteria: Implications for improving hydrological modelling. J. Hydrol. 377, 80–91. doi:10.1016/j.jhydrol.2009.08.003

Hamel, P., Riveros-Iregui, D., Ballari, D., Browning, T., Célleri, R., Chandler, D., Chun, K.P., Destouni, G., Jacobs, S., Jasechko, S., Johnson, M., Krishnaswamy, J., Poca, M., Pompeu, P.V., Rocha, H., 2017. Watershed services in the humid tropics: Opportunities from recent advances in ecohydrology. Ecohydrology e1921. doi:10.1002/eco.1921

Harman, C.J., 2015. Time-variable transit time distributions and transport: Theory and application to storage-dependent transport of chloride in a watershed. Water Resour. Res. 51, 1–30. doi:10.1002/2014WR015707

Hayashi, M., Vogt, T., Mächler, L., Schirmer, M., 2012. Diurnal fluctuations of electrical conductivity in a pre-alpine river: Effects of photosynthesis and groundwater exchange. J. Hydrol. 450–451, 93–104. doi:10.1016/J.JHYDROL.2012.05.020

Herbstritt, B., Gralher, B., Weiler, M., 2019. Continuous, near-real-time observations of water stable isotope ratios during rainfall and throughfall events. Hydrol. Earth Syst. Sci. 23, 3007–3019. doi:10.5194/HESS-23-3007-2019

Hoeg, S., Uhlenbrook, S., Leibundgut, C., 2000. Hydrograph separation in a mountainous catchment ? combining hydrochemical and isotopic tracers. Hydrol. Process. 14, 1199–1216. doi:10.1002/(SICI)1099-1085(200005)14:7<1199::AID-HYP35>3.0.CO;2-K

Hollander, M., Wolfe, D.A., Chicken, E., 2013. Nonparametric statistical methods, Wiley Series in Probability and Statistics. Wiley.

Hooper, R.P., Shoemaker, C.A., 1986. A Comparison of Chemical and Isotopic Hydrograph Separation. Water Resour. Res. 22, 1444–1454. doi:10.1029/WR022i010p01444

Hrachowitz, M., Bohte, R., Mul, M.L., Bogaard, T.A., Savenije, H.H.G., Uhlenbrook, S., 2011. On the value of combined event runoff and tracer analysis to improve understanding of catchment functioning in a data-scarce semi-arid area. Hydrol. Earth Syst. Sci. 15, 2007–2024. doi:10.5194/hess-15-2007-2011

Inamdar, S.P., Mitchell, M.J., 2007. Contributions of riparian and hillslope waters to storm runoff across multiple catchments and storm events in a glaciated forested watershed. J. Hydrol. 341, 116–130. doi:10.1016/j.jhydrol.2007.05.007

IUSS Working Group WRB, 2015. World Reference Base for Soil Resources 2014, update 2015. International soil classification system for naming soils and creating legends for soil maps. World Soil Resources Reports No. 106. FAO Rome.

Iwagami, S., Tsujimura, M., Onda, Y., Shimada, J., Tanaka, T., 2010. Role of bedrock groundwater in the rainfall-runoff process in a small headwater catchment underlain by volcanic rock. Hydrol. Process. 24, 2771–2783. doi:10.1002/hyp.7690

Iwasaki, K., Katsuyama, M., Tani, M., 2015. Contributions of bedrock groundwater to the upscaling of storm-runoff generation processes in weathered granitic headwater catchments. Hydrol. Process. 29, 1535–1548. doi:10.1002/hyp.10279

Iwasaki, K., Katsuyama, M., Tani, M., 2020. Factors affecting dominant peak-flow runoff-generation mechanisms among five neighbouring granitic headwater catchments. Hydrol. Process. 34, 1154–1166. doi:10.1002/hyp.13656

Jakeman, A.J., Hornberger, G.M., 1993. How much complexity is warranted in a rainfall-runoff model? Water Resour. Res. 29, 2637–2649. doi:10.1029/93WR00877

James, A.L., Roulet, N.T., 2009. Antecedent moisture conditions and catchment morphology as controls on spatial patterns of runoff generation in small forest catchments. J. Hydrol. 377, 351–366. doi:10.1016/J.JHYDROL.2009.08.039

Jencso, K.G., McGlynn, B.L., 2011. Hierarchical controls on runoff generation: Topographically driven hydrologic connectivity, geology, and vegetation. Water Resour. Res. 47, 11527. doi:10.1029/2011WR010666

Jencso, K.G., McGlynn, B.L., Gooseff, M.N., Bencala, K.E., Wondzell, S.M., 2010. Hillslope hydrologic connectivity controls riparian groundwater turnover: Implications of catchment structure for riparian buffering and stream water sources. Water Resour. Res. 46, 10524. doi:10.1029/2009WR008818

Johnson, K., Harpold, A., Carroll, R.W.H., Barnard, H., Raleigh, M.S., Segura, C., Li, L., Williams, K.H., Dong, W., Sullivan, P.L., 2023. Leveraging Groundwater Dynamics to Improve Predictions of Summer Low-Flow Discharges. Water Resour. Res. 59. doi:10.1029/2023WR035126

Kendall, C., McDonnell, J.J., 1998. Isotope tracers in catchment hydrology. Elsevier.

Kiewiet, L., van Meerveld, I., Seibert, J., 2020. Effects of Spatial Variability in the Groundwater Isotopic Composition on Hydrograph Separation Results for a Pre-Alpine Headwater Catchment. Water Resour. Res. 56, e2019WR026855. doi:10.1029/2019WR026855

Kim, H., Cho, S.-H., Lee, D., Jung, Y.-Y., Kim, Y.-H., Koh, D.-C., Lee, J., 2017. Influence of pre-event water on streamflow in a granitic watershed using hydrograph separation. Environ. Earth Sci. 76, 82. doi:10.1007/s12665-017-6402-6

Kirchner, J.W., Feng, X., Neal, C., Robson, A.J., 2004. The fine structure of water-quality dynamics: the (high-frequency) wave of the future. Hydrol. Process. 18, 1353–1359. doi:10.1002/HYP.5537

Klaus, J., McDonnell, J.J., 2013. Hydrograph separation using stable isotopes: Review and evaluation. J. Hydrol. 505, 47–64. doi:10.1016/j.jhydrol.2013.09.006

Krklec, K., Domínguez-Villar, D., Lojen, S., 2018. The impact of moisture sources on the oxygen isotope composition of precipitation at a continental site in central Europe. J. Hydrol. 561, 810–821. doi:10.1016/J.JHYDROL.2018.04.045

Lang, M., Ouarda, T.B.M.J., Bobée, B., 1999. Towards operational guidelines for over-threshold modeling. J. Hydrol. doi:10.1016/S0022-1694(99)00167-5

Larco, K., Mosquera, G.M., Jacobs, S.R., Cardenas, I., Crespo, P., 2023. Factors controlling the temporal variability of streamflow transit times in tropical alpine catchments. J. Hydrol. 617, 128990. doi:10.1016/J.JHYDROL.2022.128990

Laudon, H., Seibert, J., Köhler, S., Bishop, K., 2004. Hydrological flow paths during snowmelt: Congruence between hydrometric measurements and oxygen 18 in meltwater, soil water, and runoff. Water Resour. Res. 40. doi:10.1029/2003WR002455

Laudon, H., Sjöblom, V., Buffam, I., Seibert, J., Mörth, M., 2007. The role of catchment scale and landscape characteristics for runoff generation of boreal streams. J. Hydrol. 344, 198–209. doi:10.1016/j.jhydrol.2007.07.010

Laudon, H., Slaymaker, O., 1997. Hydrograph separation using stable isotopes, silica and electrical conductivity: an alpine example. J. Hydrol. 201, 82–101. doi:10.1016/S0022-1694(97)00030-9

Lazo, P.X., Mosquera, G.M., Cárdenas, I., Segura, C., Crespo, P., 2023. Flow partitioning modelling using high-resolution electrical conductivity data during variable flow conditions in a tropical montane catchment. J. Hydrol. 617, 128898. doi:10.1016/J.JHYDROL.2022.128898

Lazo, P.X., Mosquera, G.M., Cárdenas, I., Segura, C., Crespo, P., 2024. A simple mixing model using electrical conductivity yields robust hydrograph separation in a tropical montane catchment. J. Hydrol. 131632. doi:https://doi.org/10.1016/j.jhydrol.2024.131632

Lazo, P.X., Mosquera, G.M., McDonnell, J.J., Crespo, P., 2019. The role of vegetation, soils, and precipitation on water storage and hydrological services in Andean Páramo catchments. J. Hydrol. 572, 805–819. doi:10.1016/J.JHYDROL.2019.03.050

Leaney, F.W., Smettem, K.R.J., Chittleborough, D.J., 1993. Estimating the contribution of preferential flow to subsurface runoff from a hillslope using deuterium and chloride. J. Hydrol. 147, 83–103. doi:10.1016/0022-1694(93)90076-L

Lee, J.-Y., Shih, Y.-T., Lan, C.-Y., Lee, T.-Y., Peng, T.-R., Lee, C.-T., Huang, J.-C., 2020. Rainstorm Magnitude Likely Regulates Event Water Fraction and Its Transit Time in Mesoscale Mountainous Catchments: Implication for Modelling Parameterization. Water 12, 1169. doi:10.3390/w12041169

Linsley, R.K., Kohler, M.A., Paulhus, J.L.H., 1982. Hydrology for engineers. Third edition.

Litt, G.F., Gardner, C.B., Ogden, F.L., Lyons, W.B., 2015. Hydrologic tracers and

thresholds: A comparison of geochemical techniques for event-based stream hydrograph separation and flowpath interpretation across multiple land covers in the Panama Canal Watershed. Appl. Geochemistry 63, 507–518. doi:10.1016/J.APGEOCHEM.2015.04.003

Liu, F., Williams, M.W., Caine, N., 2004. Source waters and flow paths in an alpine catchment, Colorado Front Range, United States. Water Resour. Res. 40. doi:10.1029/2004WR003076

Lott, D.A., Stewart, M.T., 2016. Base flow separation: A comparison of analytical and mass balance methods. J. Hydrol. 535, 525–533. doi:10.1016/J.JHYDROL.2016.01.063

Lyon, S.W., Desilets, S.L.E., Troch, P.A., 2008. Characterizing the response of a catchment to an extreme rainfall event using hydrometric and isotopic data. Water Resour. Res. 44. doi:10.1029/2007WR006259

Maher, K., 2011. The role of fluid residence time and topographic scales in determining chemical fluxes from landscapes. Earth Planet. Sci. Lett. 312, 48–58. doi:10.1016/j.epsl.2011.09.040

Maloszewski, P., Zuber, A., 1996. Lumped parameter models for the interpretation of environmental tracer data, in Manual on Mathematical Models in Isotope Hydrogeology.

Marc, V., Didon-Lescot, J.F., Michael, C., 2001. Investigation of the hydrological processes using chemical and isotopic tracers in a small Mediterranean forested catchment during autumn recharge. J. Hydrol. 247, 215–229. doi:10.1016/S0022-1694(01)00386-9

McDonnell, J.J., Beven, K., 2014. Debates-The future of hydrological sciences: A (common) path forward? A call to action aimed at understanding velocities, celerities and residence time distributions of the headwater hydrograph. Water Resour. Res. 50, 5342–5350. doi:10.1002/2013WR015141

McDonnell, J.J., Bonell, M., Stewart, M.K., Pearce, A.J., 1990. Deuterium variations in storm rainfall: Implications for stream hydrograph separation. Water Resour. Res. 26, 455–458. doi:10.1029/WR026I003P00455

McGlynn, B.L., McDonnell, J.J., 2003. Quantifying the relative contributions of riparian and

hillslope zones to catchment runoff. Water Resour. Res. 39, n/a-n/a. doi:10.1029/2003WR002091

McGlynn, B.L., McDonnell, J.J., Seibert, J., Kendall, C., 2004. Scale effects on headwater catchment runoff timing, flow sources, and groundwater-streamflow relations. Water Resour. Res. 40. doi:10.1029/2003WR002494

McGuire, K.J., McDonnell, J.J., 2006. A review and evaluation of catchment transit time modeling. J. Hydrol. 330, 543–563. doi:10.1016/j.jhydrol.2006.04.020

McGuire, K.J., McDonnell, J.J., 2010. Hydrological connectivity of hillslopes and streams: Characteristic time scales and nonlinearities. Water Resour. Res. 46, 10543. doi:10.1029/2010WR009341

McGuire, K.J., Weiler, M., McDonnell, J.J., 2007. Integrating tracer experiments with modeling to assess runoff processes and water transit times. Adv. Water Resour. 30, 824–837. doi:10.1016/j.advwatres.2006.07.004

Mei, Y., Anagnostou, E.N., 2015. A hydrograph separation method based on information from rainfall and runoff records. J. Hydrol. 523, 636–649. doi:10.1016/J.JHYDROL.2015.01.083

Meriano, M., Howard, K.W.F., Eyles, N., 2011. The role of midsummer urban aquifer recharge in stormflow generation using isotopic and chemical hydrograph separation techniques. J. Hydrol. 396, 82–93. doi:10.1016/J.JHYDROL.2010.10.041

Merz, R., Blöschl, G., 2009. A regional analysis of event runoff coefficients with respect to climate and catchment characteristics in Austria. Water Resour. Res. 45. doi:10.1029/2008WR007163

Michel, C., Perrin, C., Andreassian, V., 2003. The exponential store: a correct formulation for rainfall—runoff modelling. Hydrol. Sci. J. 48, 109–124. doi:10.1623/hysj.48.1.109.43484

Michelon, A., Benoit, L., Beria, H., Ceperley, N., Schaefli, B., 2021. Benefits from high-density rain gauge observations for hydrological response analysis in a small alpine catchment. Hydrol. Earth Syst. Sci. 25, 2301–2325. doi:10.5194/hess-25-2301-2021

Miller, M.P., Susong, D.D., Shope, C.L., Heilweil, V.M., Stolp, B.J., 2014. Continuous

estimation of baseflow in snowmelt-dominated streams and rivers in the Upper Colorado River Basin: A chemical hydrograph separation approach. Water Resour. Res. 50, 6986–6999. doi:10.1002/2013WR014939

Monge-Salazar, M.J., Tovar, C., Cuadros-Adriazola, J., Baiker, J.R., Montesinos-Tubée, D.B., Bonnesoeur, V., Antiporta, J., Román-Dañobeytia, F., Fuentealba, B., Ochoa-Tocachi, B.F., Buytaert, W., 2022. Ecohydrology and ecosystem services of a natural and an artificial bofedal wetland in the central Andes. Sci. Total Environ. 838, 155968. doi:10.1016/j.scitotenv.2022.155968

Monteith, S.S., Buttle, J.M., Hazlett, P.W., Beall, F.D., Semkin, R.G., Jeffries, D.S., 2006. Paired-basin comparison of hydrologic response in harvested and undisturbed hardwood forests during snowmelt in central Ontario: II. Streamflow sources and groundwater residence times. Hydrol. Process. 20, 1117–1136. doi:10.1002/hyp.6073

Moore, R.B., 2004. Introduction to salt dilution gauging for streamflow measurement Part 2: Constant-rate injection. Streamline Watershed Manag. Blulletin 8, 11–15.

Morel, B., Durand, P., Jaffrézic, A., Gruau, G., Molenat, J., 2009. Sources of dissolved organic carbon during stormflow in a headwater agricultural catchment. Water Resour. Res. 23, 2888–2901. doi:https://doi.org/10.1002/hyp.7379

Mosquera, G., Lazo, P., Cárdenas, I., Crespo, P., 2012. Identificación de las principales fuentes de agua que aportan a la generación de escorrentía en zonas Andinas de páramo húmedo: mediante el uso de los isótopos estables deuterio (δ 2 H) y oxígeno-18 (δ 18 O). Maskana 3, 87–105.

Mosquera, G., Segura, C., Crespo, P., Mosquera, G.M., Segura, C., Crespo, P., 2018. Flow Partitioning Modelling Using High-Resolution Isotopic and Electrical Conductivity Data. Water 10, 904. doi:10.3390/w10070904

Mosquera, G.M., 2020. Disentangling water transport and tracer mixingmechanisms in mountainous environments influenced by volcanic features. PhD thesis. Universidad de Cuenca, Escuela Politécnica Nacional and Universidad Técnica Particular de Loja.

Mosquera, G.M., Célleri, R., Lazo, P.X., Vaché, K.B., Perakis, S.S., Crespo, P., 2016a. Combined use of isotopic and hydrometric data to conceptualize ecohydrological processes in a high-elevation tropical ecosystem. Hydrol. Process. 30, 2930–2947.

doi:10.1002/hyp.10927

Mosquera, G.M., Célleri, R., Lazo, P.X., Vaché, K.B., Perakis, S.S., Crespo, P., 2016b. Combined use of isotopic and hydrometric data to conceptualize ecohydrological processes in a high-elevation tropical ecosystem. Hydrol. Process. 30, 2930–2947. doi:10.1002/hyp.10927

Mosquera, G.M., Crespo, P., Breuer, L., Feyen, J., Windhorst, D., 2020. Water transport and tracer mixing in volcanic ash soils at a tropical hillslope: A wet layered sloping sponge. Hydrol. Process. 34, 2032–2047. doi:10.1002/HYP.13733

Mosquera, G.M., Franklin, M., Jan, F., Rolando, C., Lutz, B., David, W., Patricio, C., 2021. A field, laboratory, and literature review evaluation of the water retention curve of volcanic ash soils: How well do standard laboratory methods reflect field conditions? Hydrol. Process. 35. doi:10.1002/hyp.14011

Mosquera, G.M., Hofstede, R., Bremer, L.L., Asbjornsen, H., Carabajo-Hidalgo, A., Célleri, R., Crespo, P., Esquivel-Hernández, G., Feyen, J., Manosalvas, R., Marín, F., Mena-Vásconez, P., Montenegro-Díaz, P., Ochoa-Sánchez, A., Pesántez, J., Riveros-Iregui, D.A., Suárez, E., 2023. Frontiers in páramo water resources research: A multidisciplinary assessment. Sci. Total Environ. 892, 164373. doi:https://doi.org/10.1016/j.scitotenv.2023.164373

Mosquera, G.M., Lazo, P.X., Célleri, R., Wilcox, B.P., Crespo, P., 2015. Runoff from tropical alpine grasslands increases with areal extent of wetlands. CATENA 125, 120–128. doi:10.1016/j.catena.2014.10.010

Mosquera, G.M., Marín, F., Stern, M., Bonnesoeur, V., Ochoa-Tocachi, B.F., Román-Dañobeytia, F., Crespo, P., 2022. Progress in understanding the hydrology of high-elevation Andean grasslands under changing land use. Sci. Total Environ. 804, 150112. doi:10.1016/j.scitotenv.2021.150112

Mosquera, G.M., Segura, C., Vaché, K.B., Windhorst, D., Breuer, L., Crespo, P., 2016c. Insights into the water mean transit time in a high-elevation tropical ecosystem. Hydrol. Earth Syst. Sci. 20, 2987–3004. doi:10.5194/hess-20-2987-2016

Muñoz-Villers, L.E., McDonnell, J.J., 2012. Runoff generation in a steep, tropical montane cloud forest catchment on permeable volcanic substrate. Water Resour. Res. 48, n/a-

n/a. doi:10.1029/2011WR011316

Munyaneza, O., Wenninger, J., Uhlenbrook, S., 2012. Identification of runoff generation processes using hydrometric and tracer methods in a meso-scale catchment in Rwanda. Hydrol. Earth Syst. Sci. 16, 1991–2004. doi:10.5194/HESS-16-1991-2012

Nippgen, F., McGlynn, B.L., Emanuel, R.E., Vose, J.M., 2016. Watershed memory at the Coweeta Hydrologic Laboratory: The effect of past precipitation and storage on hydrologic response. Water Resour. Res. 52, 1673–1695. doi:https://doi.org/10.1002/2015WR018196

Nolan, K.M., Hill, B.R., 1990. Storm-runoff generation in the Permanente Creek drainage basin, west central California — An example of flood-wave effects on runoff composition. J. Hydrol. 113, 343–367. doi:10.1016/0022-1694(90)90183-X

Obradovic, M.M., Sklash, M.G., 1986. An isotopic and geochemical study of snowmelt runoff in a small arctic watershed. Hydrol. Process. 1, 15–30. doi:10.1002/HYP.3360010104

Ocampo, C.J., Oldham, C.E., Sivapalan, M., Turner, J. V., 2006. Hydrological versus biogeochemical controls on catchment nitrate export: a test of the flushing mechanism. Hydrol. Process. 20, 4269–4286. doi:10.1002/hyp.6311

Ochoa-Sánchez, A., Crespo, P., Célleri, R., 2018. Quantification of rainfall interception in the high Andean tussock grasslands. Ecohydrology e1946. doi:10.1002/eco.1946

Ochoa-Sánchez, A.E., Crespo, P., Carrillo-Rojas, G., Marín, F., Célleri, R., 2020. Unravelling evapotranspiration controls and components in tropical Andean tussock grasslands. Hydrol. Process. 34, 2117–2127. doi:10.1002/HYP.13716

Ogunkoya, O.O., Jenkins, A., 1993. Analysis of storm hydrograph and flow pathways using a three-component hydrograph separation model. J. Hydrol. 142, 71–88. doi:10.1016/0022-1694(93)90005-T

Ombadi, M., Risser, M.D., Rhoades, A.M., Varadharajan, C., 2023. A warming-induced reduction in snow fraction amplifies rainfall extremes. Nature 619, 305–310. doi:10.1038/s41586-023-06092-7

Onda, Y., Tsujimura, M., Fujihara, J., Ito, J., 2006. Runoff generation mechanisms in high-

relief mountainous watersheds with different underlying geology. J. Hydrol. 331, 659–673. doi:10.1016/j.jhydrol.2006.06.009

Orlowski, N., Kraft, P., Pferdmenges, J., Breuer, L., 2016. Exploring water cycle dynamics by sampling multiple stable water isotope pools in a developed landscape in Germany. Hydrol. Earth Syst. Sci. 20, 3873–3894. doi:10.5194/hess-20-3873-2016

Padrón, R.S., Wilcox, B.P., Crespo, P., Célleri, R., 2015. Rainfall in the Andean Páramo: New Insights from High-Resolution Monitoring in Southern Ecuador. J. Hydrometeorol. 16, 985–996. doi:10.1175/JHM-D-14-0135.1

Pearce, A.J., Stewart, M.K., Sklash, M.G., 1986. Storm Runoff Generation in Humid Headwater Catchments: 1. Where Does the Water Come From? Water Resour. Res. 22, 1263–1272. doi:10.1029/WR022i008p01263

Pellerin, B.A., Wollheim, W.M., Feng, X., Vörösmarty, C.J., 2008. The application of electrical conductivity as a tracer for hydrograph separation in urban catchments. Hydrol. Process. 22, 1810–1818. doi:10.1002/hyp.6786

Pelletier, A., Andréassian, V., 2020. Hydrograph separation: An impartial parametrisation for an imperfect method. Hydrol. Earth Syst. Sci. 24, 1171–1187. doi:10.5194/HESS-24-1171-2020

Penna, D., Meerveld, H.J. van, Oliviero, O., Zuecco, G., Assendelft, R.S., Fontana, G.D., Borga, M., 2015. Seasonal changes in runoff generation in a small forested mountain catchment. Hydrol. Process. 29, 2027–2042. doi:10.1002/HYP.10347

Penna, D., Stenni, B., Šanda, M., Wrede, S., Bogaard, T.A., Michelini, M., Fischer, B.M.C., Gobbi, A., Mantese, N., Zuecco, G., Borga, M., Bonazza, M., Sobotková, M., Čejková, B., Wassenaar, L.I., 2012. Technical note: Evaluation of between-sample memory effects in the analysis of δ2H and δ18O of water samples measured by laser spectroscopes. Hydrol. Earth Syst. Sci. 16, 3925–3933. doi:10.5194/hess-16-3925-2012

Penna, D., Tromp-van Meerveld, H.J., Gobbi, A., Borga, M., Dalla Fontana, G., 2011. The influence of soil moisture on threshold runoff generation processes in an alpine headwater catchment. Hydrol. Earth Syst. Sci. 15, 689–702. doi:10.5194/hess-15-689-2011

Pesántez, J., 2023. Bridging the gap between hydrological and biogeochemical processes in a high Andean catchment: a comprehensive tracer-aided model framework. PhD thesis. Universidad de Cuenca, Escuela Politécnica Nacional and Universidad Técnica Particular de Loja.

Pesántez, J., Birkel, C., Gaona, G., Arciniega-Esparza, S., Murray, D.S., Mosquera, G.M., Célleri, R., Mora, E., Crespo, P., 2023. Spatially distributed tracer-aided modelling to explore DOC dynamics, hot spots and hot moments in a tropical mountain catchment. Hydrol. Process. 37, e15020. doi:https://doi.org/10.1002/hyp.15020

Pesántez, J., Birkel, C., Mosquera, G.M., Peña, P., Arízaga-Idrovo, V., Mora, E., McDowell, W.H., Crespo, P., 2021. High-frequency multi-solute calibration using an in situ UV–visible sensor. Hydrol. Process. 35, e14357. doi:10.1002/HYP.14357

Pesántez, J., Mosquera, G.M., Crespo, P., Breuer, L., Windhorst, D., 2018. Effect of land cover and hydro-meteorological controls on soil water DOC concentrations in a high-elevation tropical environment. Hydrol. Process. 32, 2624–2635. doi:10.1002/hyp.13224

Petrone, K., Buffam, I., Laudon, H., 2007. Hydrologic and biotic control of nitrogen export during snowmelt: A combined conservative and reactive tracer approach. Water Resour. Res. 43. doi:10.1029/2006WR005286

Pfister, L., Kirchner, J.W., 2017. Debates—Hypothesis testing in hydrology: Theory and practice. Water Resour. Res. 53, 1792–1798. doi:10.1002/2016WR020116

Pinder, G.F., Jones, J.F., 1969. Determination of the ground-water component of peak discharge from the chemistry of total runoff. Water Resour. Res. 5, 438–445. doi:10.1029/WR005I002P00438

Pionke, H.B., Gburek, W.J., Folmar, G.J., 1993. Quantifying stormflow components in a Pennsylvania watershed when 18O input and storm conditions vary. J. Hydrol. 148, 169–187. doi:10.1016/0022-1694(93)90258-B

Potdar, A.S., Kirstetter, P.-E., Woods, D., Saharia, M., 2021. Toward Predicting Flood Event Peak Discharge in Ungauged Basins by Learning Universal Hydrological Behaviors with Machine Learning. J. Hydrometeorol. 22, 2971–2982. doi:10.1175/JHM-D-20-0302.1

Quichimbo, P., Tenorio, G., Borja, P., Cárdenas, I., Crespo, P., Célleri, R., 2012. Efectos sobre las propiedades físicas y químicas de los suelos por el cambio de la cobertura vegetal y uso del suelo: Páramo de Quimsacocha al sur del Ecuador. Suelos Ecuatoriales 42, 138–153.

Ramón, J., Correa, A., Timbe, E., Mosquera, G.M., Mora, E., Crespo, P., 2021. Do mixing models with different input requirement yield similar streamflow source contributions? Case study: A tropical montane catchment. Hydrol. Process. 35, e14209. doi:https://doi.org/10.1002/hyp.14209

Renshaw, C.E., Feng, X., Sinclair, K.J., Dums, R.H., 2003. The use of stream flow routing for direct channel precipitation with isotopically-based hydrograph separations: the role of new water in stormflow generation. J. Hydrol. 273, 205–216. doi:10.1016/S0022-1694(02)00392-X

Ribatet, M., Dutang, C., 2004. Generalized Pareto Distribution and Peaks Over Threshold.

Ribolzi, O., Vallès, V., Bariac, T., 1996. Comparison of Hydrograph Deconvolutions using Residual Alkalinity, Chloride, and Oxygen 18 as Hydrochemical Tracers. Water Resour. Res. 32, 1051–1059. doi:10.1029/95WR02967

Richardson, M., Ketcheson, S., Whittington, P., Price, J., 2012. The influences of catchment geomorphology and scale on runoff generation in a northern peatland complex. Hydrol. Process. 26, 1805–1817. doi:https://doi.org/10.1002/hyp.9322

Rinderer, M., van Meerveld, H.J., McGlynn, B.L., 2019. From Points to Patterns: Using Groundwater Time Series Clustering to Investigate Subsurface Hydrological Connectivity and Runoff Source Area Dynamics. Water Resour. Res. 55, 5784–5806. doi:10.1029/2018WR023886

Roa-García, M.C., Weiler, M., 2010. Integrated response and transit time distributions of watersheds by combining hydrograph separation and long-term transit time modeling. Hydrol. Earth Syst. Sci. 14, 1537–1549. doi:10.5194/hess-14-1537-2010

Rodhe, A., 1987. The origin of streamwater traced by oxygen-18. Uppsala University.

Rodríguez-Blanco, M.L., Taboada-Castro, M.M., Taboada-Castro, M.T., 2012. Rainfall–runoff response and event-based runoff coefficients in a humid area (northwest Spain). Hydrol. Sci. J. 57, 445–459.

doi:https://doi.org/10.1080/02626667.2012.666351

Romanowicz, R., 2010. An application of a log-transformed low-flow (LTLF) model to baseflow separation. https://doi.org/10.1080/02626667.2010.505172 55, 952–964. doi:10.1080/02626667.2010.505172

Sahraei, A., Kraft, P., Windhorst, D., Breuer, L., 2020. High-Resolution, In Situ Monitoring of Stable Isotopes of Water Revealed Insight into Hydrological Response Behavior. Water 12, 565. doi:10.3390/w12020565

Saraiva Okello, A.M.L., Uhlenbrook, S., Jewitt, G.P.W., Masih, I., Riddell, E.S., Van der Zaag, P., 2018. Hydrograph separation using tracers and digital filters to quantify runoff components in a semi-arid mesoscale catchment. Hydrol. Process. 32, 1334–1350. doi:10.1002/HYP.11491

Scaife, C.I., Band, L.E., 2017. Nonstationarity in threshold response of stormflow in southern Appalachian headwater catchments. Water Resour. Res. 53, 6579–6596. doi:10.1002/2017WR020376

Schiff, S.L., Devito, K.J., Elgood, R.J., McCrindle, P.M., Spoelstra, J., Dillon, P., 2002. Two adjacent forested catchments: Dramatically different NO 3 − export. Water Resour. Res. 38. doi:10.1029/2000WR000170

Schmeller, D.S., Loyau, A., Bao, K., Brack, W., Chatzinotas, A., De Vleeschouwer, F., Friesen, J., Gandois, L., Hansson, S. V., Haver, M., Le Roux, G., Shen, J., Teisserenc, R., Vredenburg, V.T., 2018. People, pollution and pathogens – Global change impacts in mountain freshwater ecosystems. Sci. Total Environ. 622–623, 756–763. doi:https://doi.org/10.1016/j.scitotenv.2017.12.006.

Segura, C., James, A.L., Lazzati, D., Roulet, N.T., 2012. Scaling relationships for event water contributions and transit times in small-forested catchments in Eastern Quebec. Water Resour. Res. 48, n/a-n/a. doi:10.1029/2012WR011890

Seibert, J., McDonnell, J.J., 2002. On the dialog between experimentalist and modeler in catchment hydrology: Use of soft data for multicriteria model calibration. Water Resour. Res. 38, 23-1-23–14. doi:10.1029/2001WR000978

Seibert, J., Staudinger, M., van Meerveld, H.J., 2019. Validation and over-parameterization—experiences from hydrological modeling. Comput. Simul. Valid.

Fundam. concepts, Methodol. Fram. Philos. Perspect. 811–834.

Seminario, S., 2016. INCERTIDUMBRE EN LA PRECIPITACIÓN ESPACIAL DIARIA CAUSADA POR REDES PLUVIOGRÁFICAS DISPERSAS EN UNA MICROCUENCA DE PÁRAMO DENSAMENTE MONITOREADA. Universidad de Cuenca.

Shanley, J.B., Kendall, C., Smith, T.E., Wolock, D.M., McDonnell, J.J., 2002. Controls on old and new water contributions to stream flow at some nested catchments in Vermont, USA. Hydrol. Process. 16, 589–609. doi:10.1002/hyp.312

Shope, C.L., 2016. Disentangling event-scale hydrologic flow partitioning in mountains of the Korean Peninsula under extreme precipitation. J. Hydrol. 538, 399–415. doi:10.1016/j.jhydrol.2016.04.050

Sklash, M.G., Farvolden, R.N., 1979. The role of groundwater in storm runoff. J. Hydrol. 43, 45–65. doi:10.1016/0022-1694(79)90164-1

Sklash, M.G., Farvolden, R.N., Fritz, P., 1976. A conceptual model of watershed response to rainfall, developed through the use of oxygen-18 as a natural tracer. Can. J. Earth Sci. 13, 271–283. doi:https://doi.org/10.1139/e76-029

Sklash, M.G., Stewart, M.K., Pearce, A.J., 1986. Storm Runoff Generation in Humid Headwater Catchments: 2. A Case Study of Hillslope and Low-Order Stream Response. Water Resour. Res. 22, 1273–1282. doi:10.1029/WR022I008P01273

Smakhtin, V.., 2001. Low flow hydrology: a review. J. Hydrol. 240, 147–186. doi:10.1016/S0022-1694(00)00340-1

Smith, A., Welch, C., Stadnyk, T., 2016. Assessment of a lumped coupled flow-isotope model in data scarce Boreal catchments. Hydrol. Process. 30, 3871–3884. doi:10.1002/hyp.10835

Soulsby, C., Birkel, C., Geris, J., Dick, J., Tunaley, C., Tetzlaff, D., 2015. Stream water age distributions controlled by storage dynamics and nonlinear hydrologic connectivity: Modeling with high-resolution isotope data. Water Resour. Res. 51, 7759–7776. doi:10.1002/2015WR017888

Soulsby, C., Piegat, K., Seibert, J., Tetzlaff, D., 2011. Catchment-scale estimates of flow path partitioning and water storage based on transit time and runoff modelling.

Hydrol. Process. 25, 3960–3976. doi:10.1002/hyp.8324

Sprent, P., 2011. Sign Test, in: International Encyclopedia of Statistical Science. Springer Berlin Heidelberg, Berlin, Heidelberg, pp. 1316–1317. doi:10.1007/978-3-642-04898-2_515

St Amour, N.A., Gibson, J.J., Edwards, T.W.D., Prowse, T.D., Pietroniro, A., 2005. Isotopic time-series partitioning of streamflow components in wetland-dominated catchments, lower Liard River basin, Northwest Territories, Canada. Hydrol. Process. 19, 3357–3381. doi:10.1002/HYP.5975

Stadnyk, T.A., Delavau, C., Kouwen, N., Edwards, T.W.D., 2013. Towards hydrological model calibration and validation: simulation of stable water isotopes using the isoWATFLOOD model. Hydrol. Process. 27, 3791–3810. doi:10.1002/HYP.9695

Stewart, M., Cimino, J., Ross, M., 2007. Calibration of Base Flow Separation Methods with Streamflow Conductivity. Groundwater 45, 17–27. doi:10.1111/J.1745-6584.2006.00263.X

Stockinger, M.P., Bogena, H.R., Lücke, A., Diekkrüger, B., Cornelissen, T., Vereecken, H., 2016. Tracer sampling frequency influences estimates of young water fraction and streamwater transit time distribution. J. Hydrol. 541, 952–964. doi:10.1016/J.JHYDROL.2016.08.007

Su, C.H., Costelloe, J.F., Peterson, T.J., Western, A.W., 2016. On the structural limitations of recursive digital filters for base flow estimation. Water Resour. Res. 52, 4745–4764. doi:10.1002/2015WR018067

Suecker, J.K., Ryan, J.N., Kendall, C., Jarrett, R.D., 2000. Determination of hydrologic pathways during snowmelt for alpine/subalpine basins, Rocky Mountain National Park, Colorado. Water Resour. Res. 36, 63–75. doi:10.1029/1999WR900296

Tayfur, G., Zucco, G., Brocca, L., Moramarco, T., 2014. Coupling soil moisture and precipitation observations for predicting hourly runoff at small catchment scale. J. Hydrol. 510, 363–371. doi:10.1016/j.jhydrol.2013.12.045

Tenelanda-Patiño, D., Crespo-Sánchez, P., Mosquera-Rojas, G., 2018. Umbrales en la respuesta de humedad del suelo a condiciones meteorológicas en una ladera Altoandina. Maskana 9, 53–65. doi:10.18537/mskn.09.02.07

Tetzlaff, D., Birkel, C., Dick, J., Geris, J., Soulsby, C., 2014. Storage dynamics in hydropedological units control hillslope connectivity, runoff generation, and the evolution of catchment transit time distributions. Water Resour. Res. 50, 969–985. doi:10.1002/2013WR014147

Tetzlaff, D., Buttle, J., Carey, S.K., McGuire, K., Laudon, H., Soulsby, C., 2015a. Tracer-based assessment of flow paths, storage and runoff generation in northern catchments: a review. Hydrol. Process. 29, 3475–3490. doi:10.1002/hyp.10412

Tetzlaff, D., Buttle, J., Carey, S.K., van Huijgevoort, M.H.J., Laudon, H., McNamara, J.P., Mitchell, C.P.J., Spence, C., Gabor, R.S., Soulsby, C., 2015b. A preliminary assessment of water partitioning and ecohydrological coupling in northern headwaters using stable isotopes and conceptual runoff models. Hydrol. Process. 29, 5153–5173. doi:10.1002/hyp.10515

Tetzlaff, D., Seibert, J., Soulsby, C., 2009. Inter-catchment comparison to assess the influence of topography and soils on catchment transit times in a geomorphic province; the Cairngorm mountains, Scotland. Hydrol. Process. 23, 1874–1886. doi:10.1002/hyp

Tetzlaff, D., Uhlenbrook, S., Eppert, S., Soulsby, C., 2008. Does the incorporation of process conceptualization and tracer data improve the structure and performance of a simple rainfall-runoff model in a Scottish mesoscale catchment? Hydrol. Process. 22, 2461–2474. doi:10.1002/hyp.6841

Timbe, E., Windhorst, D., Celleri, R., Timbe, L., Crespo, P., Frede, H.G., Feyen, J., Breuer, L., 2015. Sampling frequency trade-offs in the assessment of mean transit times of tropical montane catchment waters under semi-steady-state conditions. Hydrol. Earth Syst. Sci. 19, 1153–1168. doi:10.5194/HESS-19-1153-2015

Turner, J.V., Macpherson, D.K., Stokes, R.A., 1987. The mechanisms of catchment flow processes using natural variations in deuterium and oxygen-18. J. Hydrol. 94, 143–162. doi:10.1016/0022-1694(87)90037-0

Tweed, S., Munksgaard, N., Marc, V., Rockett, N., Bass, A., Forsythe, A.J., Bird, M.I., Leblanc, M., 2016. Continuous monitoring of stream δ18O and δ2H and stormflow hydrograph separation using laser spectrometry in an agricultural catchment. Hydrol.

Process. 30, 648–660. doi:10.1002/HYP.10689

U.S. Bureau of Reclamation, 2001. Water Measurement Manual. Washington DC.

Uber, M., Vandervaere, J.-P., Zin, I., Braud, I., Heistermann, M., Legoût, C., Molinié, G., Nord, G., 2018. How does initial soil moisture influence the hydrological response? A case study from southern France. Hydrol. Earth Syst. Sci. 22, 6127–6146. doi:10.5194/hess-22-6127-2018

Uchida, T., Kosugi, K., Mizuyama, T., 2001. Effects of pipeflow on hydrological process and its relation to landslide: a review of pipeflow studies in forested headwater catchments. Hydrol. Process. 15, 2151–2174. doi:10.1002/hyp.281

Uhlenbrook, S., Sieber, A., 2005. On the value of experimental data to reduce the prediction uncertainty of a process-oriented catchment model. Environ. Model. Softw. 20, 19–32. doi:10.1016/j.envsoft.2003.12.006

Vaché, K.B., McDonnell, J.J., 2006. A process-based rejectionist framework for evaluating catchment runoff model structure. Water Resour. Res. 42, 2409. doi:10.1029/2005WR004247

van Huijgevoort, M.H.J., Tetzlaff, D., Sutanudjaja, E.H., Soulsby, C., 2016. Using high resolution tracer data to constrain water storage, flux and age estimates in a spatially distributed rainfall-runoff model. Hydrol. Process. 30, 4761–4778. doi:10.1002/hyp.10902

van Kempen, G., van der Wiel, K., Melsen, L.A., 2021. The impact of hydrological model structure on the simulation of extreme runoff events. Nat. Hazards Earth Syst. Sci. 21, 961–976. doi:10.5194/nhess-21-961-2021

Vidon, P., Cuadra, P.E., 2010. Impact of precipitation characteristics on soil hydrology in tile-drained landscapes. Hydrol. Process. 24, 1821–1833. doi:10.1002/HYP.7627

von Freyberg, J., Studer, B., Kirchner, J.W., 2017. A lab in the field: high-frequency analysis of water quality and stable isotopes in stream water and precipitation. Hydrol. Earth Syst. Sci. 21, 1721–1739. doi:10.5194/hess-21-1721-2017

von Freyberg, J., Studer, B., Rinderer, M., Kirchner, J.W., 2018. Studying catchment storm response using event- and pre-event-water volumes as fractions of precipitation

rather than discharge. Hydrol. Earth Syst. Sci. 22, 5847–5865. doi:10.5194/hess-22-5847-2018

Wang, L., van Meerveld, H.J., Seibert, J., 2017. When should stream water be sampled to be most informative for event-based, multi-criteria model calibration? Hydrol. Res. 48, 1566–1584. doi:10.2166/nh.2017.197

Wang, L., van Meerveld, H.J., Seibert, J., 2018. Effect of Observation Errors on the Timing of the Most Informative Isotope Samples for Event-Based Model Calibration. Hydrol. 2018, Vol. 5, Page 4 5, 4. doi:10.3390/HYDROLOGY5010004

Wang, L., von Freyberg, J., van Meerveld, I., Seibert, J., Kirchner, J.W., 2019. What is the best time to take stream isotope samples for event-based model calibration? J. Hydrol. 577, 123950. doi:10.1016/J.JHYDROL.2019.123950

Weiler, M., McDonnell, J.J., Meerveld, I.T., Uchida, T., 2005. Subsurface Stormflow. Encycl. Hydrol. Sci. doi:10.1002/0470848944.HSA119

Weiler, M., McGlynn, B.L., McGuire, K.J., McDonnell, J.J., 2003. How does rainfall become runoff? A combined tracer and runoff transfer function approach. Water Resour. Res. 39, n/a-n/a. doi:10.1029/2003WR002331

Wen, H., Brantley, S.L., Davis, K.J., Duncan, J.M., Li, L., 2021. The Limits of Homogenization: What Hydrological Dynamics can a Simple Model Represent at the Catchment Scale? Water Resour. Res. 57, e2020WR029528. doi:10.1029/2020WR029528

Wilcoxon, F., 1945. Individual Comparisons by Ranking Methods. Biometrics Bull. 1, 80. doi:10.2307/3001968

Wilkinson, M.E., Bathurst, J.C., 2018. A multi-scale nested experiment for understanding flood wave generation across four orders of magnitude of catchment area. Hydrol. Res. 49, 597–615. doi:https://doi.org/10.2166/nh.2017.070

Willems, P., 2009. A time series tool to support the multi-criteria performance evaluation of rainfall-runoff models. Environ. Model. Softw. 24, 311–321. doi:10.1016/J.ENVSOFT.2008.09.005

Wittenberg, H., 1999. Baseflow recession and recharge as nonlinear storage processes.

Hydrol. Process. 13, 715–726. doi:10.1002/(SICI)1099-1085(19990415)13:5<715::AID-HYP775>3.0.CO;2-N

Wittenberg, H., Sivapalan, M., 1999. Watershed groundwater balance estimation using streamflow recession analysis and baseflow separation. J. Hydrol. 219, 20–33. doi:10.1016/S0022-1694(99)00040-2

Wright, C., Kagawa-Viviani, A., Gerlein-Safdi, C., Mosquera, G.M., Poca, M., Tseng, H., Chun, K.P., 2017. Advancing ecohydrology in the changing tropics: Perspectives from early career scientists. Ecohydrology e1918. doi:10.1002/eco.1918

Yang, W., Xiao, C., Liang, X., 2019. Technical note: Analytical sensitivity analysis and uncertainty estimation of baseflow index calculated by a two-component hydrograph separation method with conductivity as a tracer. Hydrol. Earth Syst. Sci. 23, 1103–1112. doi:10.5194/HESS-23-1103-2019

Zehe, E., Graeff, T., Morgner, M., Bauer, A., Bronstert, A., 2010. Plot and field scale soil moisture dynamics and subsurface wetness control on runoff generation in a headwater in the Ore Mountains. Hydrol. Earth Syst. Sci. 14, 873–889. doi:10.5194/hess-14-873-2010

Zhang, J., Zhang, Y., Song, J., Cheng, L., 2017. Evaluating relative merits of four baseflow separation methods in Eastern Australia. J. Hydrol. 549, 252–263. doi:10.1016/J.JHYDROL.2017.04.004

Zhiña, D.X., Mosquera, G.M., Esquivel-Hernández, G., Córdova, M., Sánchez-Murillo, R., Orellana-Alvear, J., Crespo, P., 2022. Hydrometeorological Factors Controlling the Stable Isotopic Composition of Precipitation in the Highlands of South Ecuador. J. Hydrometeorol. 23, 1059–1074. doi:10.1175/JHM-D-21-0180.1

Zimmer, M.A., Gannon, J.P., 2018. Run-off processes from mountains to foothills: The role of soil stratigraphy and structure in influencing run-off characteristics across high to low relief landscapes. Hydrol. Process. 32, 1546–1560. doi:https://doi.org/10.1002/hyp.11488

Zuecco, G., Rinderer, M., Penna, D., Borga, M., van Meerveld, H.J., 2019. Quantification of subsurface hydrologic connectivity in four headwater catchments using graph theory. Sci. Total Environ. 646, 1265–1280.

doi:https://doi.org/10.1016/j.scitotenv.2018.07.269

APPENDIX

Appendix 1. a) Volumetric sequential rainfall sampler located in the study site. The sampler was constructed using 4 plastic circular funnels (two of 250 mm diameter and two of 300 mm diameter) connected to ten 500 ml glass bottles. All bottles were sequentially connected by plastic tubes of 5 mm diameter. Each bottle had a glass pipette of 5 mm diameter introduced through their top while the rest of the bottle was hermetically sealed to prevent pressure decompensation. The top of the pipette was outside the glass bottle, while its bottom was inside at a level where the volume collected is 160 ml (corresponding to 1.12 mm of rainfall). Therefore, water entered the first bottle until reaching 160 ml volume, once the atmospheric pressure was equilibrated water was diverted into bottle 2 and so on until rain stopped or bottle 10 was filled. The latter almost never occurred, i.e., only 2 times during the 20 months monitoring period. The bottles were placed inside a wooden structure covered with aluminum foil and batting cotton for insulation to avoid isotopic fractionation due to evaporation, b) Sampler schematic representation showing: A-Glass bottle (500 ml volume), B-Plastic cap, C-glass pipette (5 mm diameter) to equilibrate atmospheric pressure , D-plastic tube (5 mm diameter) connecting the glass bottles in sequence, and E-Y connector).

a)

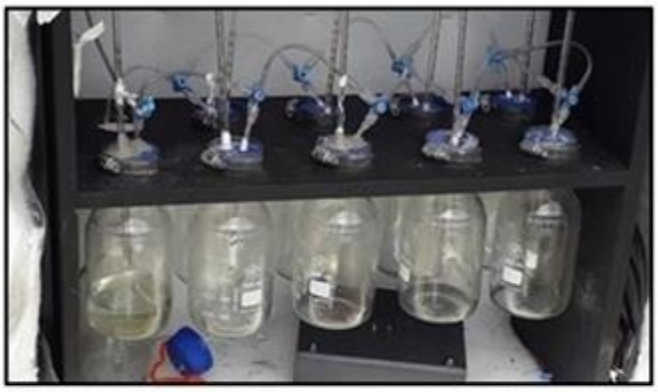

b)

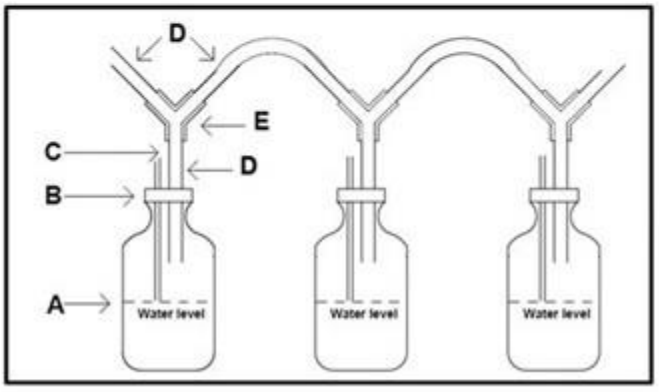

Appendix 2. Relationship between δ^2H and $\delta^{18}O$ values in precipitation water samples collected with the volumetric autosampler. Red line represents the long-term Local Meteoric Water Line for the study site obtained from Mosquera *et al*. (2016a)

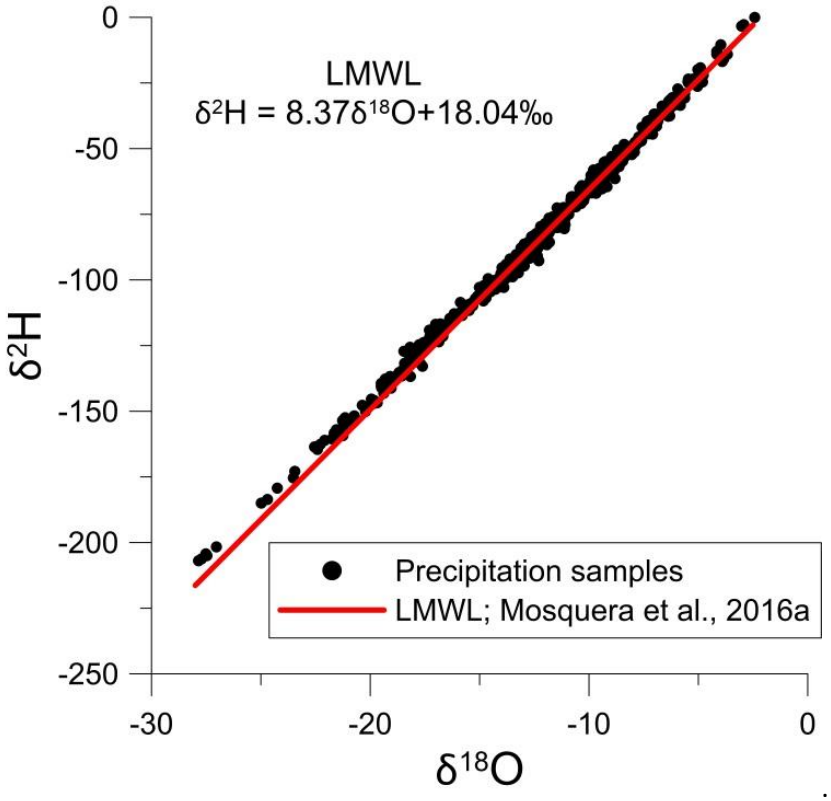

Appendix 3. Modules, equations, and parameters of the four Tracer-Based Streamflow Partitioning Analysis (TraSPAN) model structures. (Mosquera et al., 2018)

Module		Parameters and Equations		Units	Model Structure			
					1	2	3	4
1[a]	P_{eff}	Initial antecedent rainfall index, s_0		-	X	X	X	X
		Memory timescale parameter, ω		timesteps[d]	X	X	X	X
	Equations	$P_{eff}(t) = p(t)s(t)$	(1)					
		$s(t) = c \cdot p(t) - s(t-\Delta t)\left(1-\frac{1}{\omega}\right)$	(2)					
		where p is precipitation and c is the normalization constant to maintain $\sum P_{eff} = \sum Q$						
2[b]	f, constant	Fraction of effective rainfall routed as event water, f		-	X	X		
	f, variable	Normalization constant, c_f		h/mm			X	X
		Memory timescale parameter, ω_f		timesteps[d]			X	X
	Equations	$f(t) = c_f \cdot p(t) - f(t-\Delta t)\left(1-\frac{1}{\omega_f}\right)$	(3)					
3[c]	Single Reservoir	Mean transit time of event water, k_e		h	X		X	
		Time delay for the event fraction response, e_{lag}		h	X		X	
		Mean transit time of pre-event water, k_p		h	X		X	
		Time delay for the pre-event fraction response, p_{lag}		h	X		X	
	Equations	$Q_e(t) = \int_0^f h_e(\tau)P_{eff}(t-\tau)f(t-\tau)d\tau$	(4)					
		$Q_p(t) = \int_0^f h_p(\tau)P_{eff}(t-\tau)[1-f(t-\tau)]d\tau$	(5)					
		$h_e(\tau) = e_{lag} - \frac{1}{k_e}exp\left(\frac{\tau}{k_e}\right)$	(6)					
		$h_p(\tau) = e_{lag} - \frac{1}{k_p}exp\left(\frac{\tau}{k_p}\right)$	(7)					
		$C_t(t) = \frac{Q_e(t)C_e + Q_p(t)C_p}{Q_e+Q_p}$	(8)					
		where C_e is the tracer composition of event water (rainfall) and C_p is the tracer composition in pre-event water (e.g., baseflow prior to the rainstorm).						
	Two Parallel Reservoir	Fraction of water routed into the fast-responding reservoir of event water, q_e		-		X		X
		Mean transit time of the fast fraction of event water, k_{fe}		h		X		X
		Mean transit time of the slow fraction of event water, k_{se}		h		X		X
		Time delay for the event fraction response, e_{lag}		h		X		X
		Fraction of water routed into the fast-responding reservoir of pre-event water, q_p		-		X		X
		Mean transit time of the fast fraction of pre-event water, k_{fp}		h		X		X
		Mean transit time of the slow fraction of pre-event water, k_{sp}		h		X		X
		Time delay for the pre-event fraction response, p_{lag}		h		X		X
	Equations	$h_e(\tau) = -\frac{q_e}{k_{fe}}exp\left(-\frac{\tau-e_{lag}}{k_{fe}}\right) + \frac{1-q_e}{k_{se}}exp\left(\frac{\tau-e_{lag}}{k_{se}}\right)$	(9)					

$$h_p(\tau) = -\frac{q_p}{k_{fp}} exp\left(-\frac{\tau - p_{lag}}{k_{fp}}\right) + \frac{1-q_p}{k_{sp}} exp\left(\frac{\tau - p_{lag}}{k_{sp}}\right) \quad (10)$$

Equation (4), (5), and (8) are also used here.

Total number of parameters	7	11	8	12

Appendix 4. Pre-event water fractions (PEWs) estimated using model structures a) 1, b) 2, c) 3, and d) 4 and calibrated for Oxygen-18 (black dots) and electrical conductivity (EC; red dots). Vertical lines represent uncertainty in PEWs corresponding to the 5–95% confidence limits of the possible solutions from the parameter sets within the range of behavioral solutions.

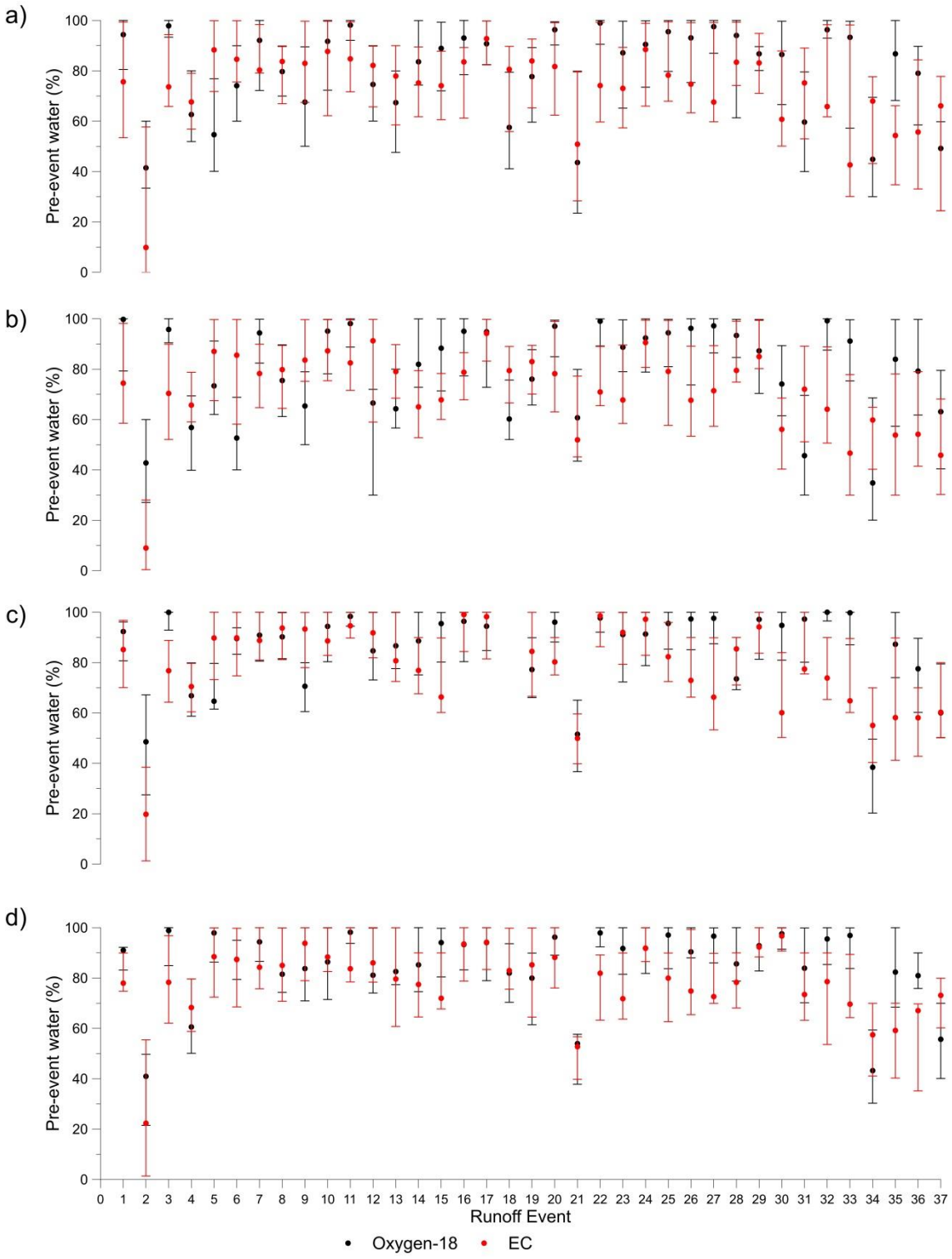

Appendix 5. Differences in pre-event water fractions (PEWs) estimated using Oxygen-18 and electrical conductivity for calibration of model structures a) 1, b) 2, c) 3, and d) 4. Dots represent the difference between the PEWs which produced the highest KGE vales for each tracer. Solid horizontal black line represents no difference (i.e., 0%). Dashed horizontal red lines represent the threshold for acceptable differences (±20%). Black vertical lines represent the differences in PEWs considering the estimated uncertainties determined for model calibration with each tracer (i.e., 5–95% confidence limits of behavioral solutions). The dots' colors correspond to events with 0 (red), 1 (black), and 2 (blue) water samples collected during peak flow. Sampling factor is equal to the total number of samples taken during an event divided by the duration of the event.

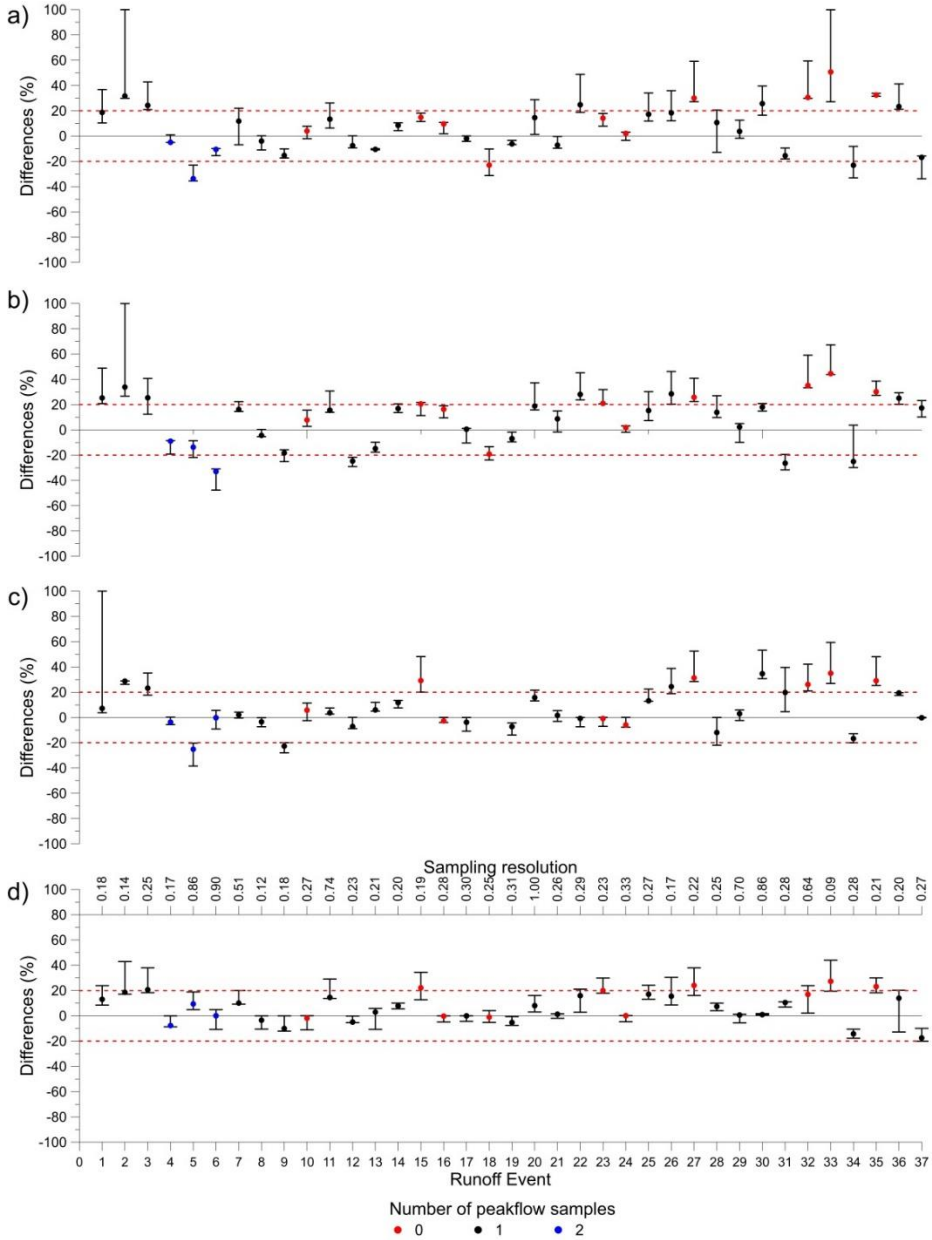

Appendix 6. Hydrograph separatioin performed during 37 rainfall-runoff events showing the pre-event water estimation obtained using the combination of C_e and C_p that showed the best results with $\delta^{18}O$ and EC. Error bars correspond to the uncertainty estimated by using the methodology proposed by Genereux (1998).

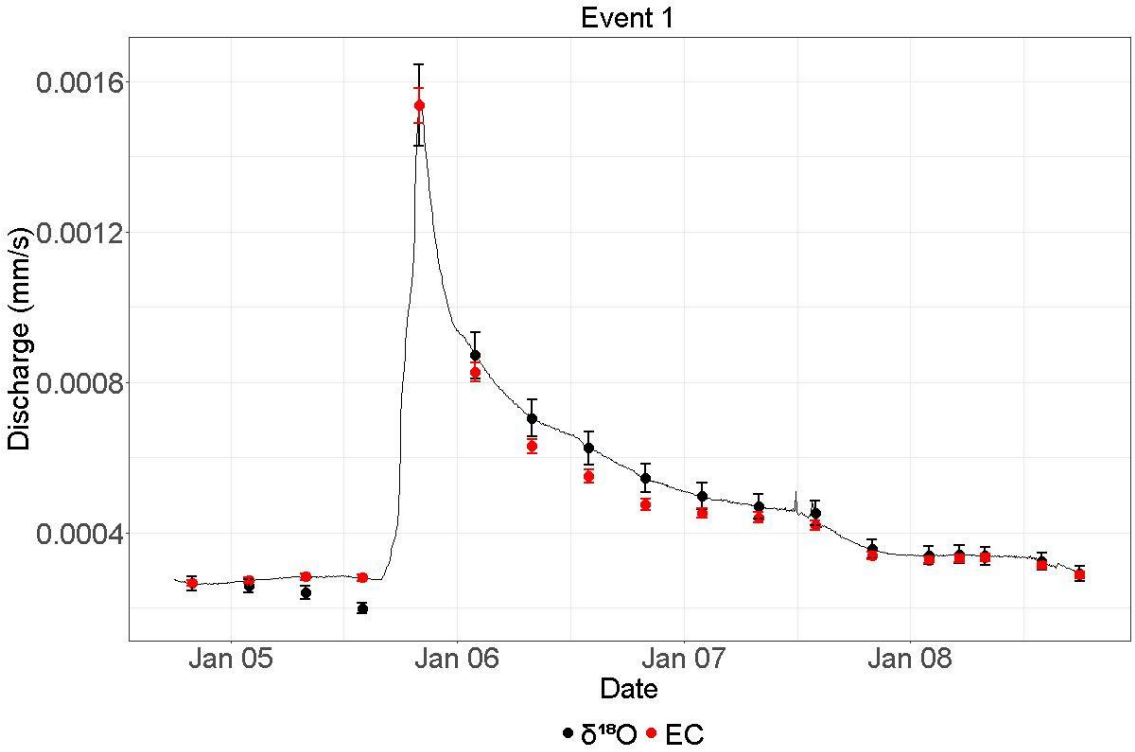

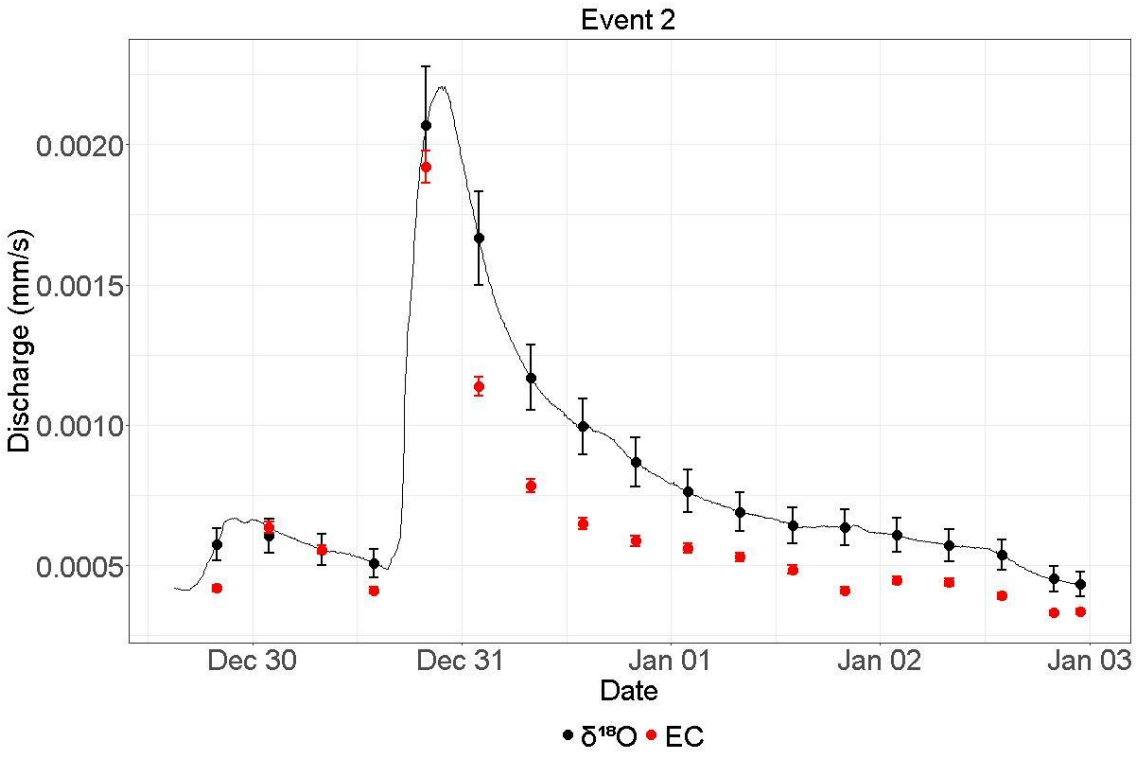
Event 2
0.0020
0.0015
0.0010
0.0005
Discharge (mm/s)
Dec 30
Dec 31
Jan 01
Jan 02
Jan 03
Date
δ¹⁸O
EC

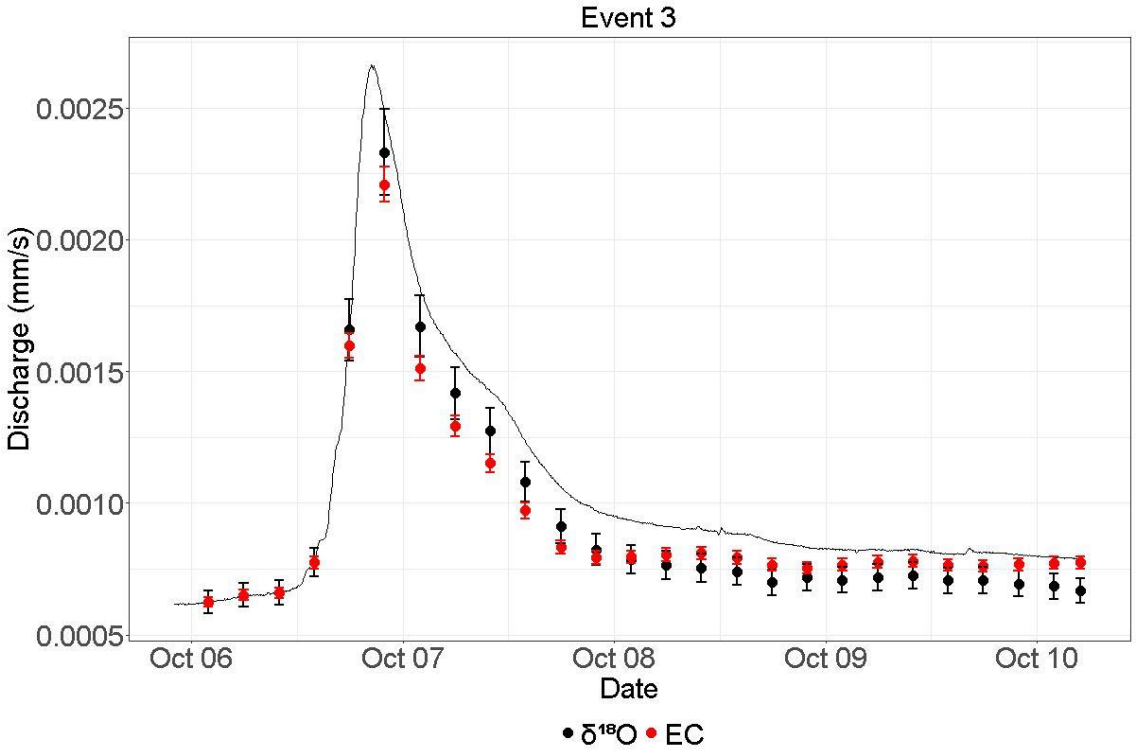
Event 3
0.0025
0.0020
0.0015
0.0010
0.0005
Discharge (mm/s)
Oct 06
Oct 07
Oct 08
Oct 09
Oct 10
Date
δ¹⁸O
EC

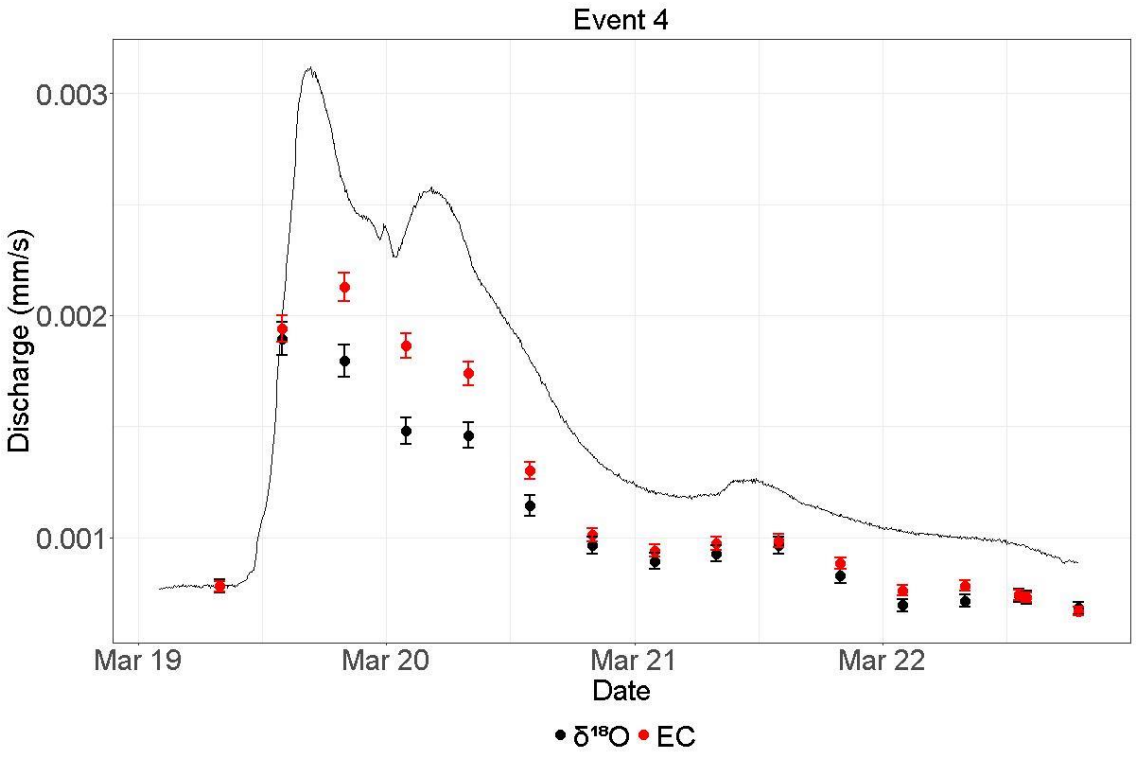
Event 4
0.003
0.002
0.001
Discharge (mm/s)
Mar 19
Mar 20
Mar 21
Mar 22
Date
δ18O
EC

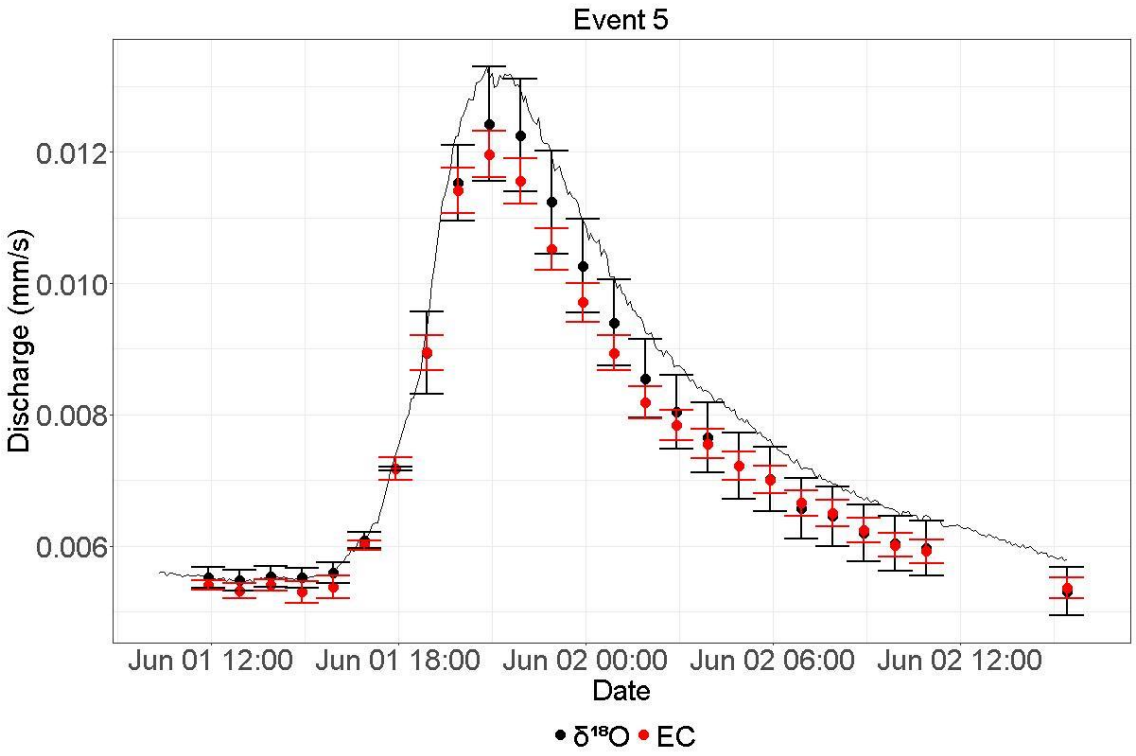
Event 5
0.012
0.010
0.008
0.006
Discharge (mm/s)
Jun 01 12:00
Jun 01 18:00
Jun 02 00:00
Jun 02 06:00
Jun 02 12:00
Date
δ18O
EC

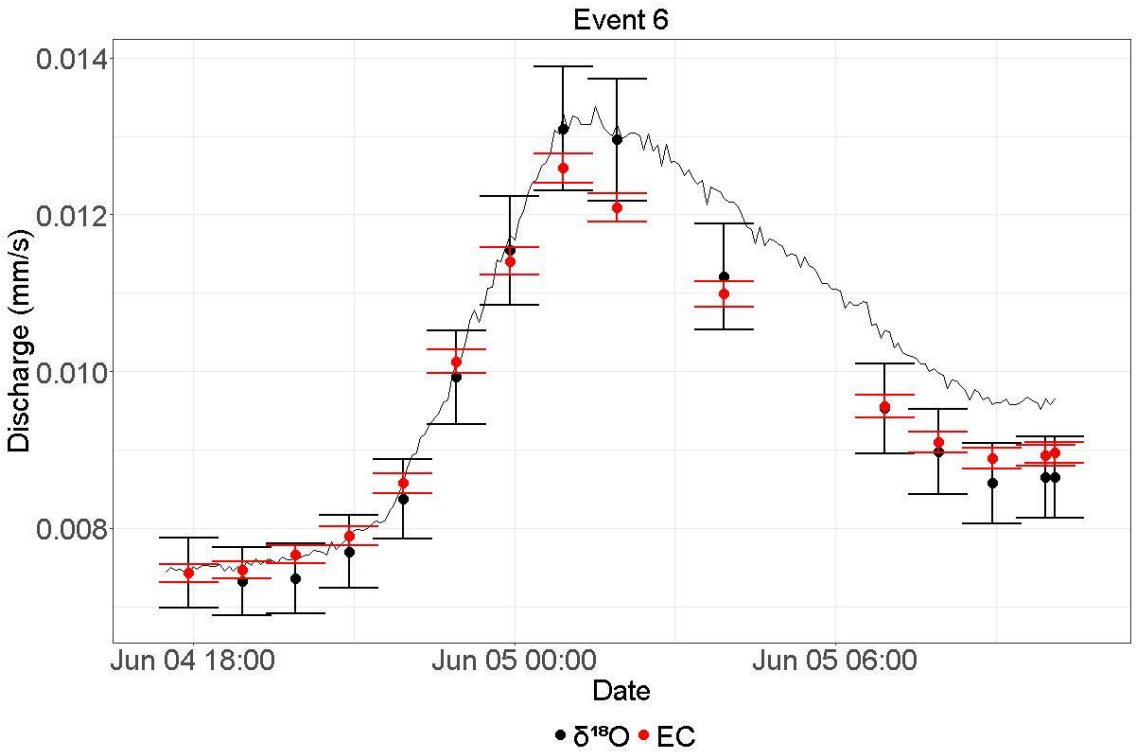
Event 6
0.014
0.012
0.010
0.008
Discharge (mm/s)
Jun 04 18:00
Jun 05 00:00
Jun 05 06:00
Date
δ¹⁸O
EC

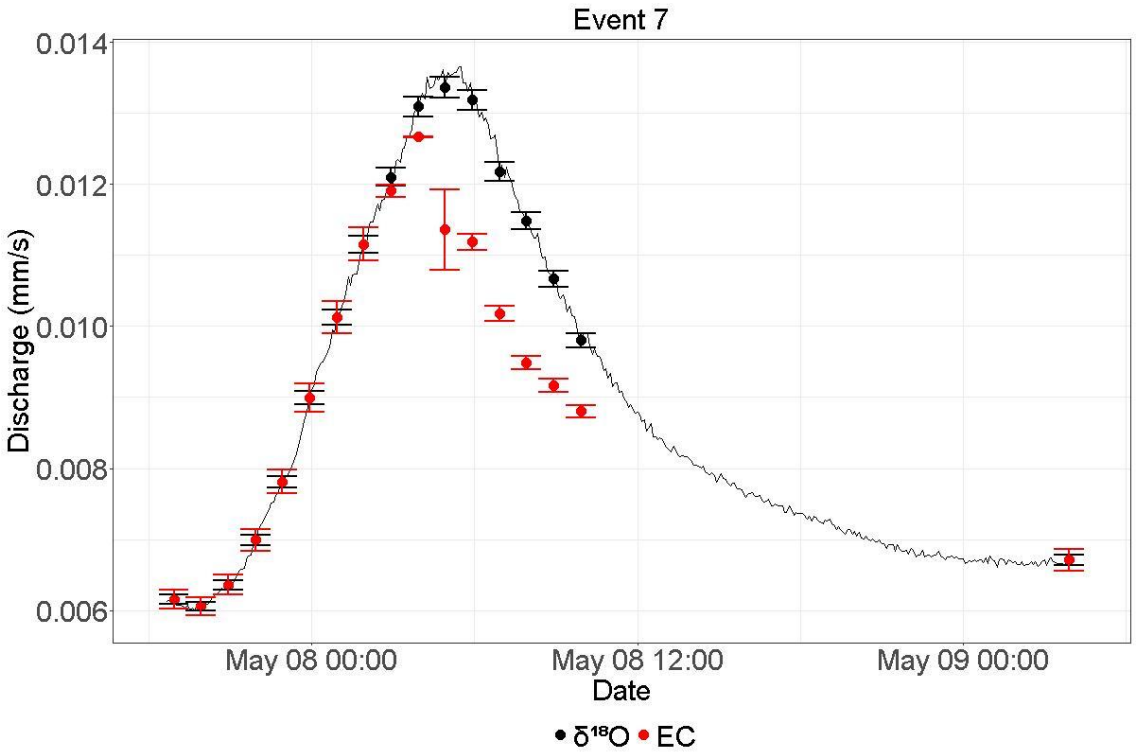
Event 7
0.014
0.012
0.010
0.008
0.006
Discharge (mm/s)
May 08 00:00
May 08 12:00
May 09 00:00
Date
δ¹⁸O
EC

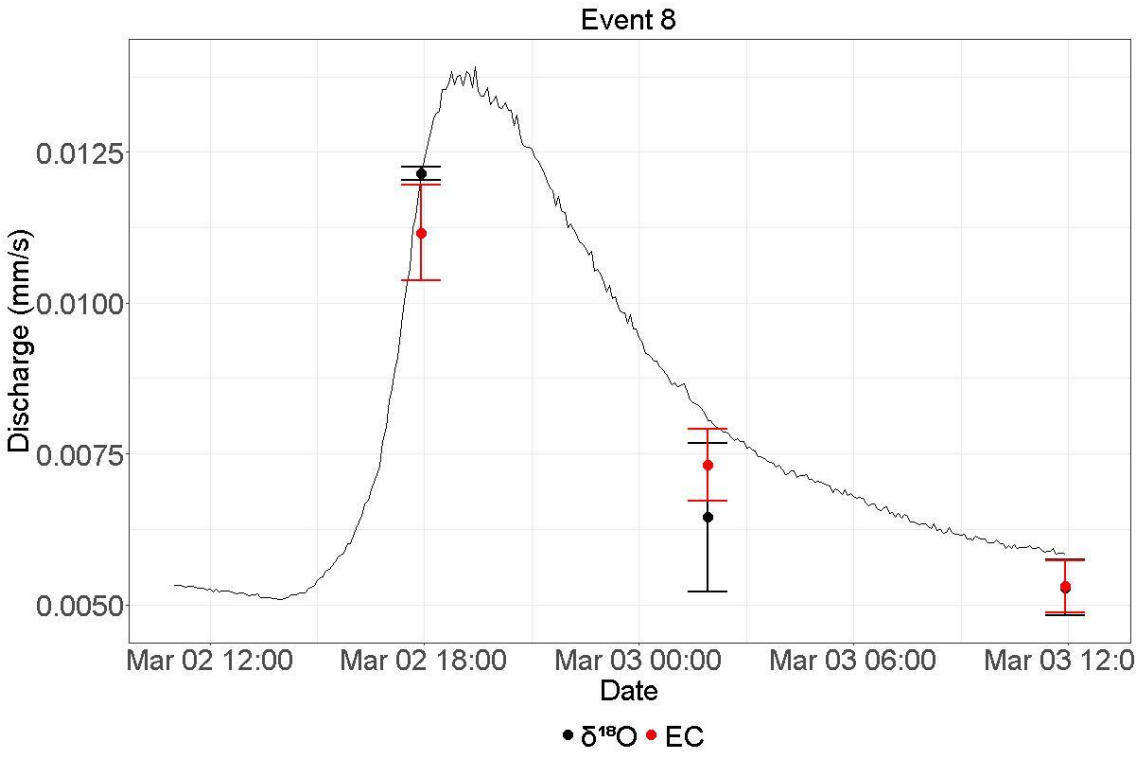
Event 8
0.0125
0.0100
0.0075
0.0050
Discharge (mm/s)
Mar 02 12:00
Mar 02 18:00
Mar 03 00:00
Mar 03 06:00
Mar 03 12:0
Date
δ¹⁸O
EC

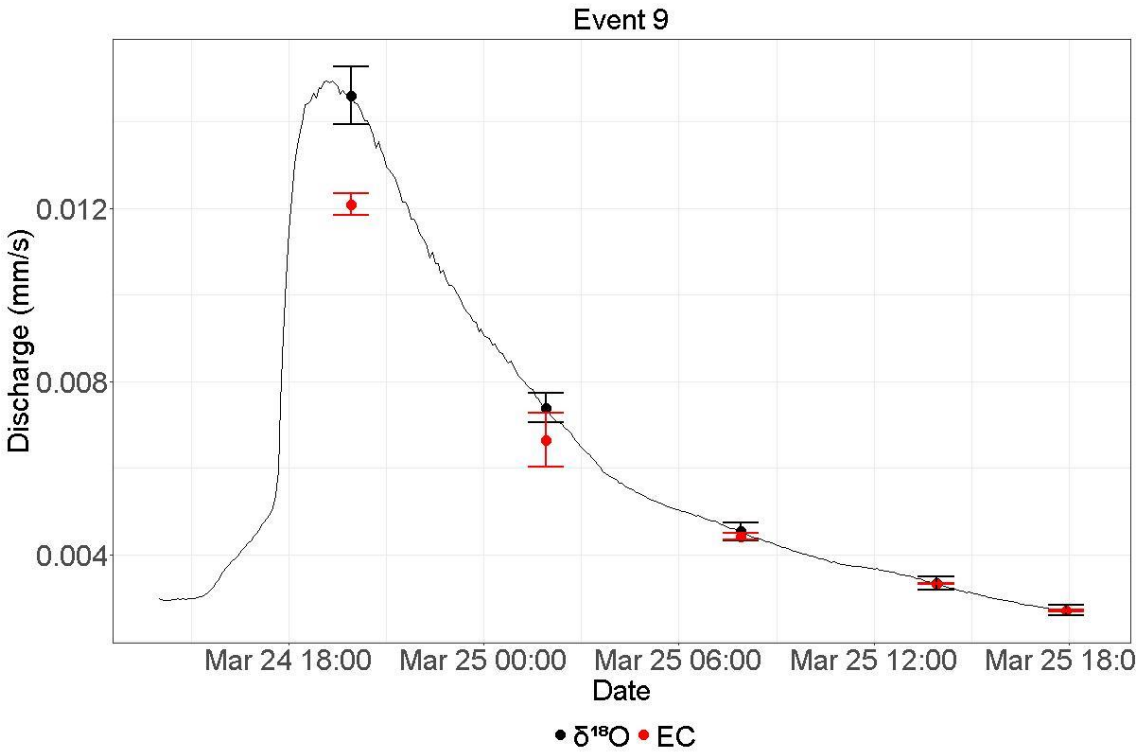
Event 9
0.012
0.008
0.004
Discharge (mm/s)
Mar 24 18:00
Mar 25 00:00
Mar 25 06:00
Mar 25 12:00
Mar 25 18:0
Date
δ¹⁸O
EC

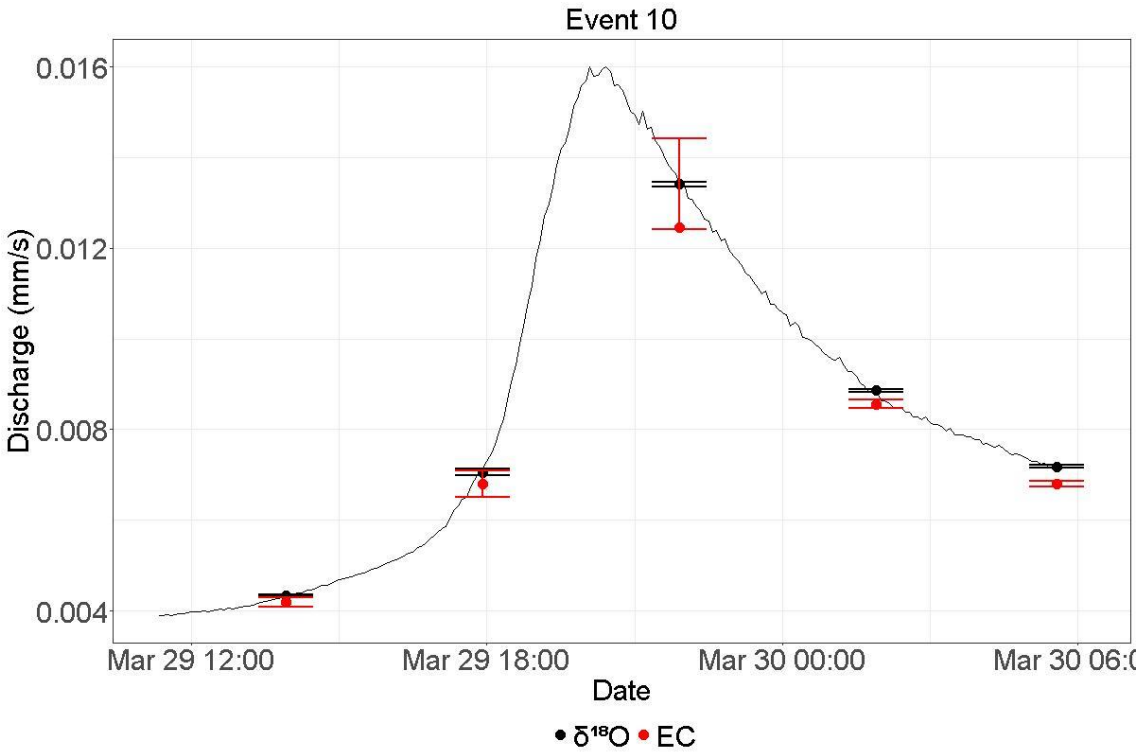
Event 10
0.016
0.012
0.008
0.004
Discharge (mm/s)
Mar 29 12:00
Mar 29 18:00
Mar 30 00:00
Mar 30 06:(
Date
δ¹⁸O
EC

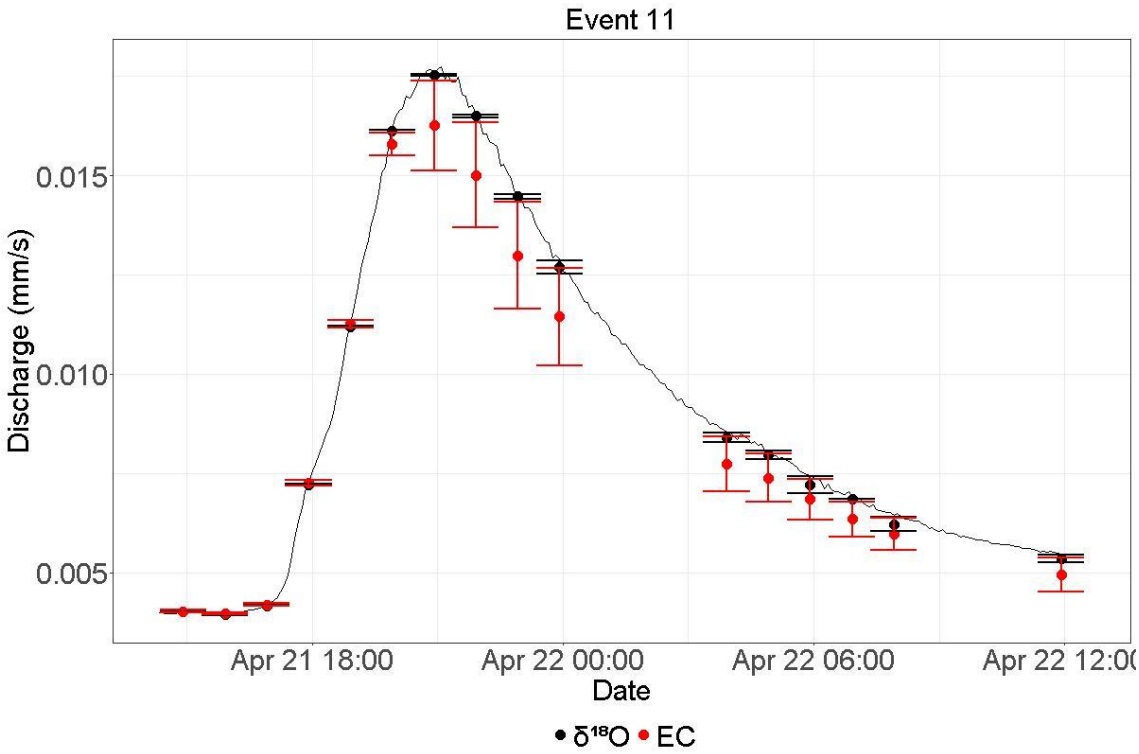
Event 11
0.015
0.010
0.005
Discharge (mm/s)
Apr 21 18:00
Apr 22 00:00
Apr 22 06:00
Apr 22 12:0(
Date
δ¹⁸O
EC

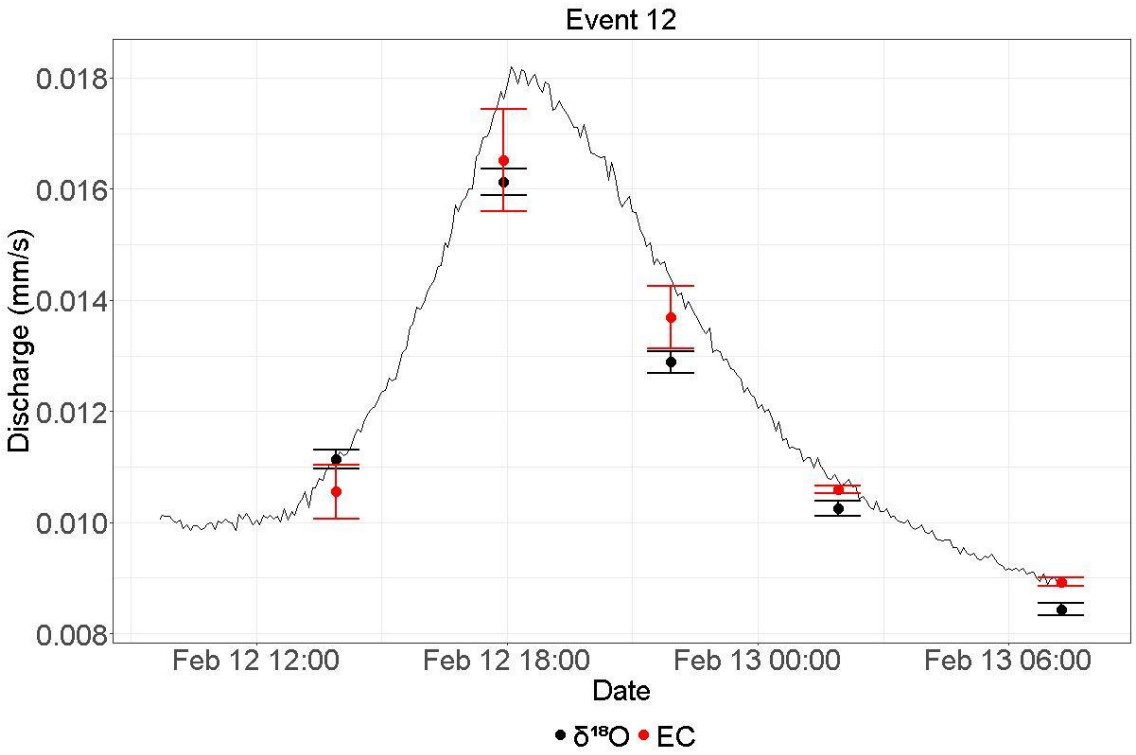
Event 12
Discharge (mm/s)
0.018
0.016
0.014
0.012
0.010
0.008
Feb 12 12:00
Feb 12 18:00
Feb 13 00:00
Feb 13 06:00
Date
δ18O
EC

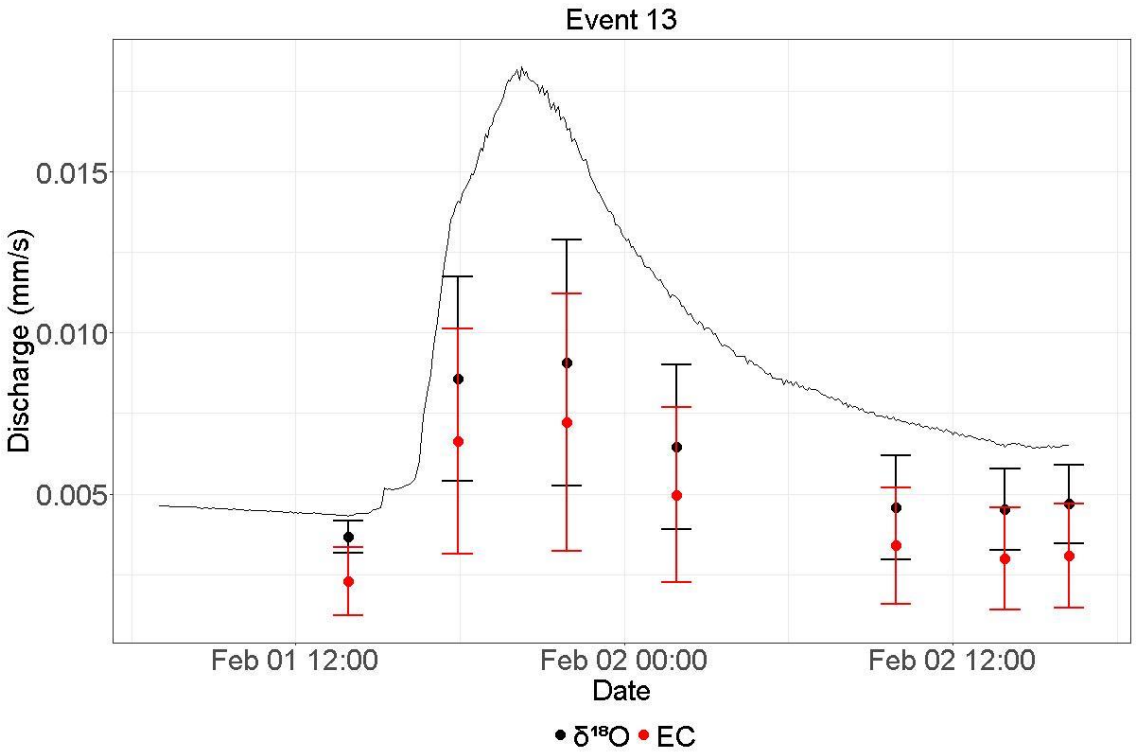
Event 13
Discharge (mm/s)
0.015
0.010
0.005
Feb 01 12:00
Feb 02 00:00
Feb 02 12:00
Date
δ18O
EC

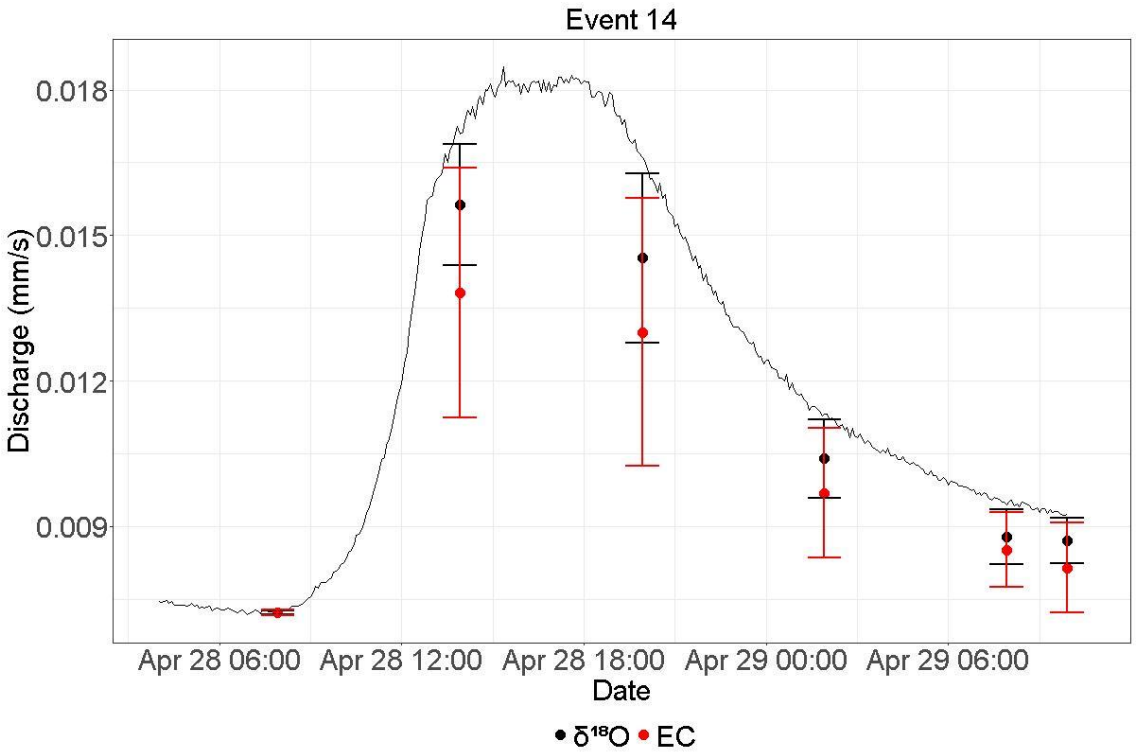
Event 14
0.018
0.015
0.012
0.009
Discharge (mm/s)
Apr 28 06:00
Apr 28 12:00
Apr 28 18:00
Apr 29 00:00
Apr 29 06:00
Date
δ¹⁸O
EC

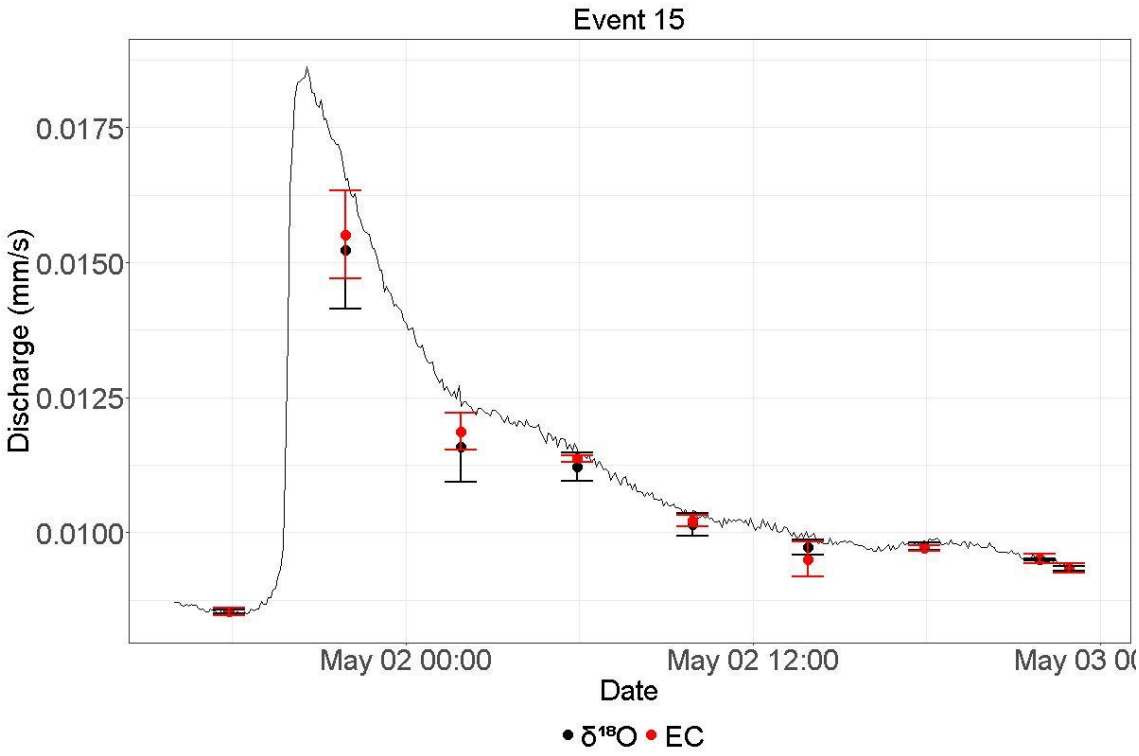
Event 15
0.0175
0.0150
0.0125
0.0100
Discharge (mm/s)
May 02 00:00
May 02 12:00
May 03 0(
Date
δ¹⁸O
EC

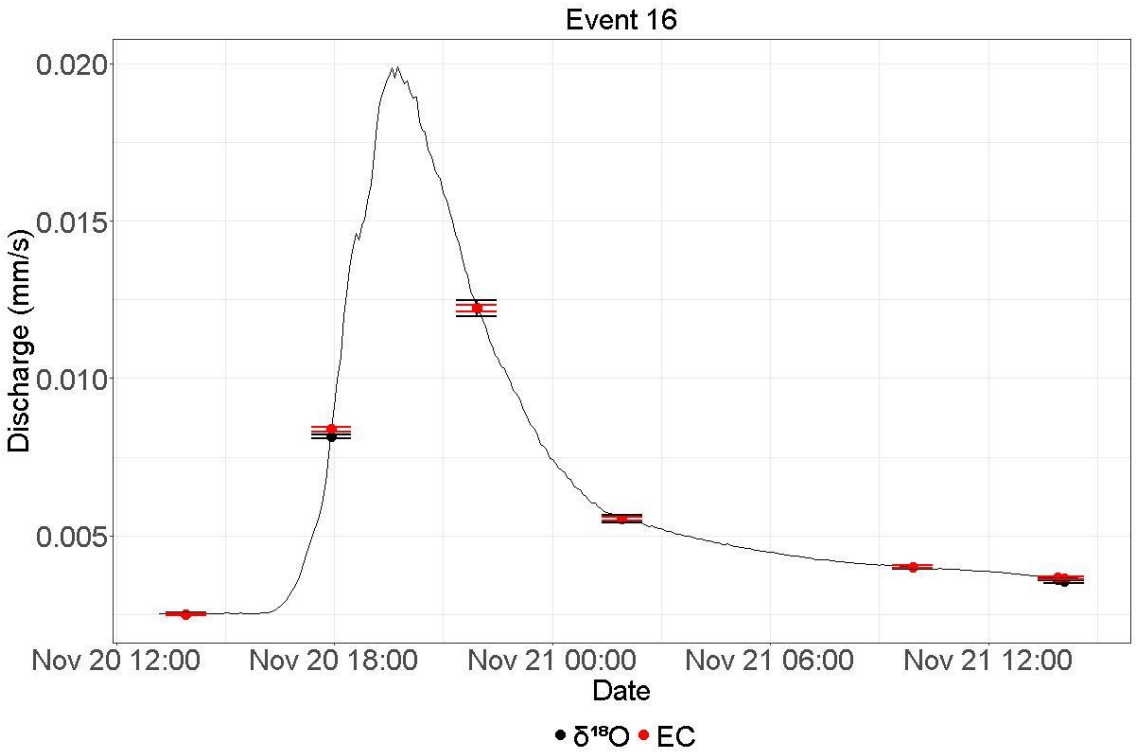
Event 16
0.020
0.015
0.010
0.005
Discharge (mm/s)
Nov 20 12:00
Nov 20 18:00
Nov 21 00:00
Nov 21 06:00
Nov 21 12:00
Date
δ¹⁸O
EC

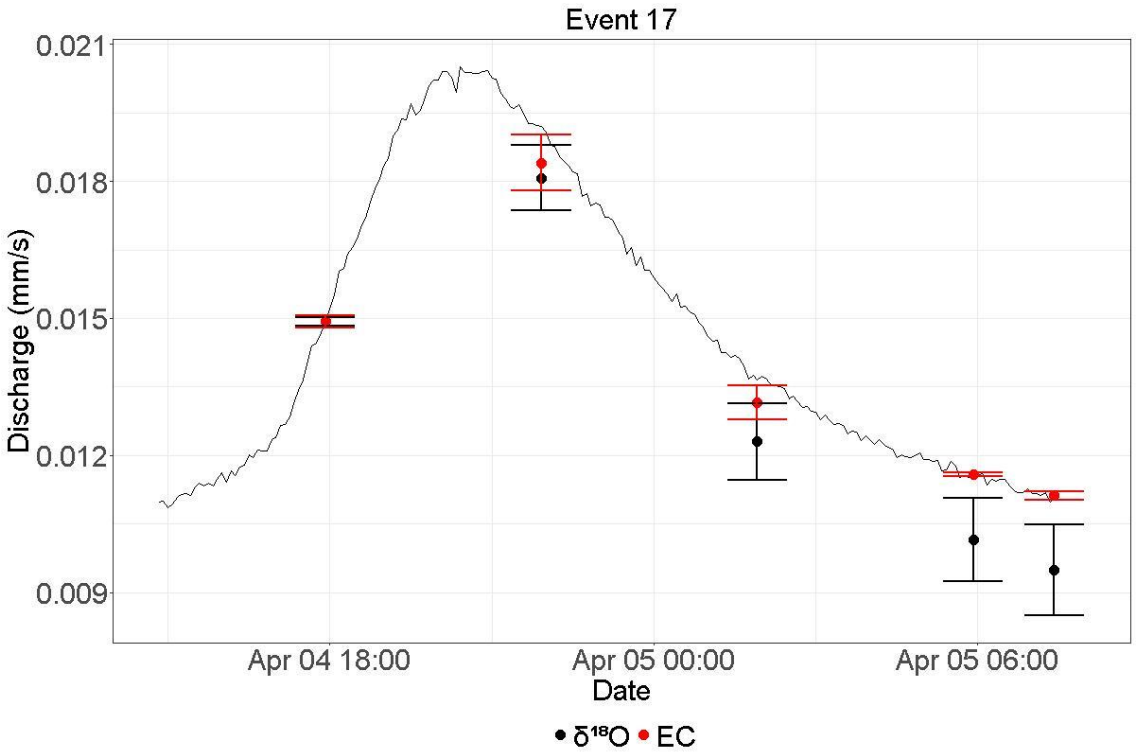
Event 17
0.021
0.018
0.015
0.012
0.009
Discharge (mm/s)
Apr 04 18:00
Apr 05 00:00
Apr 05 06:00
Date
δ¹⁸O
EC

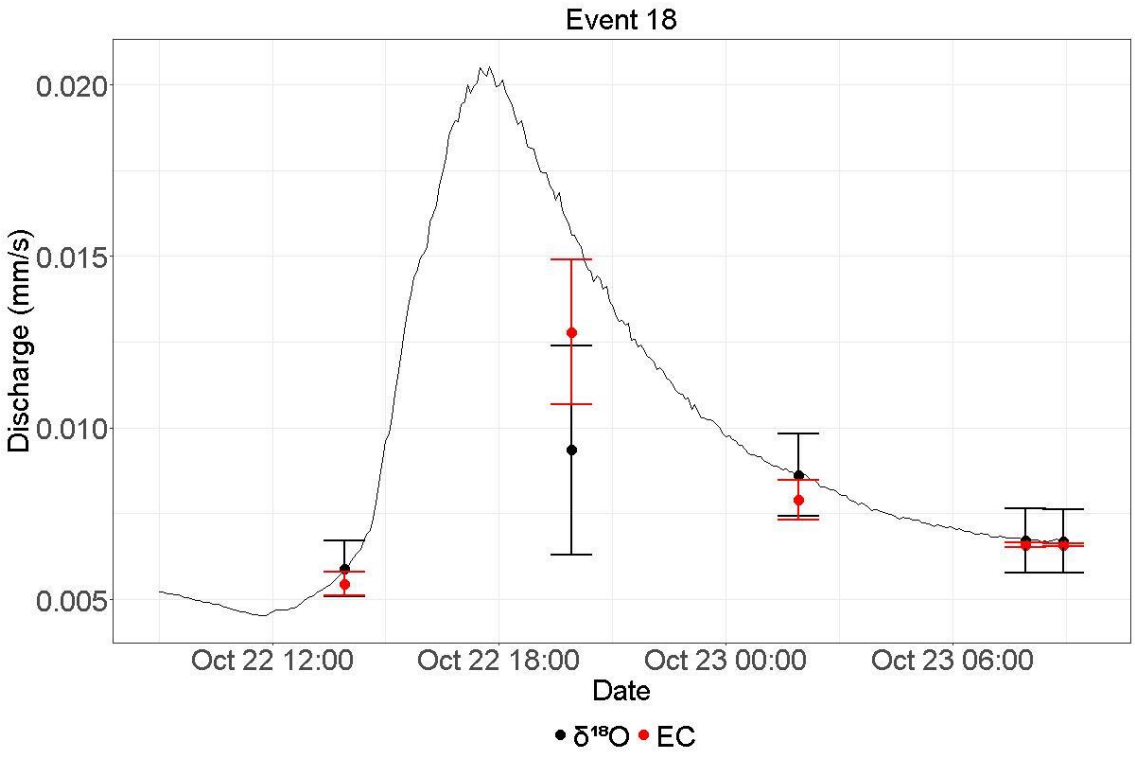
Event 18
0.020
0.015
0.010
0.005
Discharge (mm/s)
Oct 22 12:00
Oct 22 18:00
Oct 23 00:00
Oct 23 06:00
Date
δ¹⁸O
EC

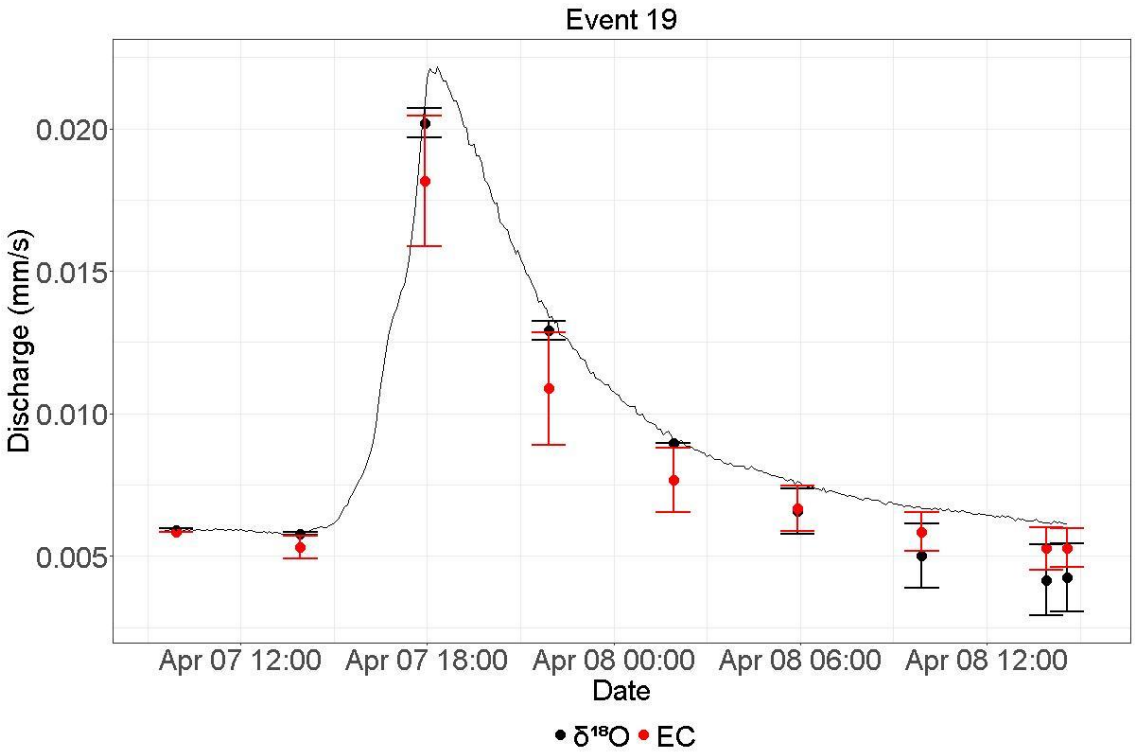
Event 19
0.020
0.015
0.010
0.005
Discharge (mm/s)
Apr 07 12:00
Apr 07 18:00
Apr 08 00:00
Apr 08 06:00
Apr 08 12:00
Date
δ¹⁸O
EC

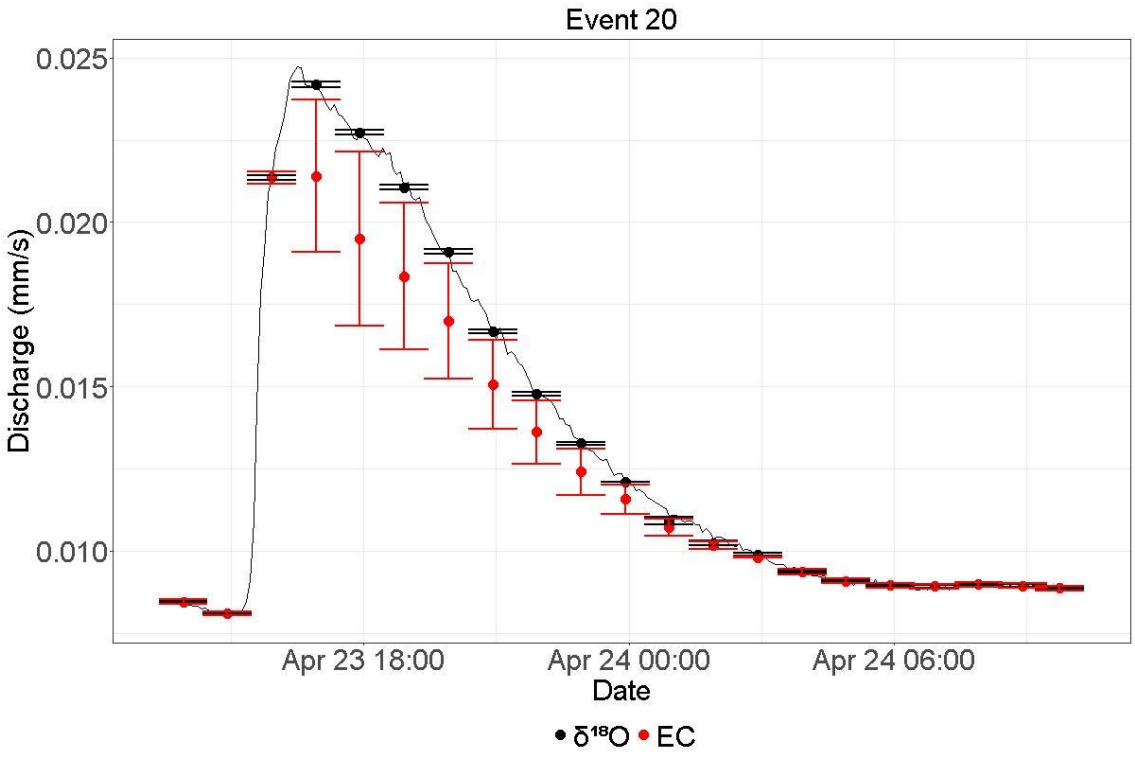
Event 20
0.025
0.020
0.015
0.010
Discharge (mm/s)
Apr 23 18:00
Apr 24 00:00
Apr 24 06:00
Date
δ¹⁸O
EC

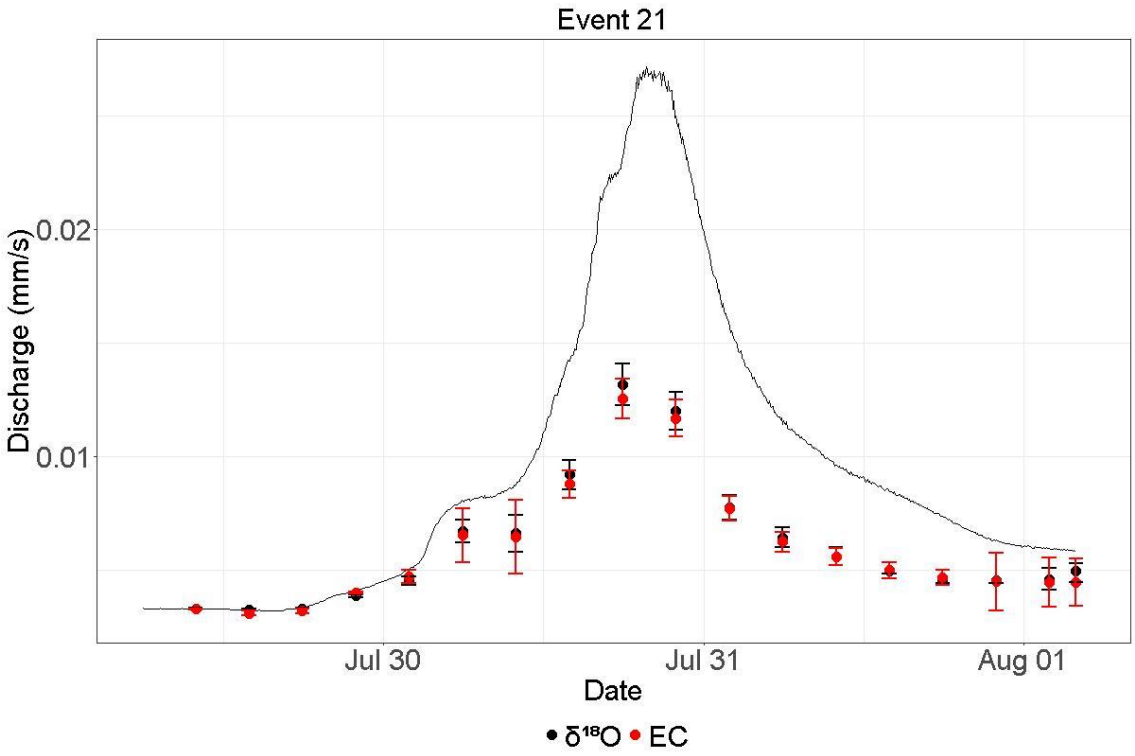
Event 21
0.02
0.01
Discharge (mm/s)
Jul 30
Jul 31
Aug 01
Date
δ¹⁸O
EC

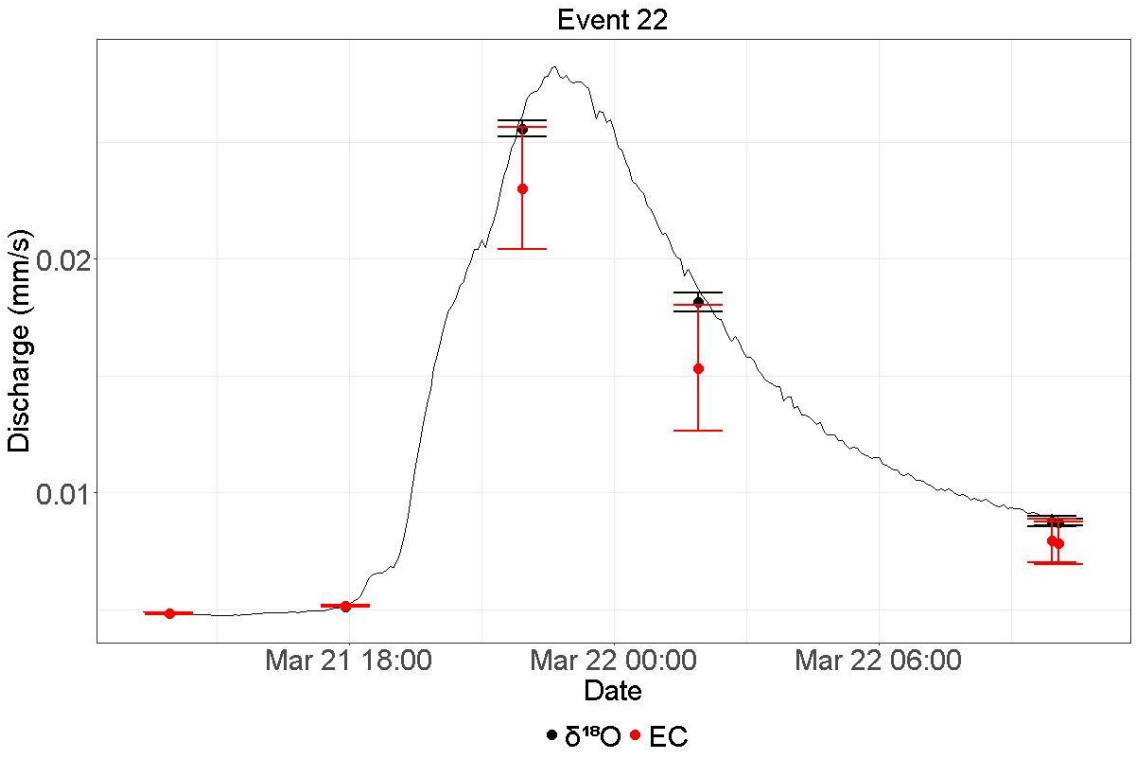
Event 22
Discharge (mm/s)
0.02
0.01
Mar 21 18:00
Mar 22 00:00
Mar 22 06:00
Date
δ¹⁸O
EC

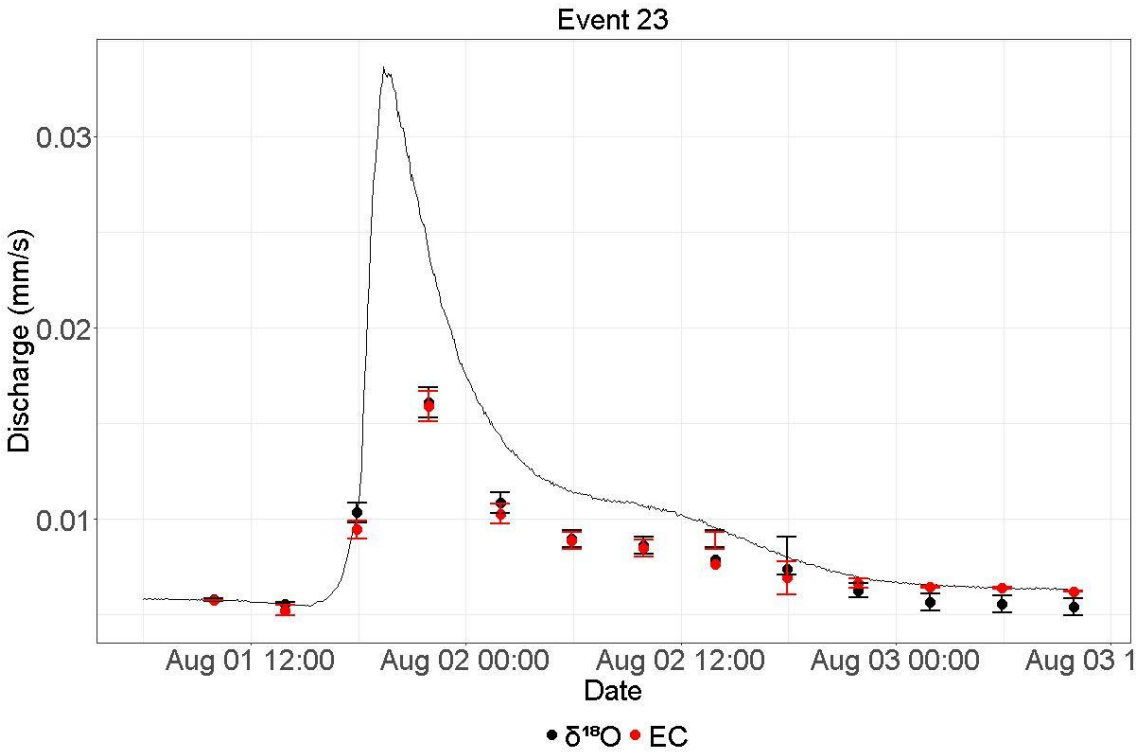
Event 23
Discharge (mm/s)
0.03
0.02
0.01
Aug 01 12:00
Aug 02 00:00
Aug 02 12:00
Aug 03 00:00
Aug 03 1
Date
δ¹⁸O
EC

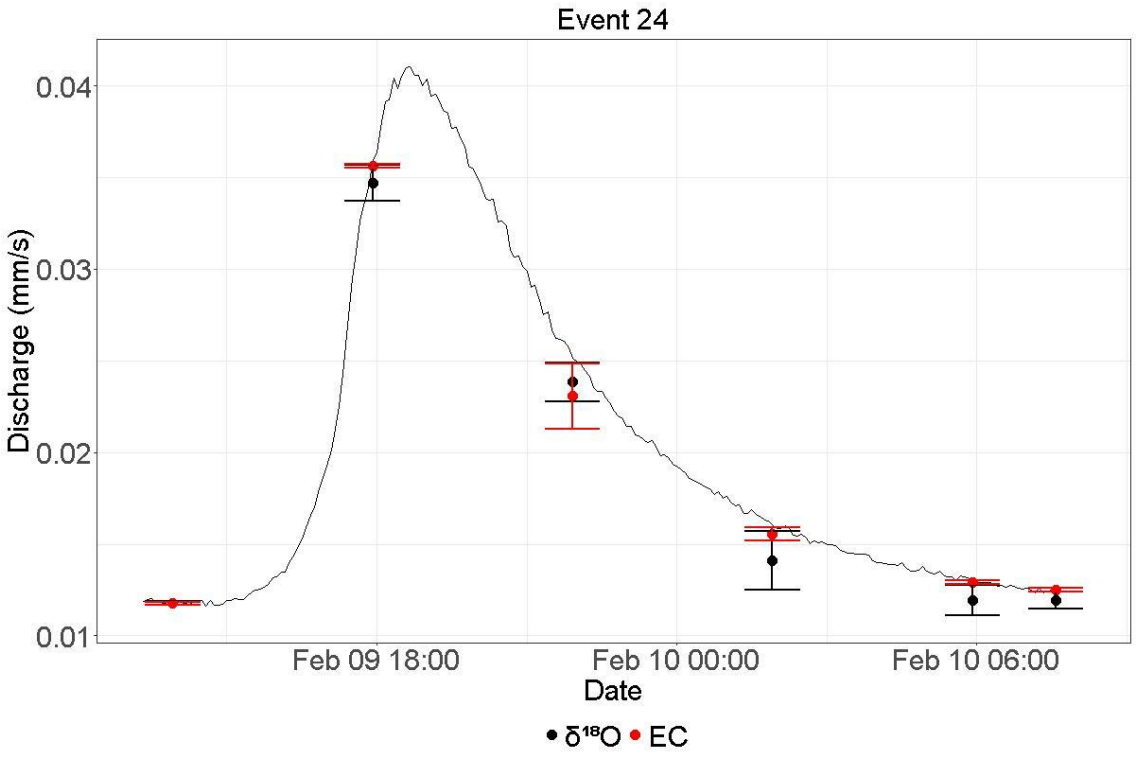
Event 24
Discharge (mm/s)
0.04
0.03
0.02
0.01
Feb 09 18:00
Feb 10 00:00
Feb 10 06:00
Date
δ¹⁸O
EC

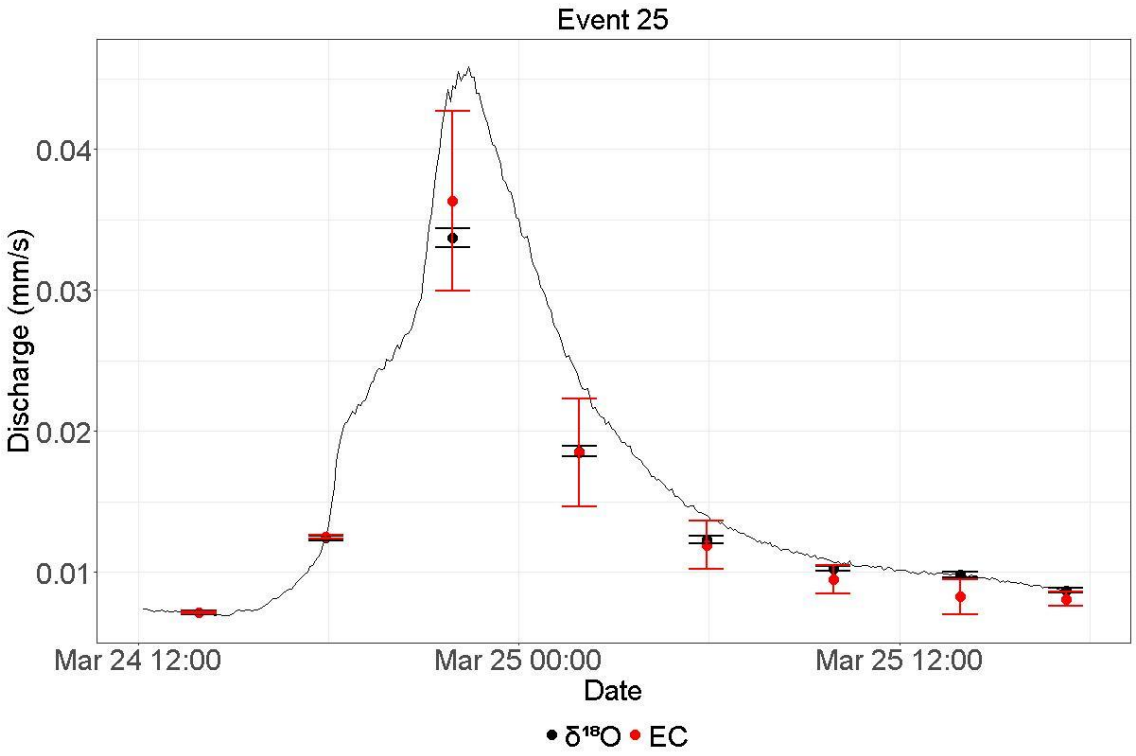
Event 25
Discharge (mm/s)
0.04
0.03
0.02
0.01
Mar 24 12:00
Mar 25 00:00
Mar 25 12:00
Date
δ¹⁸O
EC

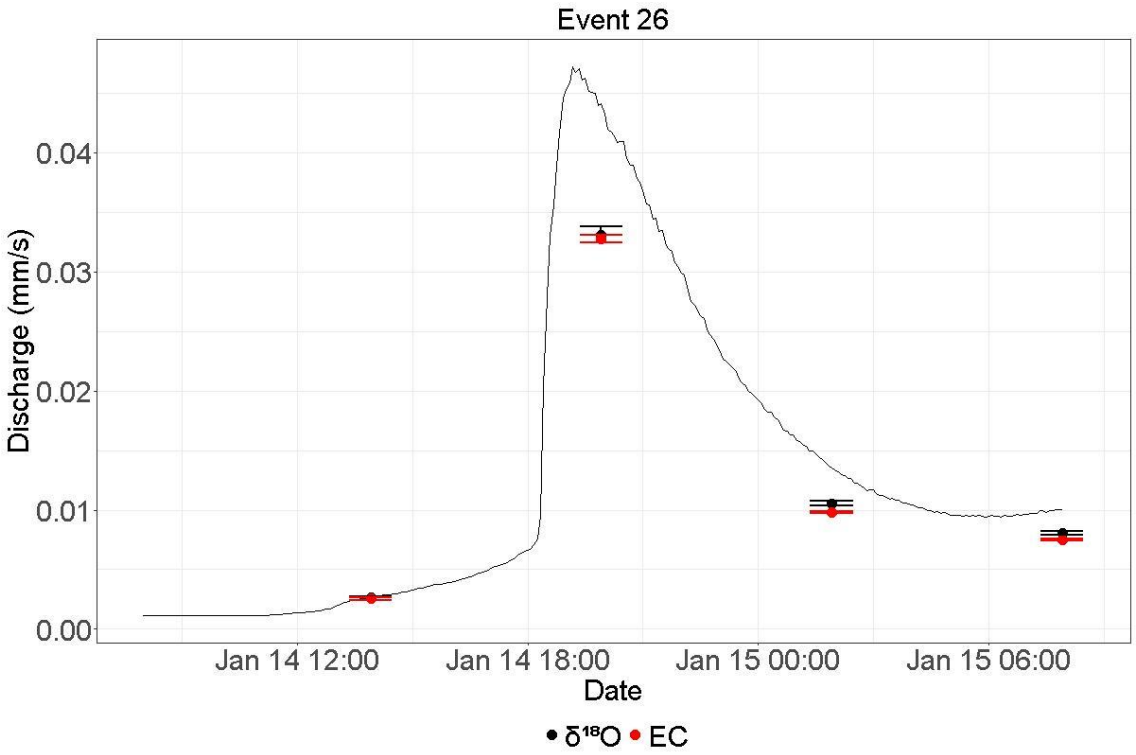
Event 26
Discharge (mm/s)
0.04
0.03
0.02
0.01
0.00
Jan 14 12:00
Jan 14 18:00
Jan 15 00:00
Jan 15 06:00
Date
δ¹⁸O
EC

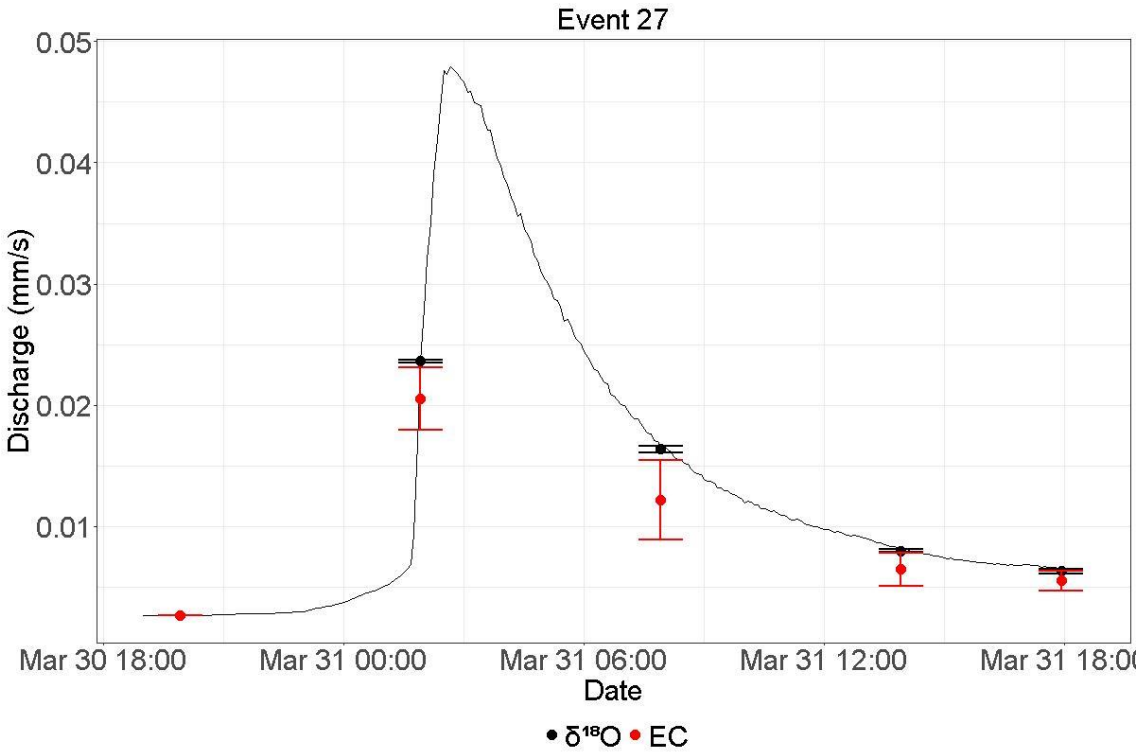
Event 27
Discharge (mm/s)
0.05
0.04
0.03
0.02
0.01
Mar 30 18:00
Mar 31 00:00
Mar 31 06:00
Mar 31 12:00
Mar 31 18:0
Date
δ¹⁸O
EC

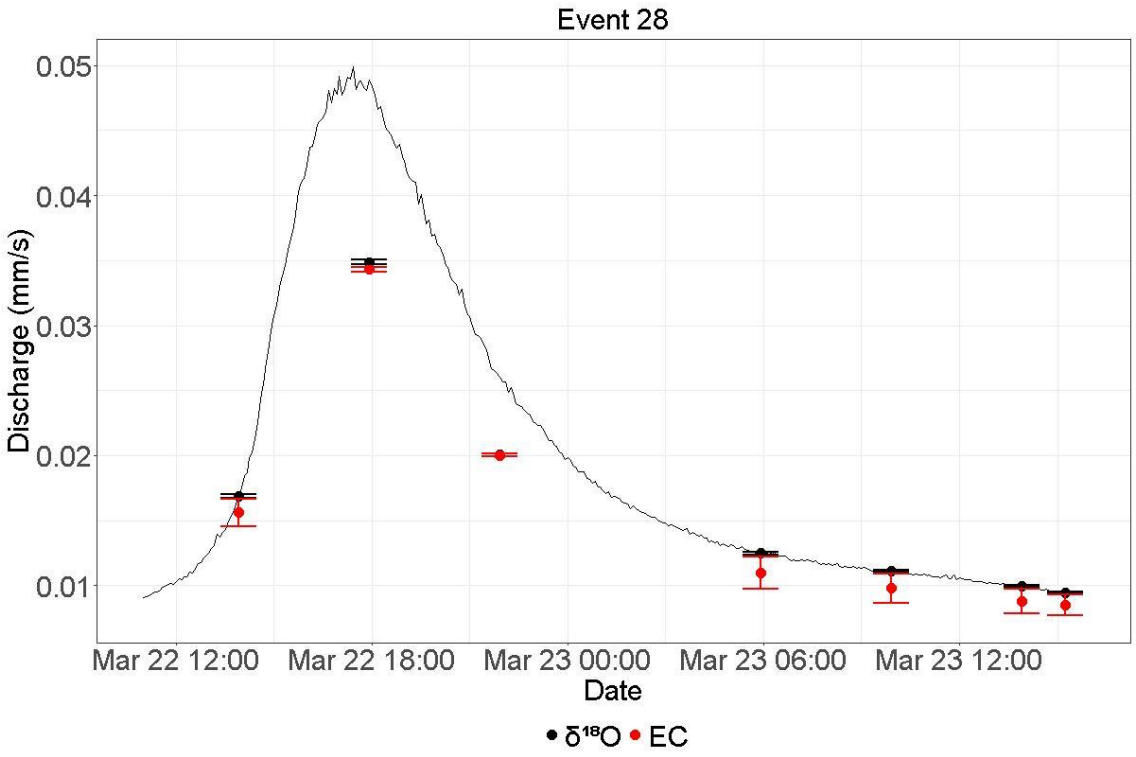
Event 28
0.05
0.04
0.03
0.02
0.01
Discharge (mm/s)
Mar 22 12:00
Mar 22 18:00
Mar 23 00:00
Mar 23 06:00
Mar 23 12:00
Date
δ¹⁸O
EC

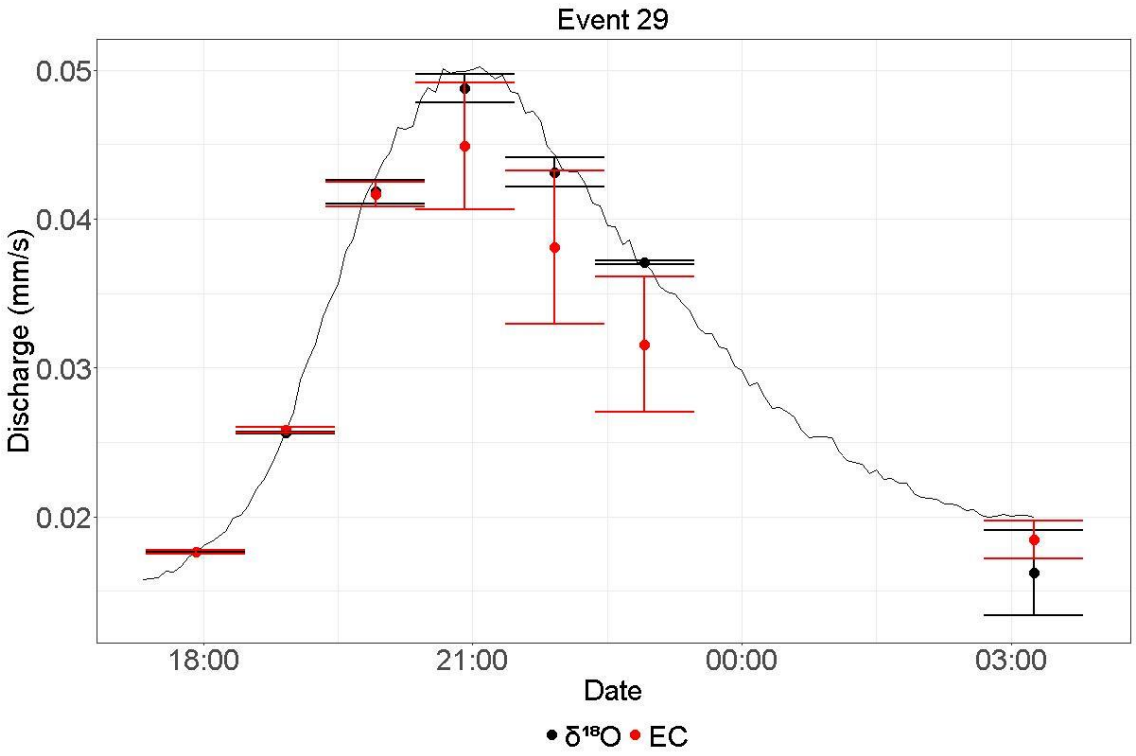
Event 29
0.05
0.04
0.03
0.02
Discharge (mm/s)
18:00
21:00
00:00
03:00
Date
δ¹⁸O
EC

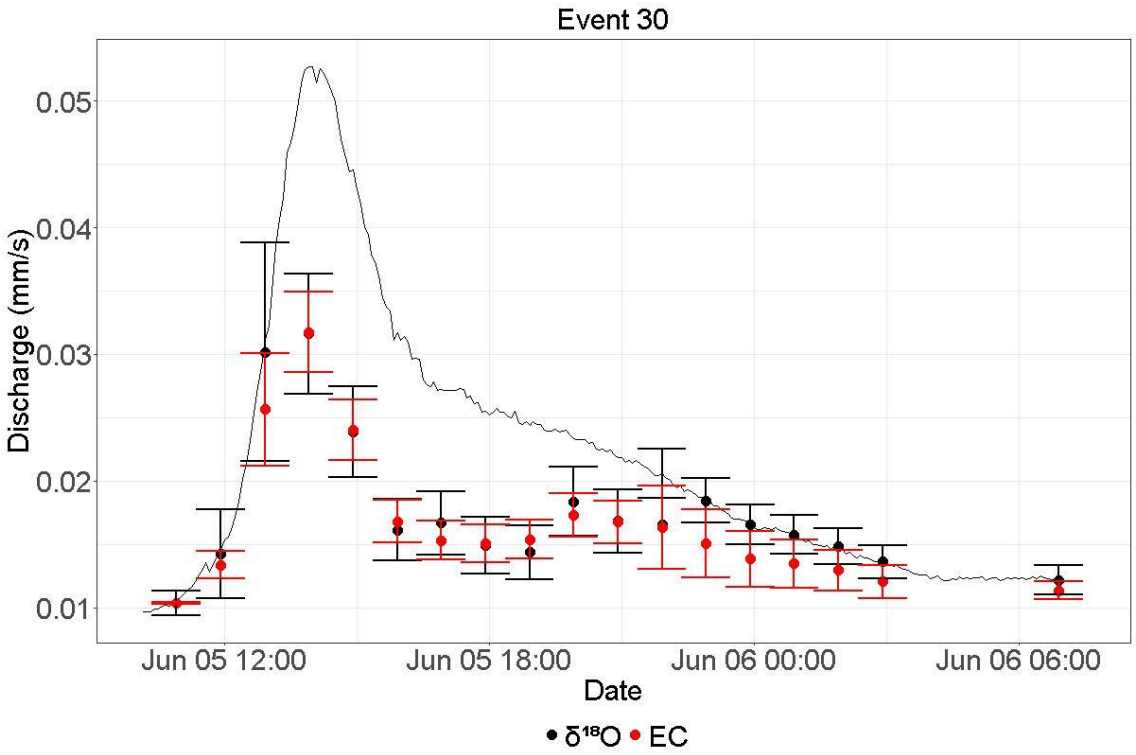
Event 30
0.05
0.04
0.03
0.02
0.01
Discharge (mm/s)
Jun 05 12:00
Jun 05 18:00
Jun 06 00:00
Jun 06 06:00
Date
δ¹⁸O
EC

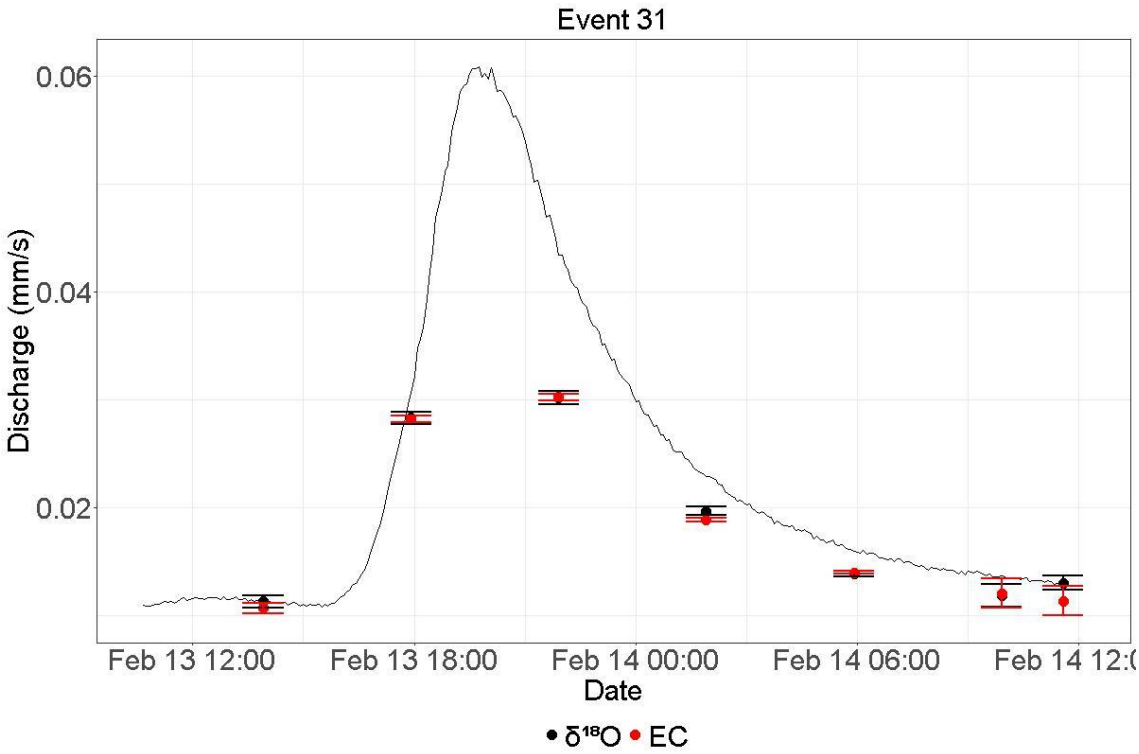
Event 31
0.06
0.04
0.02
Discharge (mm/s)
Feb 13 12:00
Feb 13 18:00
Feb 14 00:00
Feb 14 06:00
Feb 14 12:(
Date
δ¹⁸O
EC

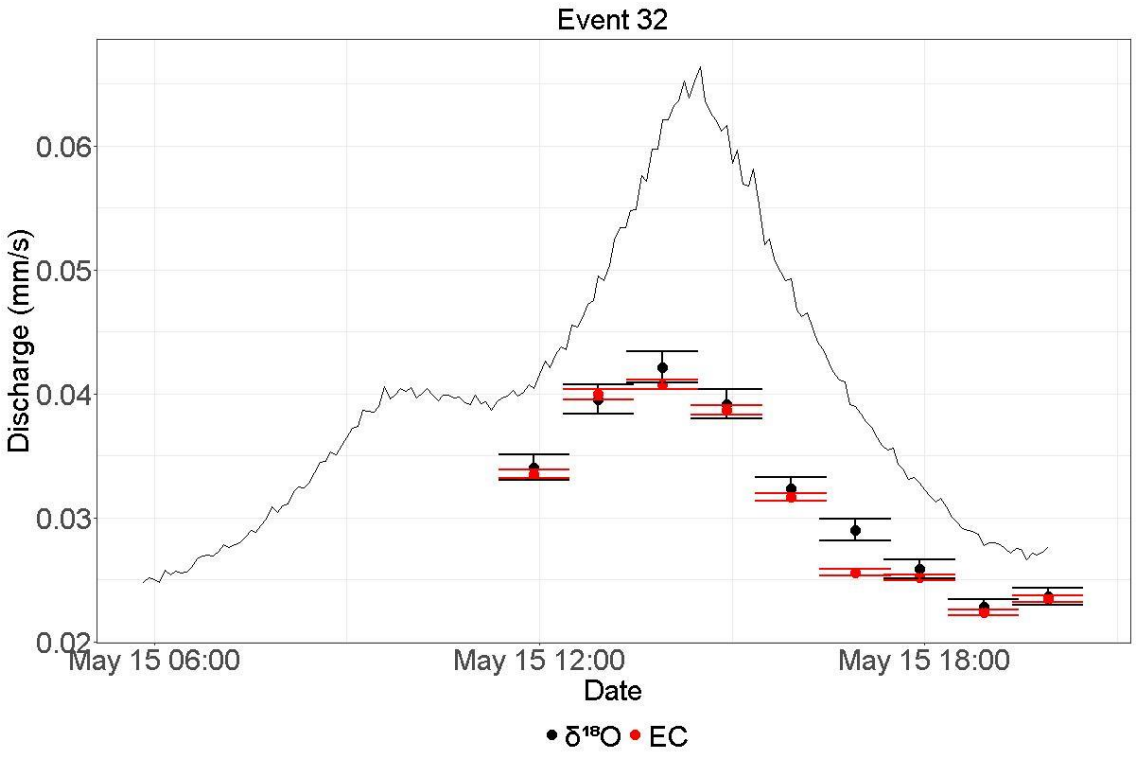
Event 32
Discharge (mm/s)
0.06
0.05
0.04
0.03
0.02
May 15 06:00
May 15 12:00
May 15 18:00
Date
δ¹⁸O
EC

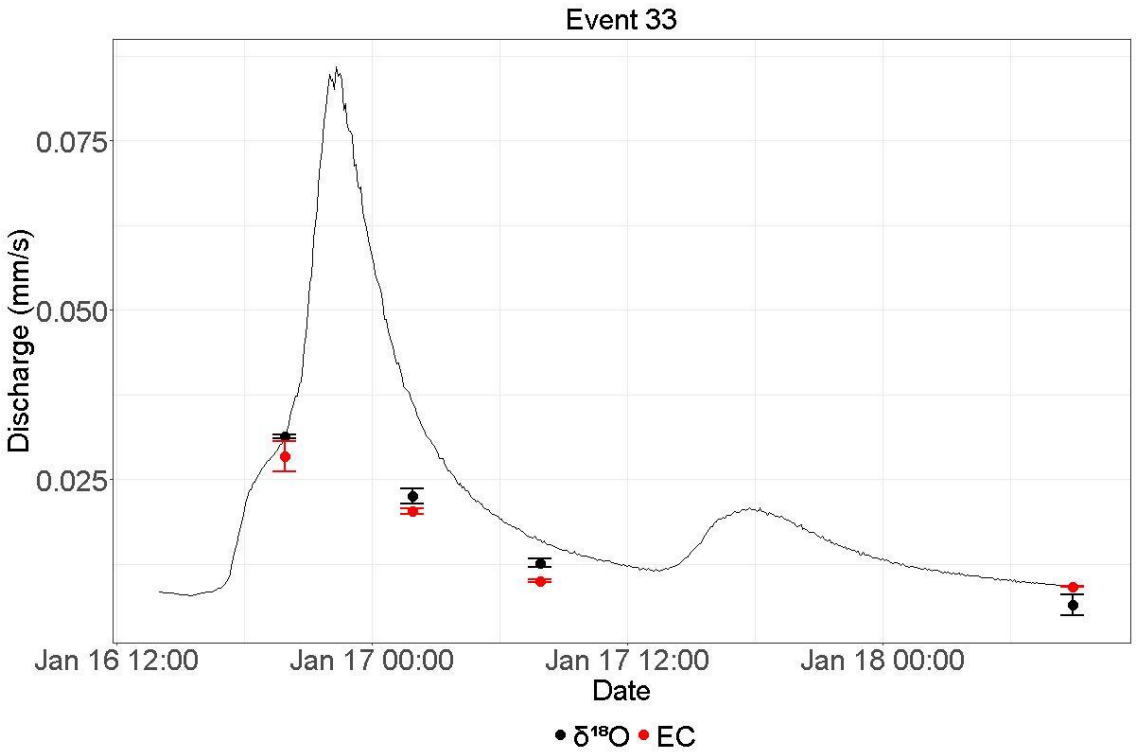
Event 33
Discharge (mm/s)
0.075
0.050
0.025
Jan 16 12:00
Jan 17 00:00
Jan 17 12:00
Jan 18 00:00
Date
δ¹⁸O
EC

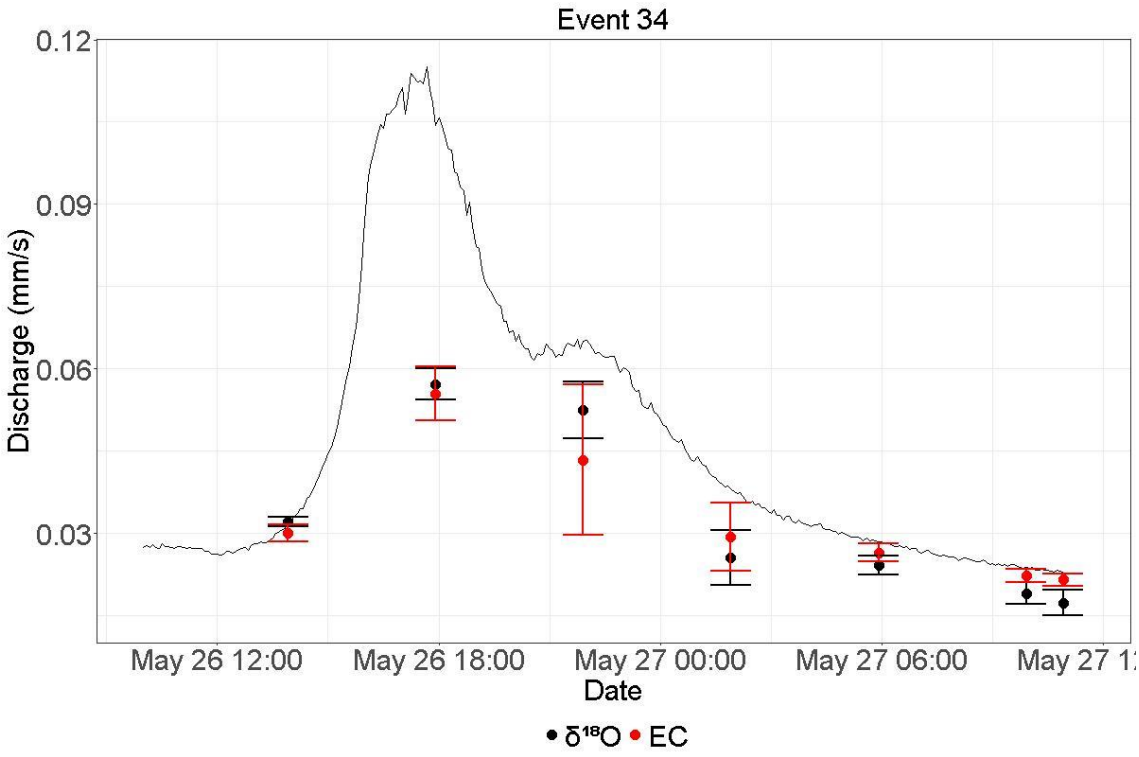
Event 34
0.12
0.09
0.06
0.03
Discharge (mm/s)
May 26 12:00
May 26 18:00
May 27 00:00
May 27 06:00
Date
δ¹⁸O
EC

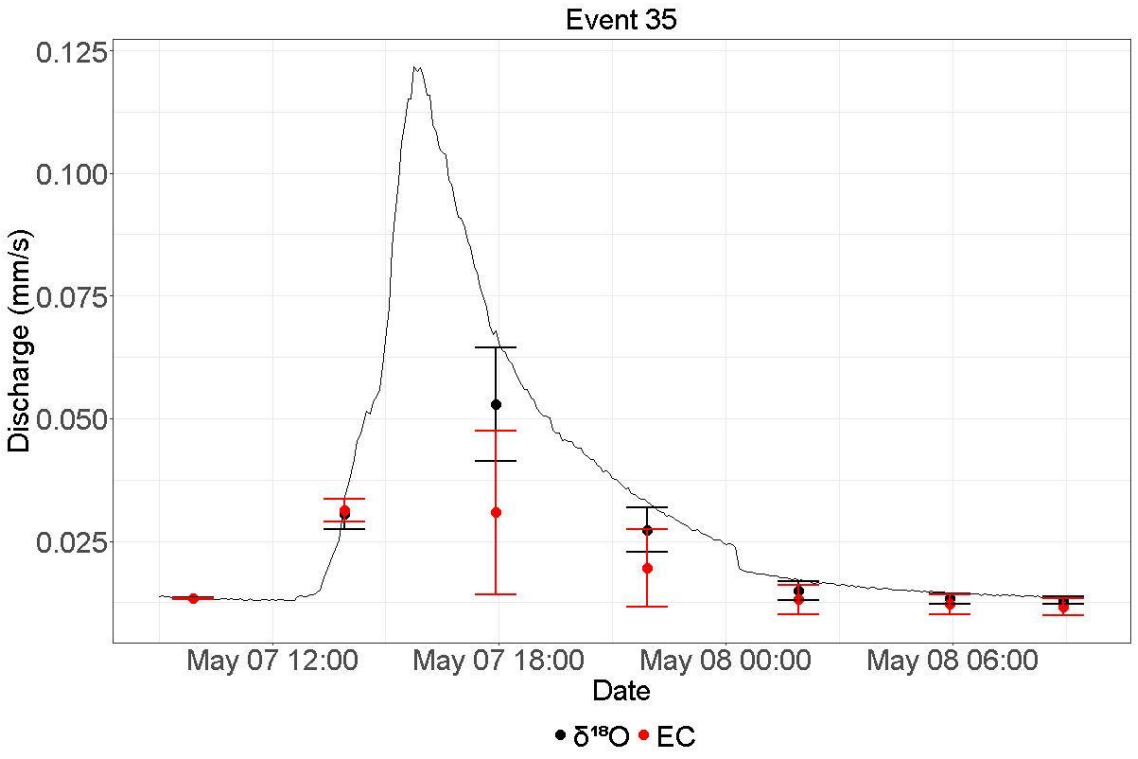
Event 35
0.125
0.100
0.075
0.050
0.025
Discharge (mm/s)
May 07 12:00
May 07 18:00
May 08 00:00
May 08 06:00
Date
δ¹⁸O
EC

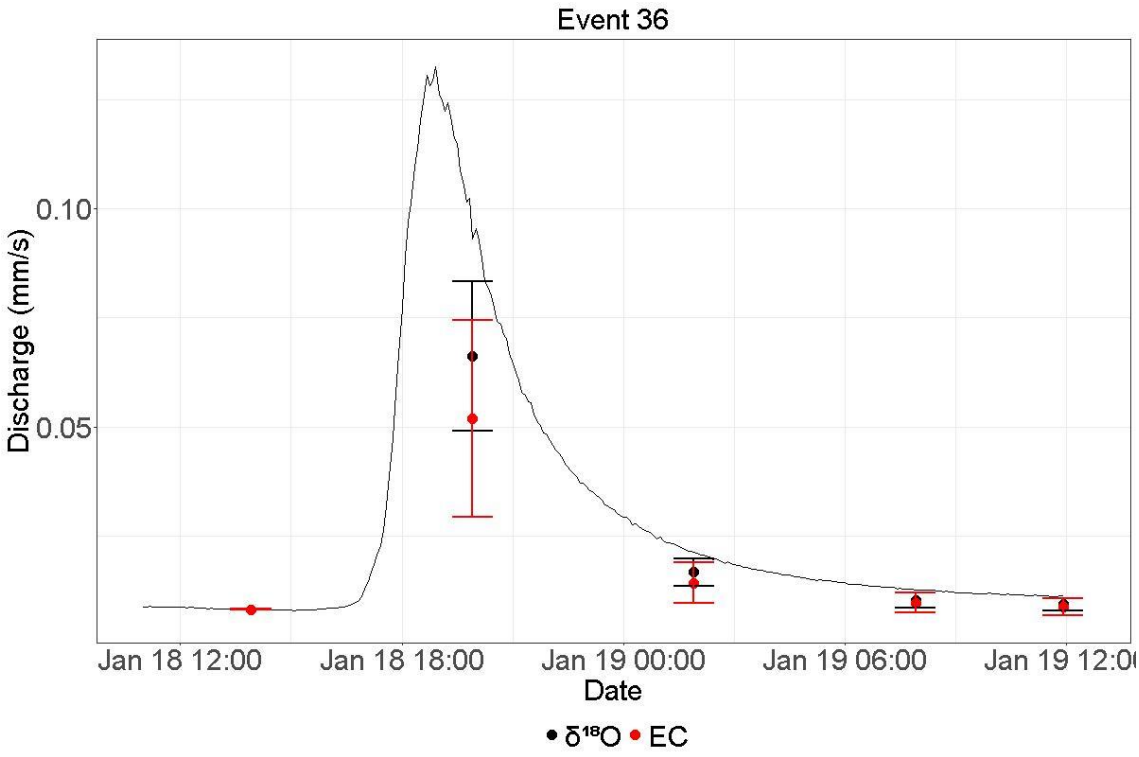
Event 36
Discharge (mm/s)
0.10
0.05
Jan 18 12:00
Jan 18 18:00
Jan 19 00:00
Jan 19 06:00
Jan 19 12:0
Date
δ¹⁸O
EC

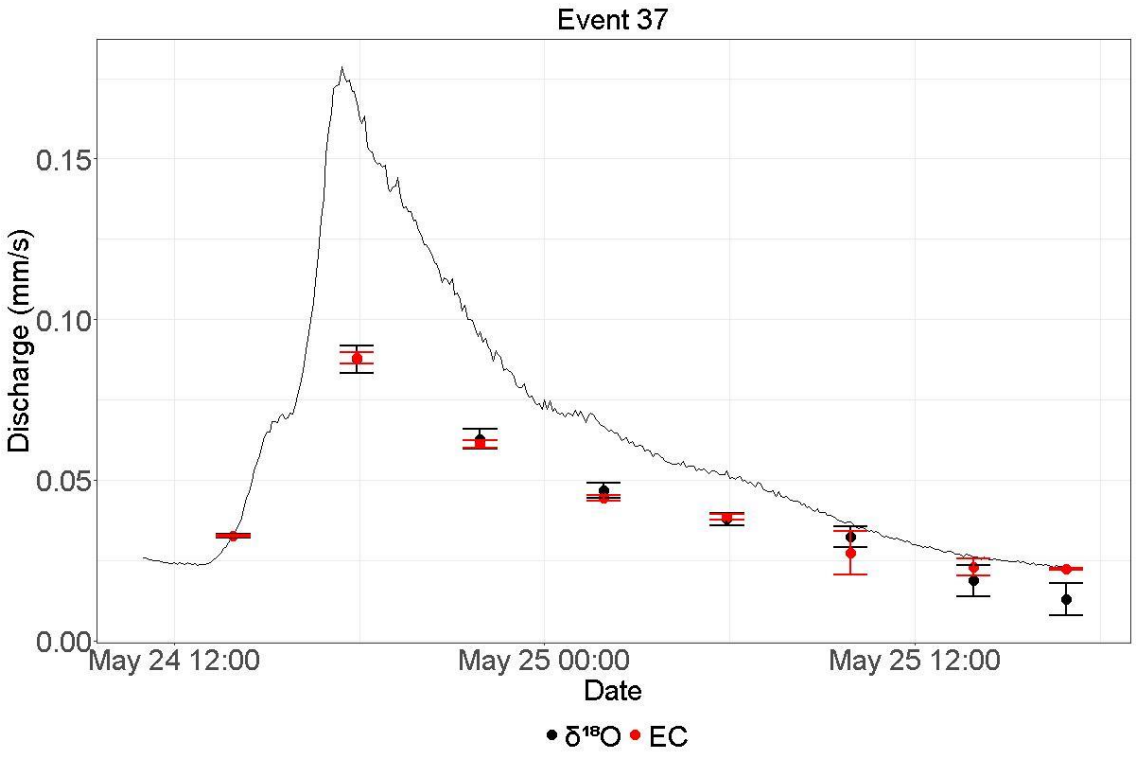
Event 37
Discharge (mm/s)
0.15
0.10
0.05
0.00
May 24 12:00
May 25 00:00
May 25 12:00
Date
δ¹⁸O
EC

Appendix 7. Stable isotopic ($\delta^{18}O$) and electrical conductivity (EC) pre-event (PE) and event (E) water concentrations for each rainfall-runoff event (n=37) using the different sample options described in Table 1 (i.e., PE1 to PE6, E2 to E6). E1 is not included in the table as it corresponds to several values depending on the number of samples collected during each monitored event as described in Table 3.1.

Event	Oxygen-18 (‰)											EC (µS/cm)										
	PE1	PE2	PE3	PE4	PE5	PE6	E2	E3	E4	E5	E6	PE1	PE2	PE3	PE4	PE5	PE6	E2	E3	E4	E5	E6
1	-9.9	-9.9	-10.3	-10.2	-10.3	-10.3	-13.0	-10.9	-10.4	-13.8	-10.4	50.2	50.0	39.9	40.2	49.5	49.4	12.9	20.0	27.2	8.5	8.5
2	-9.7	-9.7	-10.1	-10.2	-10.2	-10.3	-10.3	-9.9	-9.1	-10.4	-9.1	48.7	48.3	45.5	40.2	50.3	49.4	16.2	18.7	24.8	17.2	16.9
3	-10.5	-10.5	-10.3	-10.2	-10.3	-10.3	-12.1	-14.1	-12.4	-9.0	-9.0	52.5	52.5	39.9	40.2	49.5	49.4	4.2	2.3	3.2	6.6	1.7
4	-10.6	-10.6	-10.3	-10.2	-10.3	-10.3	-6.5	-6.0	-4.8	-7.4	-4.8	42.3	41.8	39.9	40.2	49.5	49.4	8.0	5.1	6.7	18.9	3.9
5	-12.2	-12.4	-10.0	-10.2	-9.8	-10.3	-11.2	-11.0	-10.5	-11.4	-10.5	29.1	29.1	36.7	40.2	43.6	49.4	3.3	3.5	5.0	3.0	3.0
6	-12.0	-12.0	-10.0	-10.2	-9.8	-10.3	-11.2	-12.1	-14.6	-8.7	-8.7	26.6	28.3	36.7	40.2	43.6	49.4	1.9	2.1	2.4	1.5	1.5
7	-11.6	-11.6	-10.0	-10.2	-9.8	-10.3	-8.9	-9.6	-9.8	-8.5	-8.5	27.8	27.0	36.7	40.2	43.6	49.4	19.9	6.7	2.9	26.4	2.9
8	-10.5	-10.4	-10.0	-10.2	-9.8	-10.3	-7.3	-7.1	-6.9	-7.3	-6.9	27.3	27.8	36.7	40.2	43.6	49.4	8.4	9.8	12.1	7.6	7.6
9	-8.5	-8.5	-10.3	-10.2	-10.3	-10.3	-7.9	-7.6	-7.6	-8.0	-7.6	26.0	25.3	39.9	40.2	49.5	49.4	6.8	6.2	6.2	7.2	6.2
10	-9.8	-9.8	-10.0	-10.2	-9.8	-10.3	-16.6	-16.4	-16.1	-16.7	-16.1	32.4	33.0	36.7	40.2	43.6	49.4	2.3	2.4	2.4	2.3	2.3
11	-10.3	-10.3	-10.0	-10.2	-9.8	-10.3	-20.5	-21.6	-22.1	-17.7	-17.7	30.9	31.7	36.7	40.2	43.6	49.4	3.9	3.2	4.3	5.1	3.0
12	-10.3	-10.4	-10.0	-10.2	-9.8	-10.3	-9.3	-9.1	-7.1	-9.5	-7.1	23.4	24.4	36.7	40.2	43.6	49.4	3.2	4.1	2.7	2.8	2.7
13	-9.7	-10.1	-10.0	-10.2	-9.8	-10.3	-8.8	-8.7	-8.7	-8.8	-8.7	33.7	36.3	36.7	40.2	43.6	49.4	11.3	12.3	13.5	10.7	10.7
14	-11.7	-11.8	-10.3	-10.2	-10.3	-10.3	-17.1	-16.9	-16.8	-17.2	-16.6	28.0	26.7	39.9	40.2	49.5	49.4	4.6	4.6	5.2	4.5	4.4
15	-11.8	-11.9	-10.3	-10.2	-10.3	-10.3	-18.1	-16.4	-15.0	-18.2	-15.0	26.2	26.6	39.9	40.2	49.5	49.4	5.9	13.2	20.3	5.0	4.6
16	-10.2	-10.1	-10.3	-10.2	-10.3	-10.3	-11.5	-12.1	-11.9	-11.3	-11.3	24.8	24.0	39.9	40.2	49.5	49.4	17.8	15.1	12.5	18.6	10.3
17	-9.4	-9.3	-10.0	-10.2	-9.8	-10.3	-14.0	-16.7	-16.9	-12.4	-12.4	25.8	25.5	36.7	40.2	43.6	49.4	5.2	2.9	2.7	6.6	2.7
18	-9.0	-9.0	-10.1	-10.2	-10.2	-10.3	-8.8	-8.8	-8.9	-8.8	-8.8	27.8	28.1	45.5	40.2	50.3	49.4	9.9	11.4	15.5	9.0	9.0
19	-8.9	-9.2	-10.0	-10.2	-9.8	-10.3	-11.9	-12.3	-12.4	-11.1	-11.1	31.3	31.3	36.7	40.2	43.6	49.4	4.5	4.2	6.6	4.4	3.9
20	-10.3	-10.2	-10.0	-10.2	-9.8	-10.3	-18.1	-18.0	-17.9	-19.0	-17.9	27.1	28.9	36.7	40.2	43.6	49.4	5.0	5.2	5.3	3.4	3.4
21	-10.5	-10.5	-10.3	-10.2	-10.3	-10.3	-8.4	-8.6	-5.5	-9.5	-5.5	35.0	33.5	39.9	40.2	49.5	49.4	7.4	5.9	5.3	9.3	5.2

22	-10.0	-10.3	-10.0	-10.2	-9.8	-10.3	-13.7	-13.7	-13.9	-13.6	-13.6	27.7	28.4	36.7	40.2	43.6	49.4	3.4	3.5	3.6	3.4	3.4
23	-10.4	-10.3	-10.3	-10.2	-10.3	-10.3	-12.5	-12.5	-9.5	-12.7	-9.5	29.0	27.6	39.9	40.2	49.5	49.4	6.7	7.1	9.3	6.3	5.7
24	-10.6	-10.7	-10.0	-10.2	-9.8	-10.3	-7.4	-7.3	-7.7	-7.4	-7.0	21.3	22.2	36.7	40.2	43.6	49.4	2.3	2.7	3.2	2.2	2.2
25	-10.0	-10.0	-10.0	-10.2	-9.8	-10.3	-11.4	-12.5	-13.1	-9.0	-9.0	26.0	26.9	36.7	40.2	43.6	49.4	4.6	3.7	3.4	7.2	1.0
26	-9.2	-9.3	-10.3	-10.2	-10.3	-10.3	-12.8	-11.8	-11.3	-14.0	-9.1	38.2	38.2	39.9	40.2	49.5	49.4	6.1	6.0	15.5	3.6	3.6
27	-9.4	-9.2	-10.3	-10.2	-10.3	-10.3	-14.9	-14.5	-13.9	-15.2	-13.9	29.3	28.8	39.9	40.2	49.5	49.4	4.4	4.5	4.5	4.3	4.3
28	-10.1	-10.1	-10.0	-10.2	-9.8	-10.3	-13.2	-13.4	-13.6	-13.1	-13.1	25.9	24.4	36.7	40.2	43.6	49.4	3.5	3.7	3.4	3.4	3.4
29	-12.3	-12.0	-10.0	-10.2	-9.8	-10.3	-20.4	-21.4	-24.7	-20.7	-19.9	25.1	26.9	36.7	40.2	43.6	49.4	2.4	2.4	2.5	2.7	2.3
30	-12.3	-12.0	-10.0	-10.2	-9.8	-10.3	-12.0	-6.9	-8.7	-16.6	-6.3	25.0	25.4	36.7	40.2	43.6	49.4	3.1	2.7	1.5	3.1	1.5
31	-10.2	-10.1	-10.0	-10.2	-9.8	-10.3	-9.6	-9.5	-9.5	-9.7	-9.0	23.1	23.0	36.7	40.2	43.6	49.4	2.2	2.4	2.8	2.0	2.0
32	-13.9	-12.9	-10.0	-10.2	-9.8	-10.3	-15.4	-15.3	-20.9	-11.6	-11.6	23.6	23.8	36.7	40.2	43.6	49.4	2.5	2.5	2.8	1.9	1.9
33	-10.2	-9.9	-10.3	-10.2	-10.3	-10.3	-13.4	-14.6	-14.3	-11.4	-11.4	21.0	19.8	39.9	40.2	49.5	49.4	8.3	10.9	15.5	4.4	4.4
34	-13.3	-13.3	-10.3	-10.2	-10.3	-10.3	-12.1	-12.8	-14.0	-10.7	-10.7	17.0	19.1	39.9	40.2	49.5	49.4	6.3	7.1	6.0	4.6	4.6
35	-12.6	-12.9	-10.3	-10.2	-10.3	-10.3	-19.1	-19.1	-19.1	-19.1	-18.6	24.4	24.3	39.9	40.2	49.5	49.4	5.1	5.5	7.1	4.8	4.8
36	-10.6	-10.4	-10.3	-10.2	-10.3	-10.3	-12.2	-12.2	-11.4	-12.4	-11.4	21.1	20.7	39.9	40.2	49.5	49.4	5.9	5.6	4.4	6.2	4.4
37	-14.5	-14.8	-10.3	-10.2	-10.3	-10.3	-12.8	-12.9	-13.0	-12.5	-12.3	16.6	18.0	39.9	40.2	49.5	49.4	7.4	6.7	5.3	8.1	5.3

Appendix 8. Hydrometeorological variables for each of the rainfall-runoff events at M1 microcatchment. P means precipitation, Q means streamflow, RC means Runoff Coefficient, and Ant P means antecedent precipitation with the days considered are presented within the brackets. tot, average, and max, represents total, average, and maximum values.

Event	Qtot (mm)	Ptot (mm)	Qmax (mm/s)	Duration (h)	Pmax (mm/h)	Qaverage (mm/s)	Paverage (mm/h)	Time to peak (h)	RC	Recession time (h)	Ant P. (1 day) (mm)	Ant P, (3 days) (mm)	Ant P (5 days) (mm)	Ant P (7 days) (mm)
1	0.63	6.99	0.009	11.25	3.84	0.005	0.62	2.92	0.09	8.33	7.43	7.54	8.71	8.71
2	2.02	4.33	0.020	18.00	5.16	0.009	0.24	3.50	0.47	14.50	12.35	19.67	20.95	20.95
3	0.41	1.54	0.007	8.17	1.32	0.004	0.19	0.17	0.27	8.00	7.55	7.99	13.90	17.88
4	3.40	11.46	0.018	32.25	7.68	0.009	0.36	12.33	0.30	19.92	9.09	9.53	15.44	19.20
5	1.23	1.74	0.008	16.25	2.52	0.006	0.11	3.58	0.71	12.67	9.48	20.55	21.10	26.90
6	2.32	7.22	0.018	23.00	7.68	0.008	0.31	6.33	0.32	16.67	7.29	13.66	15.40	32.91
7	1.45	2.50	0.009	16.08	5.16	0.008	0.16	5.83	0.58	10.25	7.33	20.88	20.88	32.21
8	1.85	2.69	0.024	22.08	5.16	0.007	0.12	4.17	0.69	17.92	0.11	3.60	23.49	23.49
9	2.91	15.41	0.038	16.42	10.32	0.015	0.94	6.67	0.19	9.75	6.13	19.66	26.82	26.82
10	9.17	19.32	0.180	33.50	10.32	0.023	0.58	11.50	0.47	22.00	19.61	30.02	42.23	42.23
11	2.22	4.64	0.023	12.83	19.32	0.014	0.36	3.92	0.48	8.92	16.95	37.99	74.45	87.22
12	12.25	18.89	0.034	51.67	9	0.020	0.37	14.42	0.65	37.25	5.41	26.86	63.27	83.71
13	2.04	10.31	0.007	29.00	6.48	0.006	0.36	2.00	0.20	27.00	3.45	3.45	16.21	25.96
14	14.24	29.83	0.200	26.75	18	0.044	1.12	14.42	0.48	12.33	11.41	22.47	25.18	29.69
15	7.33	10.76	0.076	28.08	14.16	0.022	0.38	4.08	0.68	24.00	29.17	52.19	53.92	59.08
16	2.69	5.16	0.017	22.50	9	0.010	0.23	4.50	0.52	18.00	2.40	32.80	60.87	69.34
17	0.60	4.09	0.004	19.33	10.32	0.003	0.21	3.33	0.15	16.00	1.20	3.26	5.55	5.55
18	0.52	1.39	0.002	21.92	3.84	0.002	0.06	0.92	0.37	21.00	5.07	7.35	9.64	9.64
19	11.13	16.95	0.297	25.08	23.16	0.037	0.68	7.58	0.66	17.50	4.41	37.52	61.90	75.32
20	2.68	11.30	0.042	17.58	18	0.013	0.64	3.58	0.24	14.00	10.95	12.03	17.95	18.28
21	1.52	11.95	0.011	21.75	14.16	0.006	0.55	4.25	0.13	17.50	8.04	9.58	24.77	25.32
22	1.39	5.57	0.008	27.92	5.16	0.004	0.20	5.50	0.25	22.42	18.81	19.03	26.34	36.20
23	3.10	13.56	0.042	25.92	11.52	0.010	0.52	9.92	0.23	16.00	6.86	10.66	14.45	25.76
24	6.11	10.62	0.088	25.25	16.68	0.020	0.42	4.42	0.58	20.83	10.81	31.77	34.58	38.37

25	2.51	5.17	0.019	17.58	3.84	0.012	0.29	4.50	0.48	13.08	10.62	34.54	44.98	45.20
26	3.59	7.50	0.021	25.00	6.48	0.012	0.30	4.42	0.48	20.58	5.17	26.60	47.56	50.37
27	5.93	12.08	0.010	94.42	5.16	0.005	0.13	22.00	0.49	72.42	2.51	2.51	16.87	19.70
28	9.99	10.95	0.173	27.33	13.08	0.030	0.40	4.33	0.91	23.00	9.79	28.97	33.14	43.88
29	1.72	3.72	0.006	34.00	3.84	0.004	0.11	12.75	0.46	21.25	0.22	2.42	14.48	14.48
30	8.45	17.15	0.039	29.42	9.12	0.024	0.58	7.58	0.49	21.83	5.36	28.08	45.28	49.78
31	3.59	4.38	0.028	16.33	14.4	0.018	0.27	5.00	0.82	11.33	12.42	33.57	61.55	64.96
32	3.58	8.46	0.019	29.42	10.44	0.010	0.29	7.67	0.42	21.75	4.51	9.33	31.84	52.58
33	2.60	6.27	0.013	23.25	3.96	0.009	0.27	11.50	0.41	11.75	4.73	13.96	18.91	40.44
34	2.26	7.02	0.010	24.83	11.76	0.008	0.28	5.75	0.32	19.08	0.22	9.79	18.25	25.18
35	1.54	4.18	0.010	17.25	6.6	0.007	0.24	6.67	0.37	10.58	7.02	9.99	19.12	32.09
36	1.55	3.63	0.007	24.83	5.28	0.005	0.15	6.50	0.43	18.33	2.97	6.71	12.74	23.30
37	1.39	3.63	0.011	14.00	5.28	0.008	0.26	5.00	0.38	9.00	4.18	11.42	21.21	31.76
38	2.26	9.38	0.011	37.58	5.16	0.005	0.25	12.83	0.24	24.75	0.11	4.05	6.80	18.31
39	4.23	10.55	0.059	10.92	9.12	0.032	0.97	7.00	0.40	3.92	8.57	14.62	27.91	32.20
40	6.53	11.44	0.079	13.42	3.96	0.041	0.85	6.50	0.57	6.92	14.95	23.74	32.54	38.79
41	19.41	26.90	0.143	27.92	17.04	0.058	0.96	6.33	0.72	21.58	21.99	32.10	42.88	50.12
42	20.68	25.71	0.171	40.58	10.44	0.042	0.63	19.92	0.80	20.67	7.92	53.73	63.29	71.32
43	2.51	4.38	0.021	15.67	15.72	0.013	0.28	4.33	0.57	11.33	1.87	11.99	37.48	83.18
44	2.94	4.03	0.007	46.75	3.84	0.005	0.09	7.50	0.73	39.25	2.59	10.04	13.65	22.58
45	11.74	22.23	0.024	81.00	23.16	0.012	0.27	24.50	0.53	56.50	0.64	7.26	15.15	18.32
46	5.74	9.79	0.025	24.08	5.28	0.020	0.41	15.25	0.59	8.83	18.30	21.71	34.09	46.77
47	4.37	9.82	0.054	19.83	7.68	0.018	0.50	7.42	0.45	12.42	13.56	24.54	24.76	28.66
48	1.42	8.45	0.011	17.92	17.04	0.007	0.47	4.33	0.17	13.58	2.20	3.63	3.74	4.07
49	1.56	5.37	0.009	21.42	10.44	0.006	0.25	4.83	0.29	16.58	0.88	17.25	20.77	20.99
50	11.64	22.06	0.152	24.92	17.04	0.039	0.89	10.08	0.53	14.83	5.37	7.24	24.82	26.25
51	5.20	7.25	0.039	21.25	13.08	0.020	0.34	5.58	0.72	15.67	22.06	28.31	44.68	48.20
52	1.68	3.32	0.013	15.67	2.52	0.009	0.21	4.25	0.51	11.42	2.26	13.76	35.30	56.15

53	4.83	11.97	0.022	59.92	23.16	0.007	0.20	4.33	0.40	55.58	0.00	6.13	17.63	39.17
54	8.73	14.47	0.067	88.92	20.52	0.008	0.16	13.83	0.60	75.08	0.99	11.97	15.84	24.76
55	2.36	5.25	0.030	10.42	11.76	0.019	0.50	3.75	0.45	6.67	0.22	38.27	41.90	46.16
56	2.09	2.86	0.014	17.25	3.96	0.010	0.17	5.75	0.73	11.50	5.06	16.26	22.64	28.36
57	2.20	5.94	0.026	9.58	3.96	0.019	0.62	4.92	0.37	4.67	15.73	21.56	21.78	21.78
58	9.97	12.68	0.075	50.67	12.84	0.016	0.25	5.92	0.79	44.75	2.42	10.35	31.48	37.77
59	6.08	12.27	0.041	41.67	25.68	0.012	0.29	2.17	0.50	39.50	0.00	13.56	22.92	44.16
60	5.62	18.30	0.075	19.00	17.04	0.025	0.96	5.08	0.31	13.92	0.88	4.94	15.79	29.79
61	2.62	4.73	0.026	12.17	3.96	0.018	0.39	7.00	0.55	5.17	18.26	28.82	29.15	29.15
62	3.51	6.17	0.013	27.08	14.16	0.011	0.23	2.75	0.57	24.33	2.18	51.89	62.95	65.66
63	2.68	7.81	0.026	22.33	7.92	0.010	0.35	4.92	0.34	17.42	9.33	12.08	12.30	12.52
64	2.29	11.19	0.031	15.58	13.08	0.012	0.72	4.25	0.20	11.33	4.18	4.73	4.73	4.73
65	1.37	3.30	0.013	12.83	2.64	0.009	0.26	4.67	0.41	8.17	13.28	15.92	15.92	15.92
66	5.15	8.80	0.027	25.67	3.96	0.017	0.34	7.00	0.59	18.67	1.98	26.26	65.15	86.14
67	0.87	0.99	0.006	13.50	1.32	0.005	0.07	4.17	0.87	9.33	0.66	4.51	16.81	21.65
68	1.42	2.97	0.006	22.83	5.28	0.005	0.13	5.67	0.48	17.17	1.43	5.39	10.87	20.88
69	2.03	11.22	0.030	11.42	3.96	0.015	0.98	5.92	0.18	5.50	5.83	10.45	10.67	10.67
70	4.92	9.14	0.021	32.67	5.16	0.013	0.28	8.25	0.54	24.42	0.66	17.71	24.29	35.75
71	1.56	5.59	0.014	21.50	6.48	0.006	0.26	3.25	0.28	18.25	5.47	8.07	12.69	27.79
72	1.07	3.79	0.003	33.17	6.48	0.003	0.11	16.67	0.28	16.50	0.22	24.49	26.03	41.22

Appendix 9. Hydrometeorological variables for each of the rainfall-runoff events at M2 microcatchment. P means precipitation, Q means streamflow, RC means Runoff Coefficient, and Ant P means antecedent precipitation with the days considered are presented within the brackets. tot, average, and max, represents total, average, and maximum values.

Event	Qtot (mm)	Ptot (mm)	Qmax (mm/s)	Duration (h)	Pmax (mm/h)	Qaverage (mm/s)	Paverage (mm/h)	Time to peak (h)	RC	Recession time (h)	Ant P. (1 day) (mm)	Ant P, (3 days) (mm)	Ant P (5 days) (mm)	Ant P (7 days) (mm)
1	0.82	6.99	0.009	11.25	3.84	0.006	0.62	2.08	0.12	9.17	7.43	7.54	8.71	8.71
2	1.92	4.33	0.014	18.00	5.16	0.009	0.24	4.42	0.44	13.58	12.35	19.67	20.95	20.95
3	0.49	1.54	0.007	8.17	1.32	0.005	0.19	0.08	0.32	8.08	7.55	7.99	13.90	17.88
4	3.71	11.46	0.018	32.25	7.68	0.010	0.36	16.92	0.32	15.33	9.09	9.53	15.44	19.20
5	1.46	1.74	0.009	16.25	2.52	0.008	0.11	2.42	0.84	13.83	9.48	20.55	21.10	26.90
6	2.80	7.22	0.015	23.00	7.68	0.010	0.31	6.58	0.39	16.42	7.29	13.66	15.40	32.91
7	1.67	2.50	0.009	16.08	5.16	0.009	0.16	5.33	0.67	10.75	7.33	20.88	20.88	32.21
8	1.39	2.69	0.007	22.08	5.16	0.005	0.12	4.67	0.51	17.42	0.11	3.60	23.49	23.49
9	2.06	15.41	0.027	16.42	10.32	0.010	0.94	6.17	0.13	10.25	6.13	19.66	26.82	26.82
10	9.52	19.32	0.116	33.50	10.32	0.024	0.58	11.58	0.49	21.92	19.61	30.02	42.23	42.23
11	2.06	4.64	0.018	12.83	19.32	0.013	0.36	3.58	0.44	9.25	16.95	37.99	74.45	87.22
12	11.42	18.89	0.026	51.67	9	0.018	0.37	14.25	0.60	37.42	5.41	26.86	63.27	83.71
13	2.55	10.31	0.008	29.00	6.48	0.007	0.36	21.17	0.25	7.83	3.45	3.45	16.21	25.96
14	15.09	29.83	0.177	26.75	18	0.047	1.12	14.58	0.51	12.17	11.41	22.47	25.18	29.69
15	7.46	10.76	0.061	28.08	14.16	0.022	0.38	3.75	0.69	24.33	29.17	52.19	53.92	59.08
16	2.95	5.16	0.016	22.50	9	0.011	0.23	3.75	0.57	18.75	2.40	32.80	60.87	69.34
17	0.92	4.09	0.006	19.33	10.32	0.004	0.21	2.42	0.22	16.92	1.20	3.26	5.55	5.55
18	0.82	1.39	0.003	21.92	3.84	0.003	0.06	6.25	0.59	15.67	5.07	7.35	9.64	9.64
19	11.80	16.95	0.288	25.08	23.16	0.039	0.68	8.17	0.70	16.92	4.41	37.52	61.90	75.32
20	2.76	11.30	0.039	17.58	18	0.013	0.64	3.17	0.24	14.42	10.95	12.03	17.95	18.28
21	2.04	11.95	0.012	21.75	14.16	0.008	0.55	4.33	0.17	17.42	8.04	9.58	24.77	25.32
22	1.96	5.57	0.010	27.92	5.16	0.006	0.20	4.58	0.35	23.33	18.81	19.03	26.34	36.20
23	3.15	13.56	0.034	25.92	11.52	0.010	0.52	9.83	0.23	16.08	6.86	10.66	14.45	25.76
24	7.52	10.62	0.109	25.25	16.68	0.025	0.42	4.67	0.71	20.58	10.81	31.77	34.58	38.37
25	2.61	5.17	0.017	17.58	3.84	0.012	0.29	3.75	0.51	13.83	10.62	34.54	44.98	45.20
26	3.46	7.50	0.016	25.00	6.48	0.012	0.30	4.08	0.46	20.92	5.17	26.60	47.56	50.37

27	7.64	12.08	0.012	94.42	5.16	0.007	0.13	21.42	0.63	73.00	2.51	2.51	16.87	19.70
28	9.85	10.95	0.126	27.33	13.08	0.030	0.40	5.08	0.90	22.25	9.79	28.97	33.14	43.88
29	2.19	3.72	0.007	34.00	3.84	0.005	0.11	12.42	0.59	21.58	0.22	2.42	14.48	14.48
30	9.05	17.15	0.045	29.42	9.12	0.026	0.58	7.58	0.53	21.83	5.36	28.08	45.28	49.78
31	3.83	4.38	0.029	16.33	14.4	0.020	0.27	4.42	0.88	11.92	12.42	33.57	61.55	64.96
32	4.43	8.46	0.019	29.42	10.44	0.013	0.29	9.67	0.52	19.75	4.51	9.33	31.84	52.58
33	3.01	6.27	0.014	23.25	3.96	0.011	0.27	11.08	0.48	12.17	4.73	13.96	18.91	40.44
34	2.80	7.02	0.012	24.83	11.76	0.009	0.28	8.17	0.40	16.67	0.22	9.79	18.25	25.18
35	1.89	4.18	0.011	17.25	6.6	0.009	0.24	6.33	0.45	10.92	7.02	9.99	19.12	32.09
36	2.25	3.63	0.009	24.83	5.28	0.008	0.15	5.67	0.62	19.17	2.97	6.71	12.74	23.30
37	1.62	3.63	0.011	14.00	5.28	0.010	0.26	4.25	0.45	9.75	4.18	11.42	21.21	31.76
38	2.76	9.38	0.011	37.58	5.16	0.006	0.25	12.67	0.29	24.92	0.11	4.05	6.80	18.31
39	3.71	10.55	0.046	10.92	9.12	0.028	0.97	6.50	0.35	4.42	8.57	14.62	27.91	32.20
40	6.17	11.44	0.063	13.42	3.96	0.038	0.85	6.42	0.54	7.00	14.95	23.74	32.54	38.79
41	19.14	26.90	0.114	27.92	17.04	0.057	0.96	8.00	0.71	19.92	21.99	32.10	42.88	50.12
42	21.26	25.71	0.149	40.58	10.44	0.044	0.63	20.08	0.83	20.50	7.92	53.73	63.29	71.32
43	2.91	4.38	0.021	15.67	15.72	0.015	0.28	3.92	0.67	11.75	1.87	11.99	37.48	83.18
44	3.76	4.03	0.009	46.75	3.84	0.007	0.09	7.17	0.93	39.58	2.59	10.04	13.65	22.58
45	11.82	22.23	0.023	81.00	23.16	0.012	0.27	23.33	0.53	57.67	0.64	7.26	15.15	18.32
46	5.39	9.79	0.022	24.08	5.28	0.019	0.41	15.00	0.55	9.08	18.30	21.71	34.09	46.77
47	5.34	9.82	0.061	19.83	7.68	0.022	0.50	7.92	0.54	11.92	13.56	24.54	24.76	28.66
48	1.92	8.45	0.012	17.92	17.04	0.009	0.47	4.08	0.23	13.83	2.20	3.63	3.74	4.07
49	1.87	5.37	0.010	21.42	10.44	0.007	0.25	4.67	0.35	16.75	0.88	17.25	20.77	20.99
50	12.15	22.06	0.132	24.92	17.04	0.041	0.89	10.42	0.55	14.50	5.37	7.24	24.82	26.25
51	5.31	7.25	0.037	21.25	13.08	0.021	0.34	6.17	0.73	15.08	22.06	28.31	44.68	48.20
52	1.80	3.32	0.013	15.67	2.52	0.010	0.21	3.92	0.54	11.75	2.26	13.76	35.30	56.15
53	7.40	11.97	0.042	59.92	23.16	0.010	0.20	5.33	0.62	54.58	0.00	6.13	17.63	39.17
54	10.59	14.47	0.062	88.92	20.52	0.010	0.16	14.67	0.73	74.25	0.99	11.97	15.84	24.76
55	2.25	5.25	0.026	10.42	11.76	0.018	0.50	4.00	0.43	6.42	0.22	38.27	41.90	46.16
56	2.32	2.86	0.014	17.25	3.96	0.011	0.17	6.17	0.81	11.08	5.06	16.26	22.64	28.36

57	2.04	5.94	0.022	9.58	3.96	0.018	0.62	5.17	0.34	4.42	15.73	21.56	21.78	21.78
58	9.80	12.68	0.056	50.67	12.84	0.016	0.25	5.58	0.77	45.08	2.42	10.35	31.48	37.77
59	7.25	12.27	0.037	41.67	25.68	0.014	0.29	2.25	0.59	39.42	0.00	13.56	22.92	44.16
60	6.38	18.30	0.078	19.00	17.04	0.028	0.96	6.42	0.35	12.58	0.88	4.94	15.79	29.79
61	2.32	4.73	0.021	12.17	3.96	0.016	0.39	7.58	0.49	4.58	18.26	28.82	29.15	29.15
62	3.91	6.17	0.016	27.08	14.16	0.012	0.23	2.58	0.63	24.50	2.18	51.89	62.95	65.66
63	3.00	7.81	0.022	22.33	7.92	0.011	0.35	4.42	0.38	17.92	9.33	12.08	12.30	12.52
64	1.98	11.19	0.021	15.58	13.08	0.011	0.72	4.33	0.18	11.25	4.18	4.73	4.73	4.73
65	1.31	3.30	0.011	12.83	2.64	0.009	0.26	4.17	0.40	8.67	13.28	15.92	15.92	15.92
66	5.94	8.80	0.027	25.67	3.96	0.019	0.34	7.00	0.68	18.67	1.98	26.26	65.15	86.14
67	0.84	0.99	0.008	13.50	1.32	0.008	0.07	2.50	0.85	11.00	0.66	4.51	16.81	21.65
68	2.11	2.97	0.009	22.83	5.28	0.008	0.13	5.17	0.71	17.67	1.43	5.39	10.87	20.88
69	1.97	11.22	0.026	11.42	3.96	0.014	0.98	5.50	0.18	5.92	5.83	10.45	10.67	10.67
70	5.12	9.14	0.020	32.67	5.16	0.013	0.28	8.83	0.56	23.83	0.66	17.71	24.29	35.75
71	1.59	5.59	0.011	21.50	6.48	0.006	0.26	3.42	0.28	18.08	5.47	8.07	12.69	27.79
72	1.55	3.79	0.004	33.17	6.48	0.004	0.11	4.08	0.41	29.08	0.22	24.49	26.03	41.22

Appendix 10. Hydrometeorological variables for each of the rainfall-runoff events at M3 microcatchment. P means precipitation, Q means streamflow, RC means Runoff Coefficient, and Ant P means antecedent precipitation with the days considered are presented within the brackets. tot, average, and max, represents total, average, and maximum values.

Event	Qtot (mm)	Ptot (mm)	Qmax (mm/s)	Duration (h)	Pmax (mm/h)	Qaverage (mm/s)	Paverage (mm/h)	Time to peak (h)	RC	Recession time (h)	Ant P. (1 day) (mm)	Ant P, (3 days) (mm)	Ant P (5 days) (mm)	Ant P (7 days) (mm)
1	0.89	6.99	0.009	11.25	3.84	0.007	0.62	2.42	0.13	8.83	7.43	7.54	8.71	8.71
2	2.35	4.33	0.020	18.00	5.16	0.011	0.24	3.75	0.54	14.25	12.35	19.67	20.95	20.95
3	0.46	1.54	0.005	8.17	1.32	0.005	0.19	0.08	0.30	8.08	7.55	7.99	13.90	17.88
4	4.39	11.46	0.024	32.25	7.68	0.011	0.36	12.08	0.38	20.17	9.09	9.53	15.44	19.20
5	1.52	1.74	0.010	16.25	2.52	0.008	0.11	3.33	0.87	12.92	9.48	20.55	21.10	26.90
6	3.56	7.22	0.025	23.00	7.68	0.013	0.31	6.50	0.49	16.50	7.29	13.66	15.40	32.91
7	1.76	2.50	0.010	16.08	5.16	0.009	0.16	5.67	0.70	10.42	7.33	20.88	20.88	32.21
8	1.27	2.69	0.005	22.08	5.16	0.005	0.12	4.67	0.47	17.42	0.11	3.60	23.49	23.49
9	4.34	15.41	0.067	16.42	10.32	0.022	0.94	6.33	0.28	10.08	6.13	19.66	26.82	26.82
10	12.27	19.32	0.144	33.50	10.32	0.031	0.58	11.58	0.63	21.92	19.61	30.02	42.23	42.23
11	2.83	4.64	0.026	12.83	19.32	0.018	0.36	4.33	0.61	8.50	16.95	37.99	74.45	87.22
12	14.72	18.89	0.045	51.67	9	0.024	0.37	14.92	0.78	36.75	5.41	26.86	63.27	83.71
13	3.12	10.31	0.011	29.00	6.48	0.009	0.36	15.17	0.30	13.83	3.45	3.45	16.21	25.96
14	23.46	29.83	0.284	26.75	18	0.073	1.12	14.50	0.79	12.25	11.41	22.47	25.18	29.69
15	9.30	10.76	0.092	28.08	14.16	0.028	0.38	4.33	0.86	23.75	29.17	52.19	53.92	59.08
16	3.19	5.16	0.017	22.50	9	0.012	0.23	4.33	0.62	18.17	2.40	32.80	60.87	69.34
17	1.09	4.09	0.006	19.33	10.32	0.005	0.21	3.75	0.27	15.58	1.20	3.26	5.55	5.55
18	1.08	1.39	0.004	21.92	3.84	0.004	0.06	6.58	0.78	15.33	5.07	7.35	9.64	9.64
19	11.08	16.95	0.191	25.08	23.16	0.037	0.68	8.50	0.65	16.58	4.41	37.52	61.90	75.32
20	2.49	11.30	0.028	17.58	18	0.012	0.64	4.25	0.22	13.33	10.95	12.03	17.95	18.28
21	4.58	11.95	0.039	21.75	14.16	0.018	0.55	2.00	0.38	19.75	8.04	9.58	24.77	25.32
22	3.81	5.57	0.026	27.92	5.16	0.011	0.20	5.08	0.68	22.83	18.81	19.03	26.34	36.20
23	5.30	13.56	0.065	25.92	11.52	0.017	0.52	10.08	0.39	15.83	6.86	10.66	14.45	25.76
24	9.02	10.62	0.128	25.25	16.68	0.030	0.42	4.00	0.85	21.25	10.81	31.77	34.58	38.37
25	3.51	5.17	0.027	17.58	3.84	0.017	0.29	4.50	0.68	13.08	10.62	34.54	44.98	45.20
26	4.53	7.50	0.025	25.00	6.48	0.015	0.30	4.83	0.60	20.17	5.17	26.60	47.56	50.37

27	8.43	12.08	0.013	94.42	5.16	0.007	0.13	26.42	0.70	68.00	2.51	2.51	16.87	19.70
28	10.51	10.95	0.149	27.33	13.08	0.032	0.40	4.83	0.96	22.50	9.79	28.97	33.14	43.88
29	2.40	3.72	0.007	34.00	3.84	0.006	0.11	13.75	0.65	20.25	0.22	2.42	14.48	14.48
30	14.99	17.15	0.116	29.42	9.12	0.042	0.58	8.08	0.87	21.33	5.36	28.08	45.28	49.78
31	4.19	4.38	0.033	16.33	14.4	0.021	0.27	5.83	0.96	10.50	12.42	33.57	61.55	64.96
32	5.38	8.46	0.026	29.42	10.44	0.015	0.29	10.67	0.64	18.75	4.51	9.33	31.84	52.58
33	3.84	6.27	0.020	23.25	3.96	0.014	0.27	6.42	0.61	16.83	4.73	13.96	18.91	40.44
34	3.92	7.02	0.021	24.83	11.76	0.013	0.28	8.50	0.56	16.33	0.22	9.79	18.25	25.18
35	2.36	4.18	0.015	17.25	6.6	0.011	0.24	6.83	0.57	10.42	7.02	9.99	19.12	32.09
36	2.60	3.63	0.012	24.83	5.28	0.009	0.15	6.33	0.72	18.50	2.97	6.71	12.74	23.30
37	2.06	3.63	0.016	14.00	5.28	0.012	0.26	4.25	0.57	9.75	4.18	11.42	21.21	31.76
38	3.17	9.38	0.013	37.58	5.16	0.007	0.25	13.17	0.34	24.42	0.11	4.05	6.80	18.31
39	4.11	10.55	0.049	10.92	9.12	0.031	0.97	6.92	0.39	4.00	8.57	14.62	27.91	32.20
40	7.11	11.44	0.076	13.42	3.96	0.044	0.85	6.92	0.62	6.50	14.95	23.74	32.54	38.79
41	23.10	26.90	0.187	27.92	17.04	0.069	0.96	6.50	0.86	21.42	21.99	32.10	42.88	50.12
42	22.00	25.71	0.149	40.58	10.44	0.045	0.63	19.83	0.86	20.75	7.92	53.73	63.29	71.32
43	3.12	4.38	0.026	15.67	15.72	0.017	0.28	5.00	0.71	10.67	1.87	11.99	37.48	83.18
44	3.88	4.03	0.009	46.75	3.84	0.007	0.09	17.08	0.96	29.67	2.59	10.04	13.65	22.58
45	12.86	22.23	0.030	81.00	23.16	0.013	0.27	24.17	0.58	56.83	0.64	7.26	15.15	18.32
46	5.95	9.79	0.025	24.08	5.28	0.021	0.41	16.00	0.61	8.08	18.30	21.71	34.09	46.77
47	7.19	9.82	0.080	19.83	7.68	0.030	0.50	7.67	0.73	12.17	13.56	24.54	24.76	28.66
48	2.50	8.45	0.018	17.92	17.04	0.012	0.47	4.75	0.30	13.17	2.20	3.63	3.74	4.07
49	2.53	5.37	0.017	21.42	10.44	0.010	0.25	5.17	0.47	16.25	0.88	17.25	20.77	20.99
50	13.30	22.06	0.123	24.92	17.04	0.044	0.89	10.50	0.60	14.42	5.37	7.24	24.82	26.25
51	6.34	7.25	0.050	21.25	13.08	0.025	0.34	5.83	0.87	15.42	22.06	28.31	44.68	48.20
52	1.91	3.32	0.012	15.67	2.52	0.010	0.21	4.00	0.58	11.67	2.26	13.76	35.30	56.15
53	9.98	11.97	0.082	59.92	23.16	0.014	0.20	4.00	0.83	55.92	0.00	6.13	17.63	39.17
54	13.65	14.47	0.107	88.92	20.52	0.013	0.16	13.42	0.94	75.50	0.99	11.97	15.84	24.76
55	2.67	5.25	0.038	10.42	11.76	0.021	0.50	4.92	0.51	5.50	0.22	38.27	41.90	46.16
56	2.51	2.86	0.015	17.25	3.96	0.012	0.17	6.17	0.88	11.08	5.06	16.26	22.64	28.36

57	2.55	5.94	0.030	9.58	3.96	0.022	0.62	4.50	0.43	5.08	15.73	21.56	21.78	21.78
58	10.47	12.68	0.086	50.67	12.84	0.017	0.25	6.17	0.83	44.50	2.42	10.35	31.48	37.77
59	5.91	12.27	0.020	41.67	25.68	0.012	0.29	3.33	0.48	38.33	0.00	13.56	22.92	44.16
60	6.70	18.30	0.086	19.00	17.04	0.029	0.96	4.83	0.37	14.17	0.88	4.94	15.79	29.79
61	3.06	4.73	0.033	12.17	3.96	0.021	0.39	6.17	0.65	6.00	18.26	28.82	29.15	29.15
62	4.56	6.17	0.018	27.08	14.16	0.014	0.23	3.42	0.74	23.67	2.18	51.89	62.95	65.66
63	4.46	7.81	0.044	22.33	7.92	0.017	0.35	4.75	0.57	17.58	9.33	12.08	12.30	12.52
64	2.66	11.19	0.039	15.58	13.08	0.014	0.72	4.33	0.24	11.25	4.18	4.73	4.73	4.73
65	1.81	3.30	0.019	12.83	2.64	0.012	0.26	3.92	0.55	8.92	13.28	15.92	15.92	15.92
66	6.44	8.80	0.035	25.67	3.96	0.021	0.34	7.42	0.73	18.25	1.98	26.26	65.15	86.14
67	0.86	0.99	0.009	13.50	1.32	0.008	0.07	2.83	0.87	10.67	0.66	4.51	16.81	21.65
68	2.41	2.97	0.011	22.83	5.28	0.009	0.13	5.42	0.81	17.42	1.43	5.39	10.87	20.88
69	3.28	11.22	0.056	11.42	3.96	0.024	0.98	5.75	0.29	5.67	5.83	10.45	10.67	10.67
70	5.62	9.14	0.023	32.67	5.16	0.014	0.28	9.00	0.61	23.67	0.66	17.71	24.29	35.75
71	1.79	5.59	0.012	21.50	6.48	0.007	0.26	3.92	0.32	17.58	5.47	8.07	12.69	27.79
72	3.04	3.79	0.011	33.17	6.48	0.008	0.11	4.75	0.80	28.42	0.22	24.49	26.03	41.22

Appendix 11. Hydrometeorological variables for each of the rainfall-runoff events at M4 microcatchment. P means precipitation, Q means streamflow, RC means Runoff Coefficient, and Ant P means antecedent precipitation with the days considered are presented within the brackets. tot, average, and max, represents total, average, and maximum values.

Event	Qtot (mm)	Ptot (mm)	Qmax (mm/s)	Duration (h)	Pmax (mm/h)	Qaverage (mm/s)	Paverage (mm/h)	Time to peak (h)	RC	Recession time (h)	Ant P. (1 day) (mm)	Ant P, (3 days) (mm)	Ant P (5 days) (mm)	Ant P (7 days) (mm)
1	0.76	6.99	0.008	11.25	3.84	0.006	0.62	4.33	0.11	6.92	7.43	7.54	8.71	8.71
2	1.96	4.33	0.018	18.00	5.16	0.009	0.24	3.67	0.45	14.33	12.35	19.67	20.95	20.95
3	0.35	1.54	0.004	8.17	1.32	0.004	0.19	0.17	0.22	8.00	7.55	7.99	13.90	17.88
4	3.67	11.46	0.019	32.25	7.68	0.009	0.36	12.75	0.32	19.50	9.09	9.53	15.44	19.20
5	1.21	1.74	0.008	16.25	2.52	0.006	0.11	3.50	0.70	12.75	9.48	20.55	21.10	26.90
6	2.95	7.22	0.022	23.00	7.68	0.011	0.31	6.83	0.41	16.17	7.29	13.66	15.40	32.91
7	1.44	2.50	0.008	16.08	5.16	0.007	0.16	5.83	0.58	10.25	7.33	20.88	20.88	32.21
8	0.99	2.69	0.004	22.08	5.16	0.004	0.12	19.33	0.37	2.75	0.11	3.60	23.49	23.49
9	3.74	15.41	0.054	16.42	10.32	0.019	0.94	6.67	0.24	9.75	6.13	19.66	26.82	26.82
10	10.81	19.32	0.128	33.50	10.32	0.027	0.58	11.83	0.56	21.67	19.61	30.02	42.23	42.23
11	2.54	4.64	0.022	12.83	19.32	0.017	0.36	4.33	0.55	8.50	16.95	37.99	74.45	87.22
12	13.45	18.89	0.038	51.67	9	0.022	0.37	15.50	0.71	36.17	5.41	26.86	63.27	83.71
13	2.45	10.31	0.009	29.00	6.48	0.007	0.36	15.33	0.24	13.67	3.45	3.45	16.21	25.96
14	20.14	29.83	0.232	26.75	18	0.063	1.12	14.67	0.68	12.08	11.41	22.47	25.18	29.69
15	9.02	10.76	0.082	28.08	14.16	0.027	0.38	4.42	0.84	23.67	29.17	52.19	53.92	59.08
16	3.11	5.16	0.016	22.50	9	0.012	0.23	4.25	0.60	18.25	2.40	32.80	60.87	69.34
17	0.92	4.09	0.005	19.33	10.32	0.004	0.21	2.67	0.22	16.67	1.20	3.26	5.55	5.55
18	0.86	1.39	0.004	21.92	3.84	0.003	0.06	6.08	0.62	15.83	5.07	7.35	9.64	9.64
19	10.16	16.95	0.173	25.08	23.16	0.034	0.68	8.33	0.60	16.75	4.41	37.52	61.90	75.32
20	2.54	11.30	0.030	17.58	18	0.012	0.64	4.33	0.23	13.25	10.95	12.03	17.95	18.28
21	3.91	11.95	0.030	21.75	14.16	0.015	0.55	2.58	0.33	19.17	8.04	9.58	24.77	25.32
22	3.23	5.57	0.020	27.92	5.16	0.010	0.20	5.00	0.58	22.92	18.81	19.03	26.34	36.20
23	4.75	13.56	0.055	25.92	11.52	0.015	0.52	10.42	0.35	15.50	6.86	10.66	14.45	25.76
24	8.50	10.62	0.112	25.25	16.68	0.028	0.42	4.42	0.80	20.83	10.81	31.77	34.58	38.37
25	3.24	5.17	0.024	17.58	3.84	0.015	0.29	4.58	0.63	13.00	10.62	34.54	44.98	45.20
26	4.19	7.50	0.022	25.00	6.48	0.014	0.30	4.83	0.56	20.17	5.17	26.60	47.56	50.37

27	6.51	12.08	0.011	94.42	5.16	0.006	0.13	26.33	0.54	68.08	2.51	2.51	16.87	19.70
28	9.33	10.95	0.127	27.33	13.08	0.028	0.40	5.08	0.85	22.25	9.79	28.97	33.14	43.88
29	1.83	3.72	0.005	34.00	3.84	0.004	0.11	13.25	0.49	20.75	0.22	2.42	14.48	14.48
30	12.82	17.15	0.097	29.42	9.12	0.036	0.58	8.42	0.75	21.00	5.36	28.08	45.28	49.78
31	3.81	4.38	0.030	16.33	14.4	0.019	0.27	5.58	0.87	10.75	12.42	33.57	61.55	64.96
32	4.51	8.46	0.022	29.42	10.44	0.013	0.29	10.58	0.53	18.83	4.51	9.33	31.84	52.58
33	3.20	6.27	0.016	23.25	3.96	0.011	0.27	6.58	0.51	16.67	4.73	13.96	18.91	40.44
34	3.20	7.02	0.017	24.83	11.76	0.011	0.28	8.50	0.46	16.33	0.22	9.79	18.25	25.18
35	1.93	4.18	0.012	17.25	6.6	0.009	0.24	6.75	0.46	10.50	7.02	9.99	19.12	32.09
36	2.07	3.63	0.009	24.83	5.28	0.007	0.15	6.33	0.57	18.50	2.97	6.71	12.74	23.30
37	1.70	3.63	0.013	14.00	5.28	0.010	0.26	4.42	0.47	9.58	4.18	11.42	21.21	31.76
38	2.45	9.38	0.010	37.58	5.16	0.005	0.25	13.42	0.26	24.17	0.11	4.05	6.80	18.31
39	3.79	10.55	0.045	10.92	9.12	0.029	0.97	7.33	0.36	3.58	8.57	14.62	27.91	32.20
40	6.41	11.44	0.070	13.42	3.96	0.040	0.85	6.92	0.56	6.50	14.95	23.74	32.54	38.79
41	21.15	26.90	0.151	27.92	17.04	0.063	0.96	6.08	0.79	21.83	21.99	32.10	42.88	50.12
42	20.56	25.71	0.134	40.58	10.44	0.042	0.63	20.00	0.80	20.58	7.92	53.73	63.29	71.32
43	2.69	4.38	0.022	15.67	15.72	0.014	0.28	4.75	0.61	10.92	1.87	11.99	37.48	83.18
44	3.02	4.03	0.007	46.75	3.84	0.005	0.09	17.33	0.75	29.42	2.59	10.04	13.65	22.58
45	10.97	22.23	0.027	81.00	23.16	0.011	0.27	24.33	0.49	56.67	0.64	7.26	15.15	18.32
46	5.33	9.79	0.023	24.08	5.28	0.018	0.41	15.92	0.54	8.17	18.30	21.71	34.09	46.77
47	6.36	9.82	0.071	19.83	7.68	0.027	0.50	8.08	0.65	11.75	13.56	24.54	24.76	28.66
48	1.94	8.45	0.013	17.92	17.04	0.009	0.47	5.58	0.23	12.33	2.20	3.63	3.74	4.07
49	1.94	5.37	0.012	21.42	10.44	0.008	0.25	4.83	0.36	16.58	0.88	17.25	20.77	20.99
50	11.91	22.06	0.112	24.92	17.04	0.040	0.89	10.75	0.54	14.17	5.37	7.24	24.82	26.25
51	5.67	7.25	0.045	21.25	13.08	0.022	0.34	6.25	0.78	15.00	22.06	28.31	44.68	48.20
52	1.78	3.32	0.011	15.67	2.52	0.009	0.21	4.75	0.54	10.92	2.26	13.76	35.30	56.15
53	8.86	11.97	0.065	59.92	23.16	0.012	0.20	5.17	0.74	54.75	0.00	6.13	17.63	39.17
54	11.76	14.47	0.079	88.92	20.52	0.011	0.16	13.83	0.81	75.08	0.99	11.97	15.84	24.76
55	2.32	5.25	0.031	10.42	11.76	0.019	0.50	4.75	0.44	5.67	0.22	38.27	41.90	46.16
56	2.11	2.86	0.013	17.25	3.96	0.010	0.17	5.75	0.74	11.50	5.06	16.26	22.64	28.36

57	2.74	5.94	0.033	9.58	3.96	0.024	0.62	4.75	0.46	4.83	15.73	21.56	21.78	21.78
58	9.20	12.68	0.070	50.67	12.84	0.015	0.25	6.00	0.73	44.67	2.42	10.35	31.48	37.77
59	5.50	12.27	0.023	41.67	25.68	0.011	0.29	3.33	0.45	38.33	0.00	13.56	22.92	44.16
60	5.91	18.30	0.067	19.00	17.04	0.026	0.96	5.58	0.32	13.42	0.88	4.94	15.79	29.79
61	3.30	4.73	0.035	12.17	3.96	0.023	0.39	6.50	0.70	5.67	18.26	28.82	29.15	29.15
62	4.52	6.17	0.018	27.08	14.16	0.014	0.23	3.50	0.73	23.58	2.18	51.89	62.95	65.66
63	3.70	7.81	0.037	22.33	7.92	0.014	0.35	4.58	0.47	17.75	9.33	12.08	12.30	12.52
64	2.84	11.19	0.038	15.58	13.08	0.015	0.72	4.83	0.25	10.75	4.18	4.73	4.73	4.73
65	1.94	3.30	0.019	12.83	2.64	0.013	0.26	4.50	0.59	8.33	13.28	15.92	15.92	15.92
66	5.75	8.80	0.032	25.67	3.96	0.019	0.34	7.58	0.65	18.08	1.98	26.26	65.15	86.14
67	0.98	0.99	0.007	13.50	1.32	0.007	0.07	4.58	0.99	8.92	0.66	4.51	16.81	21.65
68	1.88	2.97	0.008	22.83	5.28	0.007	0.13	6.42	0.63	16.42	1.43	5.39	10.87	20.88
69	3.32	11.22	0.056	11.42	3.96	0.024	0.98	5.75	0.30	5.67	5.83	10.45	10.67	10.67
70	4.79	9.14	0.020	32.67	5.16	0.012	0.28	12.58	0.52	20.08	0.66	17.71	24.29	35.75
71	1.63	5.59	0.010	21.50	6.48	0.006	0.26	4.83	0.29	16.67	5.47	8.07	12.69	27.79
72	2.53	3.79	0.009	33.17	6.48	0.006	0.11	4.67	0.67	28.50	0.22	24.49	26.03	41.22

Appendix 12. Hydrometeorological variables for each of the rainfall-runoff events at M5 microcatchment. P means precipitation, Q means streamflow, RC means Runoff Coefficient, and Ant P means antecedent precipitation with the days considered are presented within the brackets. tot, average, and max, represents total, average, and maximum values.

Event	Qtot (mm)	Ptot (mm)	Qmax (mm/s)	Duration (h)	Pmax (mm/h)	Qaverage (mm/s)	Paverage (mm/h)	Time to peak (h)	RC	Recession time (h)	Ant P. (1 day) (mm)	Ant P, (3 days) (mm)	Ant P (5 days) (mm)	Ant P (7 days) (mm)
1	1.06	6.99	0.011	11.25	3.84	0.008	0.62	5.42	0.15	5.83	7.43	7.54	8.71	8.71
2	2.54	4.33	0.022	18.00	5.16	0.012	0.24	4.17	0.59	13.83	12.35	19.67	20.95	20.95
3	0.65	1.54	0.007	8.17	1.32	0.007	0.19	3.50	0.42	4.67	7.55	7.99	13.90	17.88
4	4.64	11.46	0.023	32.25	7.68	0.012	0.36	13.58	0.41	18.67	9.09	9.53	15.44	19.20
5	1.72	1.74	0.012	16.25	2.52	0.010	0.11	5.08	0.99	11.17	9.48	20.55	21.10	26.90
6	3.96	7.22	0.028	23.00	7.68	0.014	0.31	6.17	0.55	16.83	7.29	13.66	15.40	32.91
7	2.07	2.50	0.012	16.08	5.16	0.011	0.16	6.75	0.83	9.33	7.33	20.88	20.88	32.21
8	1.80	2.69	0.010	22.08	5.16	0.007	0.12	7.67	0.67	14.42	0.11	3.60	23.49	23.49
9	4.68	15.41	0.077	16.42	10.32	0.024	0.94	6.75	0.30	9.67	6.13	19.66	26.82	26.82
10	2.75	19.32	0.111	11.75	10.32	0.020	0.58	11.67	0.17	0.08	19.61	30.02	42.23	42.23
11	2.80	4.64	0.024	12.83	19.32	0.018	0.36	5.33	0.60	7.50	16.95	37.99	74.45	87.22
12	15.44	18.89	0.051	51.67	9	0.025	0.37	15.08	0.82	36.58	5.41	26.86	63.27	83.71
13	3.31	10.31	0.012	29.00	6.48	0.009	0.36	15.00	0.32	14.00	3.45	3.45	16.21	25.96
14	20.94	29.83	0.262	26.75	18	0.065	1.12	14.67	0.70	12.08	11.41	22.47	25.18	29.69
15	9.46	10.76	0.091	28.08	14.16	0.028	0.38	4.58	0.88	23.50	29.17	52.19	53.92	59.08
16	4.11	5.16	0.022	22.50	9	0.015	0.23	5.25	0.80	17.25	2.40	32.80	60.87	69.34
17	1.23	4.09	0.009	19.33	10.32	0.005	0.21	2.67	0.30	16.67	1.20	3.26	5.55	5.55
18	1.05	1.39	0.005	21.92	3.84	0.004	0.06	6.50	0.75	15.42	5.07	7.35	9.64	9.64
19	11.44	16.95	0.223	22.67	23.16	0.042	0.68	6.25	0.68	16.42	4.41	37.52	61.90	75.32
20	2.71	11.30	0.037	17.58	18	0.013	0.64	4.75	0.24	12.83	10.95	12.03	17.95	18.28
21	2.45	11.95	0.015	21.75	14.16	0.009	0.55	5.67	0.20	16.08	8.04	9.58	24.77	25.32
22	2.71	5.57	0.013	27.92	5.16	0.008	0.20	6.50	0.49	21.42	18.81	19.03	26.34	36.20
23	5.63	13.56	0.083	25.92	11.52	0.018	0.52	10.50	0.42	15.42	6.86	10.66	14.45	25.76
24	9.65	10.62	0.119	25.25	16.68	0.032	0.42	4.33	0.91	20.92	10.81	31.77	34.58	38.37
25	3.50	5.17	0.022	17.58	3.84	0.017	0.29	5.75	0.68	11.83	10.62	34.54	44.98	45.20

26	4.89	7.50	0.024	25.00	6.48	0.016	0.30	5.83	0.65	19.17	5.17	26.60	47.56	50.37
27	8.01	12.08	0.012	94.42	5.16	0.007	0.13	26.75	0.66	67.67	2.51	2.51	16.87	19.70
28	10.33	10.95	0.188	27.33	13.08	0.041	0.40	4.92	0.94	22.42	9.79	28.97	33.14	43.88
29	2.36	3.72	0.007	34.00	3.84	0.006	0.11	15.17	0.63	18.83	0.22	2.42	14.48	14.48
30	17.15	17.15	0.146	29.42	9.12	0.052	0.58	8.33	1.00	21.08	5.36	28.08	45.28	49.78
31	4.06	4.38	0.037	16.33	14.4	0.026	0.27	6.08	0.93	10.25	12.42	33.57	61.55	64.96
32	5.53	8.46	0.024	29.42	10.44	0.016	0.29	10.42	0.65	19.00	4.51	9.33	31.84	52.58
33	4.09	6.27	0.019	23.25	3.96	0.015	0.27	7.75	0.65	15.50	4.73	13.96	18.91	40.44
34	3.67	7.02	0.017	24.83	11.76	0.012	0.28	8.83	0.52	16.00	0.22	9.79	18.25	25.18
35	2.44	4.18	0.014	17.25	6.6	0.012	0.24	8.92	0.58	8.33	7.02	9.99	19.12	32.09
36	2.45	3.63	0.010	24.83	5.28	0.008	0.15	8.33	0.67	16.50	2.97	6.71	12.74	23.30
37	2.16	3.63	0.015	14.00	5.28	0.013	0.26	5.83	0.59	8.17	4.18	11.42	21.21	31.76
38	3.17	9.38	0.012	37.58	5.16	0.007	0.25	15.50	0.34	22.08	0.11	4.05	6.80	18.31
39	4.58	10.55	0.057	10.92	9.12	0.035	0.97	7.42	0.43	3.50	8.57	14.62	27.91	32.20
40	9.06	11.44	0.100	13.42	3.96	0.056	0.85	6.83	0.79	6.58	14.95	23.74	32.54	38.79
41	26.45	26.90	0.228	27.92	17.04	0.088	0.96	6.25	0.98	21.67	21.99	32.10	42.88	50.12
42	25.27	25.71	0.175	40.58	10.44	0.056	0.63	20.50	0.98	20.08	7.92	53.73	63.29	71.32
43	3.44	4.38	0.025	15.67	15.72	0.018	0.28	5.83	0.79	9.83	1.87	11.99	37.48	83.18
44	4.02	4.03	0.009	46.75	3.84	0.007	0.09	18.92	1.00	27.83	2.59	10.04	13.65	22.58
45	14.20	22.23	0.029	81.00	23.16	0.015	0.27	25.17	0.64	55.83	0.64	7.26	15.15	18.32
46	7.09	9.79	0.030	24.08	5.28	0.025	0.41	16.33	0.72	7.75	18.30	21.71	34.09	46.77
47	6.05	9.82	0.060	19.83	7.68	0.025	0.50	8.83	0.62	11.00	13.56	24.54	24.76	28.66
48	1.96	8.45	0.012	17.92	17.04	0.009	0.47	7.08	0.23	10.83	2.20	3.63	3.74	4.07
49	2.25	5.37	0.011	21.42	10.44	0.009	0.25	8.00	0.42	13.42	0.88	17.25	20.77	20.99
50	13.53	22.06	0.132	24.92	17.04	0.045	0.89	10.67	0.61	14.25	5.37	7.24	24.82	26.25
51	6.41	7.25	0.043	21.25	13.08	0.025	0.34	7.08	0.88	14.17	22.06	28.31	44.68	48.20
52	2.24	3.32	0.014	15.67	2.52	0.012	0.21	6.50	0.67	9.17	2.26	13.76	35.30	56.15
53	6.72	11.97	0.024	59.92	23.16	0.009	0.20	7.00	0.56	52.92	0.00	6.13	17.63	39.17
54	11.40	14.47	0.062	88.92	20.52	0.011	0.16	14.25	0.79	74.67	0.99	11.97	15.84	24.76
55	3.34	5.25	0.042	10.42	11.76	0.027	0.50	5.33	0.64	5.08	0.22	38.27	41.90	46.16

56	2.85	2.86	0.017	17.25	3.96	0.014	0.17	7.50	1.00	9.75	5.06	16.26	22.64	28.36
57	2.76	5.94	0.032	9.58	3.96	0.024	0.62	4.33	0.46	5.25	15.73	21.56	21.78	21.78
58	11.87	12.68	0.101	50.67	12.84	0.021	0.25	6.42	0.94	44.25	2.42	10.35	31.48	37.77
59	7.78	12.27	0.038	41.67	25.68	0.016	0.29	3.42	0.63	38.25	0.00	13.56	22.92	44.16
60	7.87	18.30	0.094	19.00	17.04	0.035	0.96	5.50	0.43	13.50	0.88	4.94	15.79	29.79
61	3.21	4.73	0.033	12.17	3.96	0.022	0.39	6.67	0.68	5.50	18.26	28.82	29.15	29.15
62	4.99	6.17	0.019	27.08	14.16	0.015	0.23	4.25	0.81	22.83	2.18	51.89	62.95	65.66
63	4.04	7.81	0.036	22.33	7.92	0.015	0.35	5.67	0.52	16.67	9.33	12.08	12.30	12.52
64	2.93	11.19	0.040	15.58	13.08	0.016	0.72	5.33	0.26	10.25	4.18	4.73	4.73	4.73
65	1.89	3.30	0.017	12.83	2.64	0.012	0.26	5.33	0.57	7.50	13.28	15.92	15.92	15.92
66	6.94	8.80	0.034	25.67	3.96	0.023	0.34	8.00	0.79	17.67	1.98	26.26	65.15	86.14
67	0.89	0.99	0.008	13.50	1.32	0.008	0.07	5.58	0.90	7.92	0.66	4.51	16.81	21.65
68	2.20	2.97	0.009	22.83	5.28	0.008	0.13	8.58	0.74	14.25	1.43	5.39	10.87	20.88
69	2.95	11.22	0.052	11.42	3.96	0.022	0.98	6.33	0.26	5.08	5.83	10.45	10.67	10.67
70	6.15	9.14	0.024	32.67	5.16	0.016	0.28	9.67	0.67	23.00	0.66	17.71	24.29	35.75
71	1.72	5.59	0.012	21.50	6.48	0.007	0.26	5.33	0.31	16.17	5.47	8.07	12.69	27.79
72	2.49	3.79	0.008	33.17	6.48	0.006	0.11	5.33	0.66	27.83	0.22	24.49	26.03	41.22

Appendix 13. Hydrometeorological variables for each of the rainfall-runoff events at M6 microcatchment. P means precipitation, Q means streamflow, RC means Runoff Coefficient, and Ant P means antecedent precipitation with the days considered are presented within the brackets. tot, average, and max, represents total, average, and maximum values.

Event	Qtot (mm)	Ptot (mm)	Qmax (mm/s)	Duration (h)	Pmax (mm/h)	Qaverage (mm/s)	Paverage (mm/h)	Time to peak (h)	RC	Recession time (h)	Ant P. (1 day) (mm)	Ant P, (3 days) (mm)	Ant P (5 days) (mm)	Ant P (7 days) (mm)
1	0.48	2.09	0.004	11.25	3.84	0.004	0.62	6.08	0.23	5.17	7.43	7.54	8.71	8.71
2	1.06	1.09	0.008	18.00	5.16	0.005	0.24	4.67	0.97	13.33	12.35	19.67	20.95	20.95
3	0.28	1.65	0.003	8.17	1.32	0.003	0.20	3.08	0.17	5.08	7.55	7.99	13.90	17.88
4	2.39	12.54	0.012	32.25	7.68	0.006	0.39	13.17	0.19	19.08	9.09	9.53	15.44	19.20
5	0.96	1.74	0.006	16.25	1.32	0.005	0.03	6.42	0.55	9.83	9.48	20.55	21.10	26.90
6	2.81	6.68	0.021	23.00	7.68	0.010	0.29	6.00	0.42	17.00	7.29	13.66	15.40	32.91
7	1.36	2.28	0.008	16.08	5.16	0.007	0.14	6.17	0.60	9.92	7.33	20.88	20.88	32.21
8	0.98	2.58	0.005	22.08	5.16	0.004	0.12	8.25	0.38	13.83	0.11	3.60	23.49	23.49
9	3.39	16.63	0.047	16.42	10.32	0.017	0.94	5.75	0.20	10.67	6.13	19.66	26.82	26.82
10	9.28	16.81	0.100	33.42	10.32	0.023	0.58	10.75	0.55	22.67	19.61	30.02	42.23	42.23
11	2.16	5.62	0.018	12.75	19.32	0.014	0.36	4.42	0.38	8.33	16.95	37.99	74.45	87.22
12	12.15	17.69	0.036	51.75	9	0.020	0.37	14.25	0.69	37.50	5.41	26.86	63.27	83.71
13	1.79	8.60	0.007	29.00	6.48	0.005	0.36	16.67	0.21	12.33	3.45	3.45	16.21	25.96
14	19.74	29.17	0.219	26.75	18	0.062	1.12	13.25	0.68	13.50	11.41	22.47	25.18	29.69
15	7.53	14.31	0.066	28.08	14.16	0.022	0.38	3.33	0.53	24.75	29.17	52.19	53.92	59.08
16	2.52	2.69	0.016	22.50	9	0.011	0.23	4.33	0.94	18.17	2.40	32.80	60.87	69.34
17	0.88	0.99	0.005	19.33	10.32	0.004	0.21	4.42	0.89	14.92	1.20	3.26	5.55	5.55
18	0.74	1.39	0.003	21.92	3.84	0.003	0.06	6.50	0.53	15.42	5.07	7.35	9.64	9.64
19	8.52	17.28	0.132	25.08	23.16	0.028	0.68	7.50	0.49	17.58	4.41	37.52	61.90	75.32
20	1.75	11.96	0.018	17.58	18	0.008	0.64	4.42	0.15	13.17	10.95	12.03	17.95	18.28
21	1.93	4.67	0.014	21.75	14.16	0.007	0.55	4.92	0.41	16.83	8.04	9.58	24.77	25.32
22	2.11	5.24	0.015	27.92	5.16	0.006	0.20	4.83	0.40	23.08	18.81	19.03	26.34	36.20
23	3.91	13.24	0.048	25.92	11.52	0.013	0.52	9.25	0.29	16.67	6.86	10.66	14.45	25.76
24	7.58	11.27	0.097	25.25	16.68	0.025	0.42	3.17	0.67	22.08	10.81	31.77	34.58	38.37
25	2.41	3.55	0.016	17.58	3.84	0.011	0.29	5.00	0.68	12.58	10.62	34.54	44.98	45.20
26	3.38	6.86	0.018	25.00	6.48	0.011	0.30	4.33	0.49	20.67	5.17	26.60	47.56	50.37

27	5.03	10.90	0.009	94.42	5.16	0.004	0.13	26.42	0.46	68.00	2.51	2.51	16.87	19.70
28	9.99	10.95	0.122	27.33	13.08	0.030	0.40	3.50	0.91	23.83	9.79	28.97	33.14	43.88
29	1.52	3.28	0.004	34.00	3.84	0.004	0.11	16.50	0.46	17.50	0.22	2.42	14.48	14.48
30	15.20	17.15	0.125	29.42	9.12	0.043	0.58	6.92	0.89	22.50	5.36	28.08	45.28	49.78
31	3.55	4.38	0.024	16.33	14.4	0.018	0.27	5.17	0.81	11.17	12.42	33.57	61.55	64.96
32	4.24	8.13	0.020	29.42	10.44	0.012	0.29	8.83	0.52	20.58	4.51	9.33	31.84	52.58
33	3.11	6.16	0.015	23.25	3.96	0.011	0.26	6.75	0.51	16.50	4.73	13.96	18.91	40.44
34	3.14	8.56	0.016	24.83	11.76	0.011	0.34	8.08	0.37	16.75	0.22	9.79	18.25	25.18
35	1.87	4.40	0.010	17.25	5.28	0.009	0.26	7.08	0.42	10.17	7.02	9.99	19.12	32.09
36	1.77	3.63	0.007	24.83	5.28	0.006	0.15	7.75	0.49	17.08	2.97	6.71	12.74	23.30
37	1.59	2.20	0.011	14.00	5.28	0.009	0.16	4.75	0.72	9.25	4.18	11.42	21.21	31.76
38	2.16	9.49	0.008	37.58	5.16	0.005	0.25	15.08	0.23	22.50	0.11	4.05	6.80	18.31
39	3.12	10.88	0.036	10.92	9.12	0.024	1.00	6.08	0.29	4.83	8.57	14.62	27.91	32.20
40	6.09	10.34	0.063	13.42	3.96	0.038	0.77	5.83	0.59	7.58	14.95	23.74	32.54	38.79
41	21.99	25.80	0.179	27.92	17.04	0.066	0.92	5.08	0.85	22.83	21.99	32.10	42.88	50.12
42	18.84	24.17	0.115	40.58	10.44	0.039	0.60	19.17	0.78	21.42	7.92	53.73	63.29	71.32
43	2.42	4.38	0.017	15.67	15.72	0.013	0.28	4.75	0.55	10.92	1.87	11.99	37.48	83.18
44	2.65	6.91	0.006	46.75	23.16	0.005	0.15	17.83	0.38	28.92	2.59	10.04	13.65	22.58
45	10.54	18.91	0.023	81.00	15.48	0.011	0.23	24.00	0.56	57.00	0.64	7.26	15.15	18.32
46	4.60	8.14	0.019	24.08	5.28	0.016	0.34	14.83	0.56	9.25	18.30	21.71	34.09	46.77
47	5.15	10.57	0.049	19.83	7.68	0.022	0.53	7.42	0.49	12.42	13.56	24.54	24.76	28.66
48	1.30	6.49	0.009	17.92	6.6	0.006	0.36	7.50	0.20	10.42	2.20	3.63	3.74	4.07
49	1.53	5.37	0.008	21.42	10.44	0.006	0.25	7.92	0.28	13.50	0.88	17.25	20.77	20.99
50	10.00	22.72	0.091	24.92	17.04	0.033	0.91	9.50	0.44	15.42	5.37	7.24	24.82	26.25
51	4.79	6.59	0.033	21.25	13.08	0.019	0.31	5.50	0.73	15.75	22.06	28.31	44.68	48.20
52	1.26	2.57	0.008	15.67	2.52	0.007	0.16	6.33	0.49	9.33	2.26	13.76	35.30	56.15
53	4.21	10.46	0.022	59.83	23.16	0.006	0.17	5.50	0.40	54.33	0.00	6.13	17.63	39.17
54	7.29	14.47	0.043	88.92	20.52	0.007	0.16	14.08	0.50	74.83	0.99	11.97	15.84	24.76
55	2.39	5.25	0.028	10.42	11.76	0.019	0.50	4.17	0.46	6.25	0.22	38.27	41.90	46.16
56	1.94	2.31	0.011	17.17	3.96	0.009	0.13	6.33	0.84	10.83	5.06	16.26	22.64	28.36

57	1.70	4.18	0.018	9.58	3.96	0.015	0.44	3.42	0.41	6.17	15.73	21.56	21.78	21.78
58	9.42	21.46	0.065	50.58	25.68	0.016	0.42	5.50	0.44	45.08	2.42	10.35	31.48	37.77
59	5.32	12.27	0.019	41.67	3.84	0.011	0.08	3.08	0.43	38.58	0.00	13.56	22.92	44.16
60	5.20	19.18	0.059	19.00	17.04	0.023	1.01	5.42	0.27	13.58	0.88	4.94	15.79	29.79
61	2.00	3.52	0.019	12.17	3.96	0.014	0.39	5.92	0.57	6.25	18.26	28.82	29.15	29.15
62	3.68	5.09	0.014	27.08	14.16	0.011	0.23	7.08	0.72	20.00	2.18	51.89	62.95	65.66
63	3.19	5.83	0.028	22.33	7.92	0.012	0.35	4.33	0.55	18.00	9.33	12.08	12.30	12.52
64	2.09	11.85	0.025	15.58	13.08	0.011	0.72	4.33	0.18	11.25	4.18	4.73	4.73	4.73
65	1.41	1.54	0.013	12.83	2.64	0.009	0.26	4.25	0.91	8.58	13.28	15.92	15.92	15.92
66	5.00	8.03	0.024	25.67	3.96	0.016	0.34	7.17	0.62	18.50	1.98	26.26	65.15	86.14
67	0.87	0.99	0.006	13.50	1.32	0.005	0.07	5.50	0.88	8.00	0.66	4.51	16.81	21.65
68	1.53	2.97	0.007	22.75	5.28	0.006	0.13	7.42	0.52	15.33	1.43	5.39	10.87	20.88
69	2.17	12.54	0.034	11.50	3.96	0.016	0.98	5.33	0.17	6.17	5.83	10.45	10.67	10.67
70	4.67	9.14	0.018	32.67	5.16	0.012	0.28	9.42	0.51	23.25	0.66	17.71	24.29	35.75
71	1.22	2.48	0.008	21.50	3.84	0.005	0.12	5.75	0.49	15.75	5.47	8.07	12.69	27.79
72	1.35	3.79	0.005	33.00	6.48	0.003	0.11	8.00	0.36	25.00	0.22	24.49	26.03	41.22

Appendix 14. Hydrometeorological variables for each of the rainfall-runoff events at M7 microcatchment. P means precipitation, Q means streamflow, RC means Runoff Coefficient, and Ant P means antecedent precipitation with the days considered are presented within the brackets. tot, average, and max, represents total, average, and maximum values.

Event	Qtot (mm)	Ptot (mm)	Qmax (mm/s)	Duration (h)	Pmax (mm/h)	Qaverage (mm/s)	Paverage (mm/h)	Time to peak (h)	RC	Recession time (h)	Ant P. (1 day) (mm)	Ant P, (3 days) (mm)	Ant P (5 days) (mm)	Ant P (7 days) (mm)
1	0.41	2.09	0.004	11.25	3.84	0.003	0.19	3.58	0.20	7.67	7.43	7.54	8.71	8.71
2	0.85	1.09	0.006	18.00	5.16	0.004	0.06	5.75	0.78	12.25	12.35	19.67	20.95	20.95
3	0.14	1.65	0.002	8.17	1.32	0.001	0.20	4.25	0.08	3.92	7.55	7.99	13.90	17.88
4	1.37	12.54	0.007	32.25	7.68	0.004	0.39	14.17	0.11	18.08	9.09	9.53	15.44	19.20
5	0.37	0.44	0.004	16.25	1.32	0.003	0.03	4.67	0.84	11.58	9.48	20.55	21.10	26.90
6	2.62	6.68	0.022	23.00	7.68	0.010	0.29	5.50	0.39	17.50	7.29	13.66	15.40	32.91
7	1.27	2.28	0.008	16.08	5.16	0.007	0.14	6.92	0.56	9.17	7.33	20.88	20.88	32.21
8	0.85	2.58	0.004	22.08	5.16	0.003	0.12	17.08	0.33	5.00	0.11	3.60	23.49	23.49
9	3.40	16.63	0.051	16.42	10.32	0.017	1.01	6.00	0.20	10.42	6.13	19.66	26.82	26.82
10	9.46	16.81	0.100	33.50	10.32	0.024	0.50	11.33	0.56	22.17	19.61	30.02	42.23	42.23
11	2.24	5.62	0.018	12.75	19.32	0.015	0.44	4.50	0.40	8.25	16.95	37.99	74.45	87.22
12	13.81	17.69	0.038	51.75	9.00	0.022	0.34	16.17	0.78	35.58	5.41	26.86	63.27	83.71
13	1.17	8.60	0.005	29.00	6.48	0.003	0.30	16.58	0.14	12.42	3.45	3.45	16.21	25.96
14	22.96	29.17	0.222	26.75	18.00	0.072	1.09	12.75	0.79	14.00	11.41	22.47	25.18	29.69
15	9.06	14.31	0.072	28.08	14.16	0.027	0.51	3.75	0.63	24.33	29.17	52.19	53.92	59.08
16	2.61	2.69	0.023	22.50	9.00	0.013	0.12	4.58	0.97	17.92	2.40	32.80	60.87	69.34
17	0.20	0.22	0.004	19.33	10.32	0.003	0.01	5.50	0.91	13.83	1.20	3.26	5.55	5.55
18	0.61	1.39	0.003	21.92	3.84	0.002	0.06	5.42	0.44	16.50	5.07	7.35	9.64	9.64
19	7.72	17.28	0.101	25.08	23.16	0.026	0.69	8.08	0.45	17.00	4.41	37.52	61.90	75.32
20	1.01	11.96	0.010	17.58	18.00	0.005	0.68	5.42	0.08	12.17	10.95	12.03	17.95	18.28
21	1.83	4.67	0.011	21.75	14.16	0.007	0.21	4.75	0.39	17.00	8.04	9.58	24.77	25.32
22	2.65	5.24	0.016	27.92	5.16	0.008	0.19	5.75	0.51	22.17	18.81	19.03	26.34	36.20
23	4.72	13.24	0.045	25.92	11.52	0.015	0.51	9.50	0.36	16.42	6.86	10.66	14.45	25.76
24	10.76	11.27	0.113	25.25	16.68	0.036	0.45	3.33	0.95	21.92	10.81	31.77	34.58	38.37
25	3.15	3.55	0.019	17.58	3.84	0.015	0.20	5.42	0.89	12.17	10.62	34.54	44.98	45.20
26	4.26	6.86	0.021	25.00	6.48	0.014	0.27	4.67	0.62	20.33	5.17	26.60	47.56	50.37

27	4.79	10.90	0.007	94.42	5.16	0.004	0.12	27.00	0.44	67.42	2.51	2.51	16.87	19.70
28	9.89	10.95	0.136	27.33	13.08	0.042	0.40	3.75	0.90	23.58	9.79	28.97	33.14	43.88
29	1.04	3.28	0.003	34.00	3.84	0.003	0.10	17.00	0.32	17.00	0.22	2.42	14.48	14.48
30	16.33	17.15	0.138	29.42	9.12	0.060	0.58	8.33	0.95	21.08	5.36	28.08	45.28	49.78
31	4.36	4.38	0.029	16.33	14.40	0.022	0.27	5.42	1.00	10.92	12.42	33.57	61.55	64.96
32	5.76	8.13	0.037	29.42	10.44	0.016	0.28	8.42	0.71	21.00	4.51	9.33	31.84	52.58
33	4.10	6.16	0.021	23.25	3.96	0.015	0.26	9.67	0.67	13.58	4.73	13.96	18.91	40.44
34	4.61	8.56	0.027	24.83	11.76	0.015	0.34	6.83	0.54	18.00	0.22	9.79	18.25	25.18
35	2.49	4.40	0.014	17.25	5.28	0.012	0.26	7.25	0.57	10.00	7.02	9.99	19.12	32.09
36	1.74	3.63	0.007	24.83	5.28	0.006	0.15	8.17	0.48	16.67	2.97	6.71	12.74	23.30
37	1.92	2.20	0.013	14.00	5.28	0.011	0.16	5.25	0.87	8.75	4.18	11.42	21.21	31.76
38	1.57	9.49	0.006	37.58	5.16	0.003	0.25	16.42	0.17	21.17	0.11	4.05	6.80	18.31
39	2.96	10.88	0.035	10.92	9.12	0.023	1.00	7.00	0.27	3.92	8.57	14.62	27.91	32.20
40	6.99	10.34	0.073	13.42	3.96	0.043	0.77	5.42	0.68	8.00	14.95	23.74	32.54	38.79
41	24.15	25.80	0.149	27.92	17.04	0.072	0.92	5.67	0.94	22.25	21.99	32.10	42.88	50.12
42	20.56	24.17	0.117	40.58	10.44	0.042	0.60	19.75	0.85	20.83	7.92	53.73	63.29	71.32
43	2.46	4.38	0.017	15.67	15.72	0.013	0.28	5.25	0.56	10.42	1.87	11.99	37.48	83.18
44	1.81	6.91	0.005	46.75	23.16	0.003	0.15	18.50	0.26	28.25	2.59	10.04	13.65	22.58
45	8.91	18.91	0.028	81.00	15.48	0.009	0.23	22.58	0.47	58.42	0.64	7.26	15.15	18.32
46	4.82	8.14	0.021	24.08	5.28	0.017	0.34	4.33	0.59	19.75	18.30	21.71	34.09	46.77
47	8.99	10.57	0.093	19.83	7.68	0.038	0.53	4.42	0.85	15.42	13.56	24.54	24.76	28.66
48	1.15	6.49	0.007	17.92	6.60	0.005	0.36	9.58	0.18	8.33	2.20	3.63	3.74	4.07
49	1.38	5.37	0.007	21.42	10.44	0.005	0.25	8.42	0.26	13.00	0.88	17.25	20.77	20.99
50	9.29	22.72	0.088	24.92	17.04	0.031	0.91	10.25	0.41	14.67	5.37	7.24	24.82	26.25
51	4.46	6.59	0.029	21.25	13.08	0.017	0.31	5.42	0.68	15.83	22.06	28.31	44.68	48.20
52	1.55	2.57	0.009	15.67	2.52	0.008	0.16	7.67	0.60	8.00	2.26	13.76	35.30	56.15
53	5.18	10.46	0.017	59.92	23.16	0.007	0.17	6.08	0.50	53.83	0.00	6.13	17.63	39.17
54	9.01	14.47	0.035	88.92	20.52	0.008	0.16	16.17	0.62	72.75	0.99	11.97	15.84	24.76
55	2.77	5.25	0.035	10.42	11.76	0.022	0.50	5.00	0.53	5.42	0.22	38.27	41.90	46.16
56	2.10	2.31	0.012	17.25	3.96	0.010	0.13	7.25	0.91	10.00	5.06	16.26	22.64	28.36

57	1.62	4.18	0.017	9.58	3.96	0.014	0.44	4.08	0.39	5.50	15.73	21.56	21.78	21.78
58	8.52	21.46	0.061	50.67	25.68	0.014	0.42	5.50	0.40	45.17	2.42	10.35	31.48	37.77
59	3.40	3.49	0.012	41.67	3.84	0.008	0.08	4.58	0.98	37.08	0.00	13.56	22.92	44.16
60	5.16	19.18	0.059	19.00	17.04	0.023	1.01	4.75	0.27	14.25	0.88	4.94	15.79	29.79
61	2.17	3.52	0.020	12.17	3.96	0.015	0.29	6.17	0.62	6.00	18.26	28.82	29.15	29.15
62	4.20	5.09	0.018	27.08	14.16	0.013	0.19	5.83	0.82	21.25	2.18	51.89	62.95	65.66
63	2.87	5.83	0.023	22.33	7.92	0.011	0.26	4.92	0.49	17.42	9.33	12.08	12.30	12.52
64	1.79	11.85	0.022	15.58	13.08	0.010	0.76	4.83	0.15	10.75	4.18	4.73	4.73	4.73
65	1.27	1.54	0.012	12.83	2.64	0.008	0.12	4.92	0.82	7.92	13.28	15.92	15.92	15.92
66	5.09	8.03	0.024	25.67	3.96	0.017	0.31	7.50	0.63	18.17	1.98	26.26	65.15	86.14
67	0.84	0.99	0.006	13.50	1.32	0.005	0.01	2.17	0.85	11.33	0.66	4.51	16.81	21.65
68	1.48	2.97	0.006	22.83	5.28	0.005	0.13	6.58	0.50	16.25	1.43	5.39	10.87	20.88
69	2.16	12.54	0.034	11.50	3.96	0.016	1.09	4.83	0.17	6.67	5.83	10.45	10.67	10.67
70	3.82	9.14	0.016	32.67	5.16	0.010	0.28	12.75	0.42	19.92	0.66	17.71	24.29	35.75
71	0.92	2.48	0.005	21.50	3.84	0.004	0.12	7.33	0.37	14.17	5.47	8.07	12.69	27.79
72	2.68	3.79	0.027	33.17	6.48	0.007	0.11	0.67	0.71	32.50	0.22	24.49	26.03	41.22

Appendix 15. Linear regression between the hydrometeorological variables presenting the highest correlation with the event water fraction (Q_e) at catchment M1. P = precipitation, Q = streamflow.

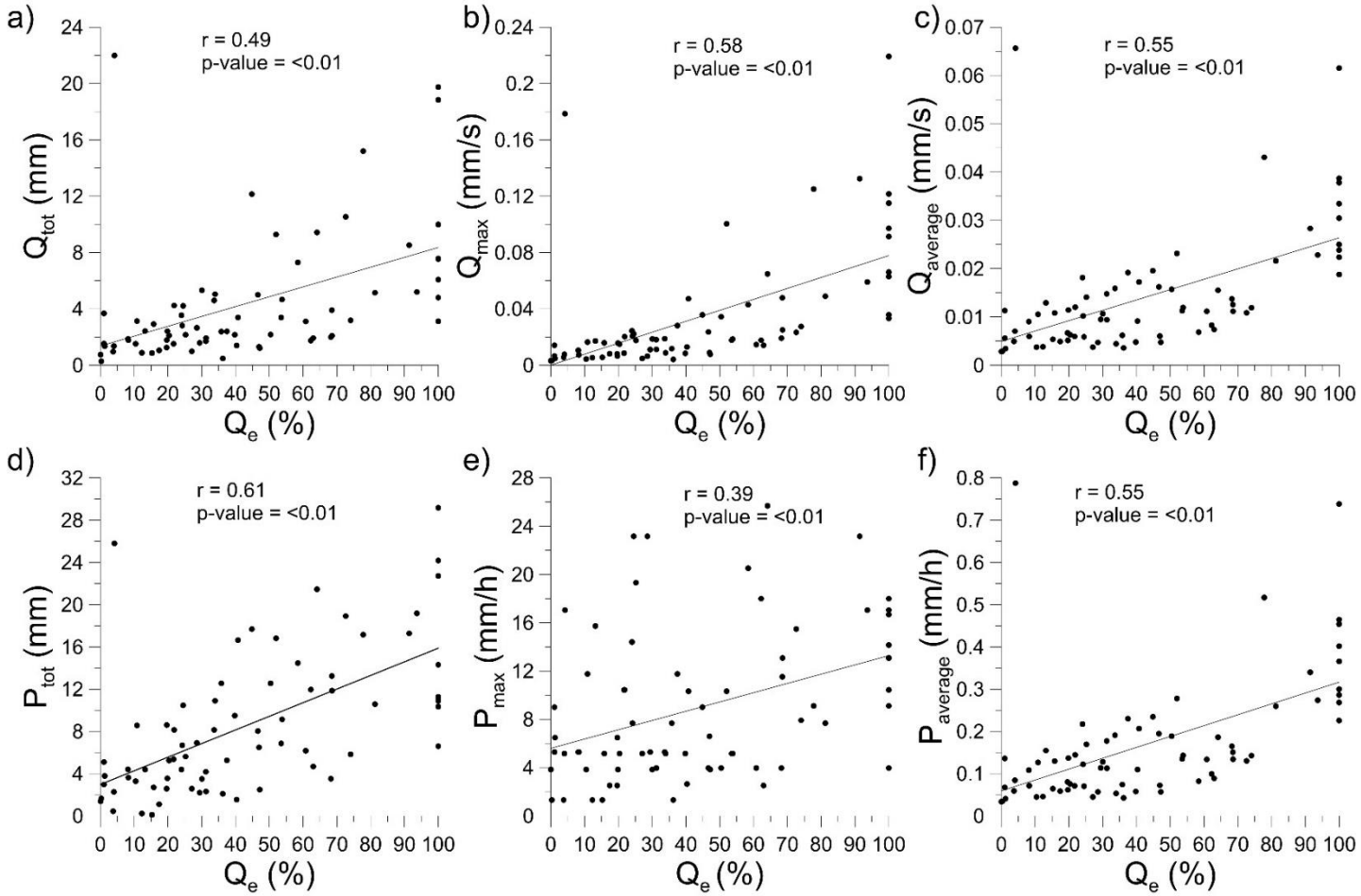

Appendix 16. Linear regression between the hydrometeorological variables presenting the highest correlation with the event water fraction (Q_e) at catchment M2. P = precipitation, Q = streamflow.

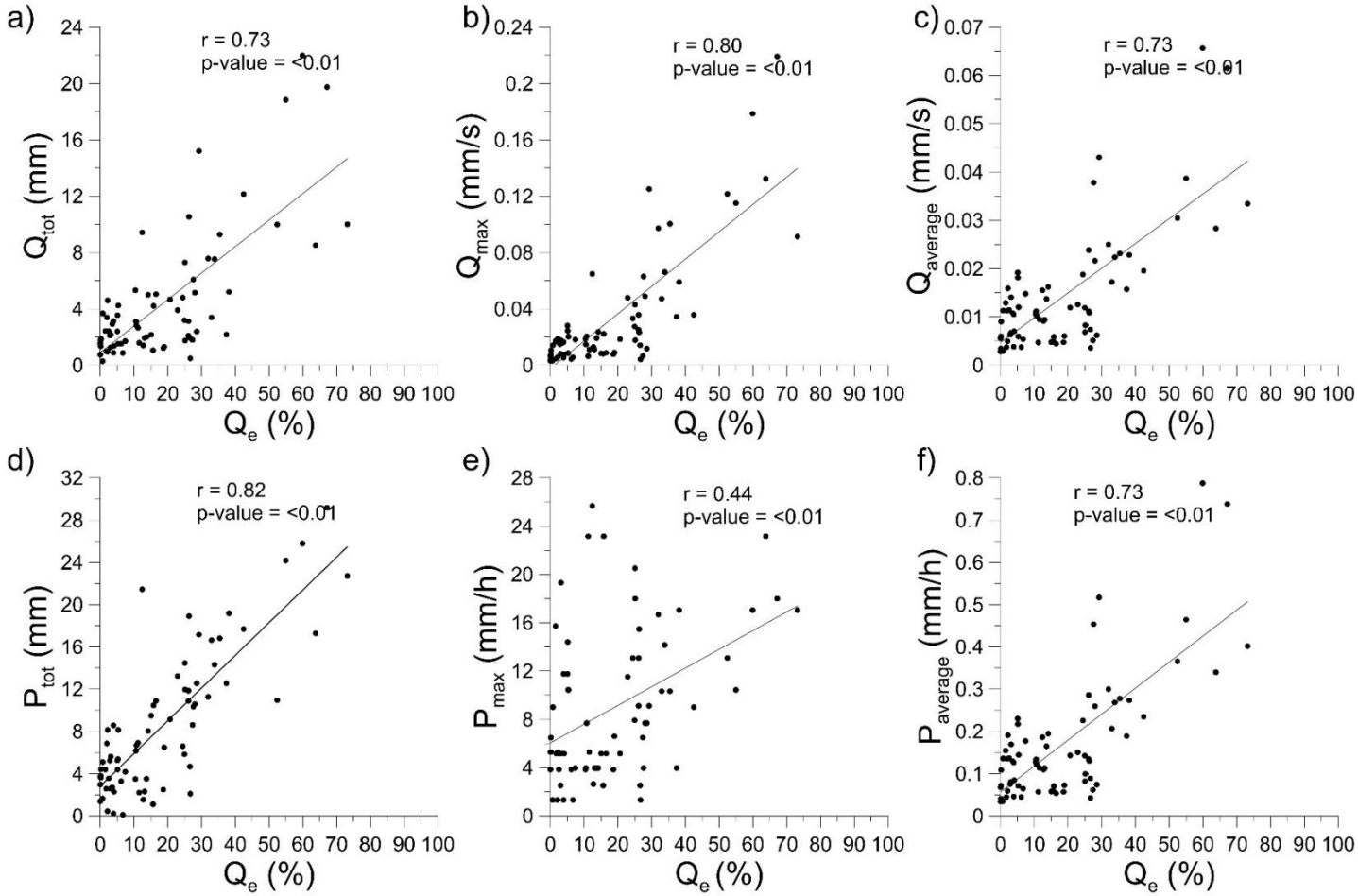

Appendix 17. Linear regression between the hydrometeorological variables presenting the highest correlation with the event water fraction (Q_e) at catchment M3. P = precipitation, Q = streamflow.

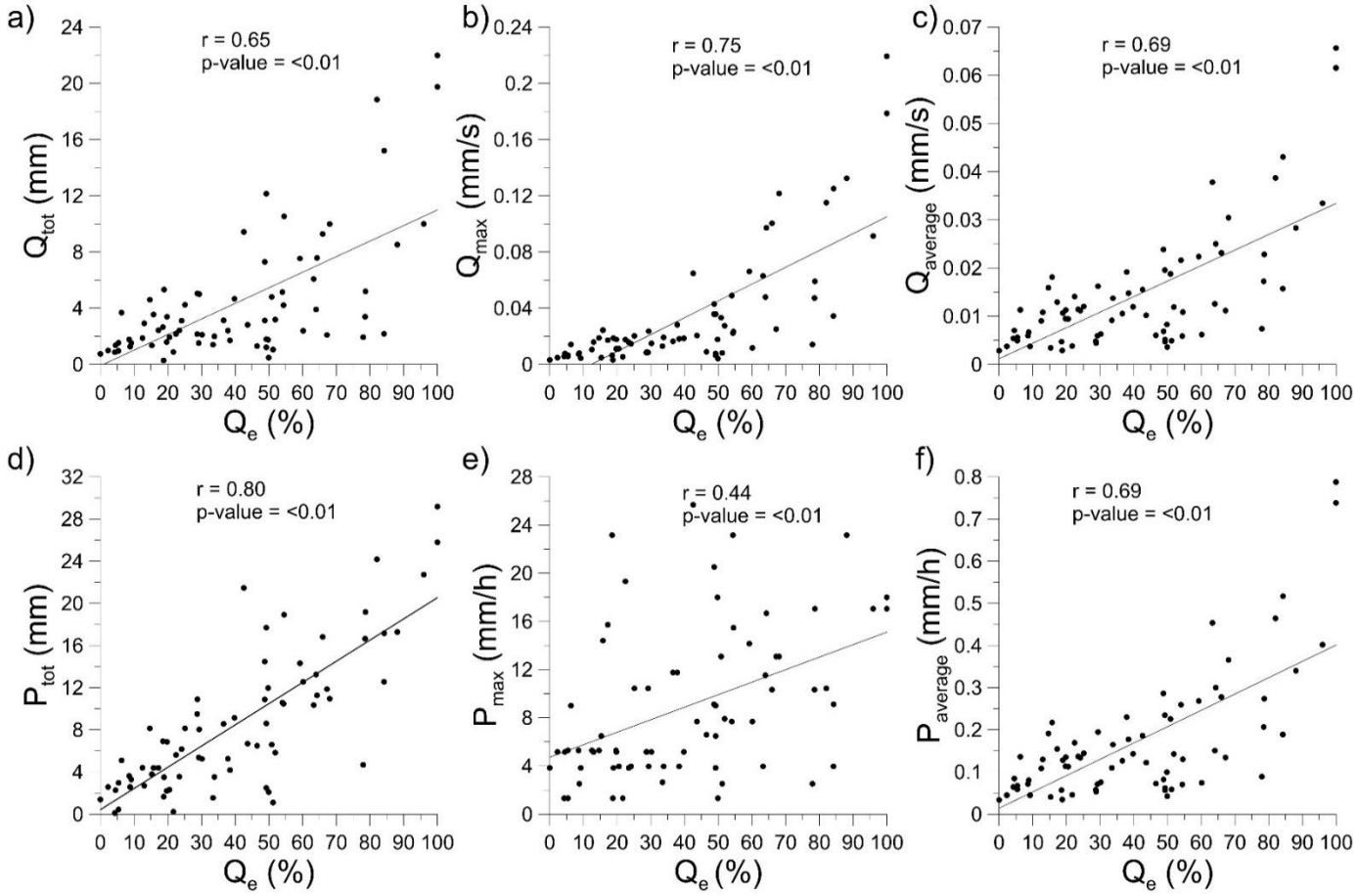

Appendix 18. Linear regression between the hydrometeorological variables presenting the highest correlation with the event water fraction (Q_e) at catchment M4. P = precipitation, Q = streamflow.

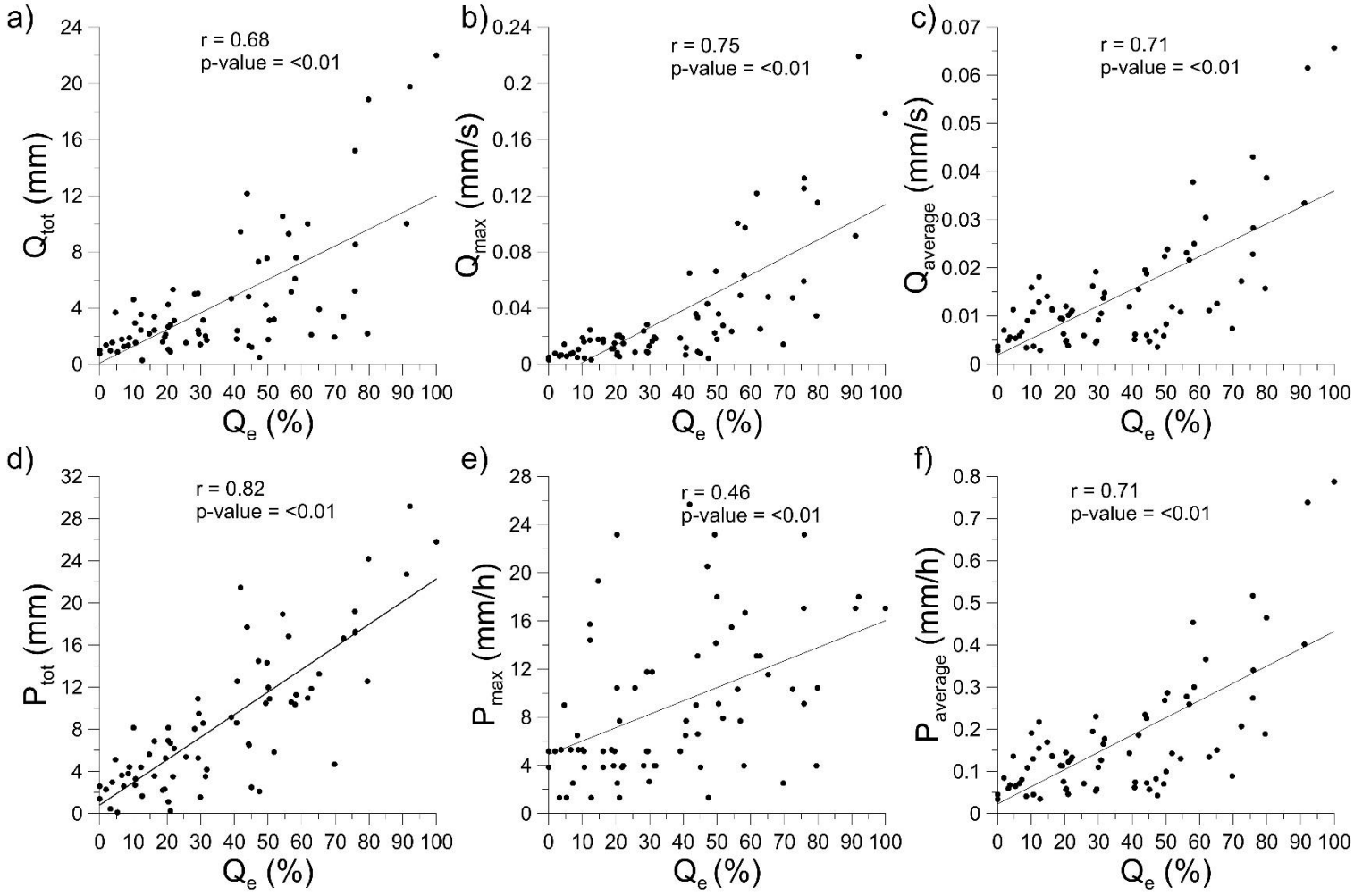

Appendix 19. Linear regression between the hydrometeorological variables presenting the highest correlation with the event water fraction (Q_e) at catchment M5. P = precipitation, Q = streamflow.

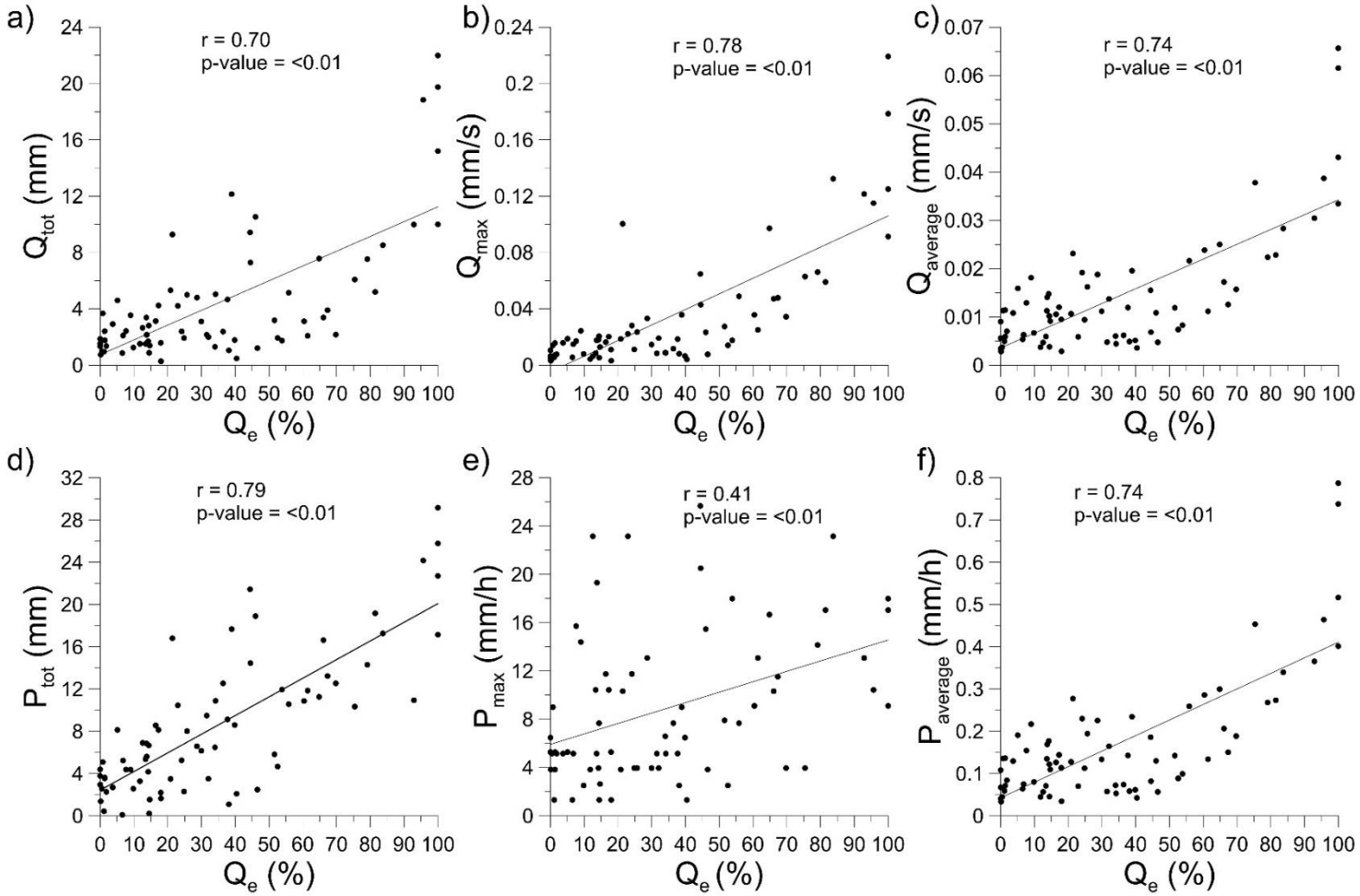
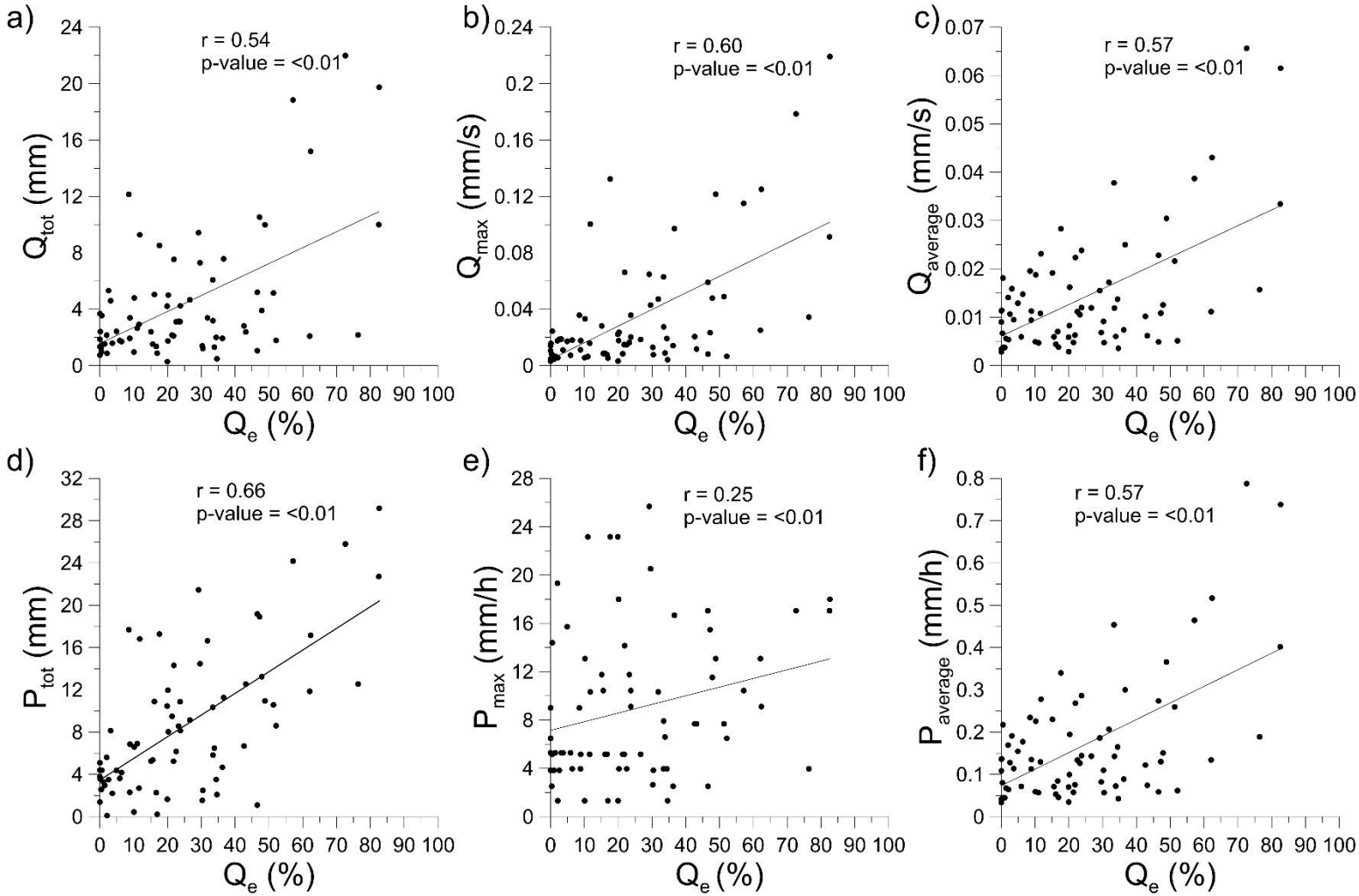
Appendix 20. Linear regression between the hydrometeorological variables presenting the highest correlation with the event water fraction (Q_e) at catchment M7. P = precipitation, Q = streamflow.